PERIODIC OPERATION OF A CONTINUOUS FLOW STIRRED TANK REACTOR WITH SIMULTANEOUS HYDROLYSIS REACTIONS

A THESIS

Presented to

The Faculty of the Division of Graduate

Studies and Research

by

Robert Charles Schucker

In Partial Fulfillment

of the Requirements for the Degree

Doctor of Philosophy in the School of Chemical Engineering

Georgia Institute of Technology

March, 1974

PERIODIC OPERATION OF A CONTINUOUS FLOW STIRRED TANK REACTOR

WITH SIMULTANEOUS HYDROLYSIS REACTIONS

Approved:

Dr. J. T. Sommerfeld, Chairman

Dr. C. W. Gorton

Dr. H. M. Neumann

Date Approved by Chairman Feb. 28, 1974

DEDICATION

To Becky

ACKNOWLEDGEMENTS

The author wishes to thank his thesis advisor, Dr. Jude T. Sommerfeld, for his advice and guidance throughout the course of this work. His suggestion of a research area and continual help were invaluable in its completion.

Appreciation is also given to Dr. C. W. Gorton and Dr. H. M. Neumann for having served on the thesis advisory committee and for their encouragement and advice during many consultations. In addition, appreciation is extended to Dr. H. C. Lewis and Dr. M. J. Matteson for having served on the orals committee.

Dr. G. L. Bridger is thanked for providing Graduate Teaching Assistantships during the academic year 1971-72, for the Procter and Gamble Fellowship during the academic year 1972-73 and for DuPont and Fiber Industries Fellowships during other quarters.

I would like to thank Dr. C. L. Liotta, Mr. Henry Harris and Mr. Tom Henson for assistance in organic reaction technology and analysis, and Dr. J. A. Knight, Mr. Pete Elston and Mr. Dave Hurst for their excellent help in the area of gas chromatography.

Appreciation is also extended to Mr. Jim Nabors and Mr. Charles Blackwood for their help in the construction of the equipment used in this work.

Thanks is given to Dr. Tomas F. Camacho for many hours of conversation and advice concerning this research, and to Mrs. Marie LaBoon for her excellent work in the typing of the final draft of this disser-

tation.

Last, but not least, I wish to thank my wife Becky for her help and encouragement during the difficult periods of this work. Without her constant support, this research would have been much more difficult.

TABLE OF CONTENTS

TABLE OF CONTENTS (CONTINUED)

TABLE OF CONTENTS (CONTINUED)

LIST OF TABLES

LIST OF TABLES (CONTINUED)

LIST OF ILLUSTRATIONS

LIST OF ILLUSTRATIONS (CONTINUED)

NOMENCLATURE

Symbol	Meaning	Units
C	concentration	gmole/liter
C_p	heat capacity	cal/gm-^oK
E	activation energy	cal/gmole
k	reaction rate constant	liter/gmole-min
M	objective function	none
Q_F	volumetric flow rate	liter/min
q	heat flux to the CSTR	cal/min
R	gas constant	cal/gmole-^oK
T	temperature	^oK
t	dimensionless time	none
t'	real time	min.
t_c	length of cycle	min.
u	dimensionless control variable	none
U	control variable vector	none
V	reaction volume	liter
x	dimensionless state variable	none
X	state variable vector	none
y	dimensionless control variable	none
ρ	ratio of activation energies (E_2/E_1)	none
ρ_ℓ	reaction liquid density	gm/ml
ϕ	fraction of cycle during which the control variable is at lower limit	none

Symbol	Meaning	Units
ψ	dimensionless adjoint variable	none
τ	length of cycle in dimensionless time	none
$\mathcal{H}$	Hamiltonian function	none
ξ	maximum function	none

SUMMARY

Numerous studies have been made of continuous flow stirred tank reactors (CSTR's); however, most of the work has centered about steady-state operation. In this work the periodic (deliberate unsteady-state) operation of an experimental CSTR, in which two simultaneous hydrolysis reactions were carried out, was studied by monitoring the time-averaged yield of the products of these reactions under various periodic conditions. The objective of this work was to show that actual increases in yield of 5-10% above the conventional steady-state could be obtained by the periodic operation of the CSTR.

The reactor system consisted of reactant feed tanks, constant head flow controllers, reactant rotameters, a reactant cooler and CSTR. The reactants were gravity fed to the constant head flow controllers which assured a constant flow to the rotameters. Fine adjustments to the flow rate were made with needle valves in the rotameters. Reactants entered the CSTR, were mixed with a three-blade impeller while reacting and overflowed into a receiving vessel where the reactions were quenched. The volume of liquid in the reactor was maintained constant at two liters.

The reactions studied, over the temperature range of -10°C to 60°C, were the simultaneous alkaline hydrolyses of methyl acetate and ethyl benzoate in an acetone-water solution. The latter hydrolysis, being much slower than the first, was made competitive by fixing the ethyl benzoate feed concentration to be ten times that of either the methyl acetate or sodium hydroxide. Reaction rate constants for these

two reactions were determined experimentally; the frequency factors and activation energies were found to be:

$k_{10} = 1.8552 \cdot 10^{7}$ liter/gmole-min $\qquad E_1 = 8{,}800$ cal/gmole

$k_{20} = 1.0283 \cdot 10^{10}$ liter/gmole-min $\qquad E_2 = 14{,}750$ cal/gmole

when the reactant solution consisted of 70 parts by volume acetone made up to 100 parts by the addition of distilled water plus reactants.

The experimental method consisted of generating a periodic heat flux (maximum of 2.3 KW) to the reactor by means of an electrical heating element. The heat flux was caused to be periodic by a cycle timer, which allowed control of the amount of time the heat flux was on and off. The subsequent result was a square-wave variation in the heat flux.

During operation the concentrations of the reactants and products vary as a function of time; their time-averaged values over one cycle, however, approach a constant or pseudo-steady-state value after a small number of cycles. These pseudo-steady-state concentrations were measured by allowing the reactor effluent to accumulate over one cycle in a receiving vessel and measuring the product concentrations in this composite sample.

Experimental runs were made at $\phi = 0.95$, 0.90, 0.80, 0.70 and 0.60 (ϕ is the fraction of the cycle during which the heat flux is at its lower limit of zero). The concentration of ethanol (one of the products of the reaction with the higher activation energy) in the

composite samples was measured with a Perkin-Elmer gas chromatograph equipped with a flame ionization detector. Experimental results were compared with results of a computer simulation of this operation and agreed favorably. Improvements of up to 11% were observed in the pseudo-steady-state yield of ethanol over its conventional steady-state yield. The yields of the products of the other reaction were found to decrease.

CHAPTER I

INTRODUCTION

Many studies (3,39) of continuous flow stirred tank reactors (CSTR's) have been made in the past; however, most of the work has been centered about steady-state operation. This is primarily due to the fact that steady-state operation is the simplest to describe mathematically and often the simplest to implement physically. In many reaction systems, such as competitive reactions of different orders or consecutive reactions, there is usually an upper limit to the possible yield of a desired product in a CSTR. This upper limit will be referred to as the optimum steady-state value. This optimum steady-state may be either a global optimum, where within the range of operating conditions the change of the desired variable with respect to the control variable is actually zero, or a local optimum, where further increase in the desired variable is prevented by some physical restraint (such as boiling point, heat transfer rate, flow rate, etc.). Both types of systems occur in practice and were examined in this work.

An alternative to steady-state operation is unsteady operation, which has many forms, one of which is periodic reactor operation. In periodic reactor operation, one or more of the control variables of the reactor is varied periodically with respect to time until a pseudo-steady-state is reached. This pseudo-steady-state is similar to conventional steady-state in that the time-averaged value of the state

variables (rather than the state variables themselves) over the period of the variation approach a constant value. Although the state variables are a function of time, they have the same values at the end of the period of variation that they did at the beginning, once pseudo-steady-state has been reached. The form of the periodic variation of the control variable may be a triangular wave, sine wave, square wave, etc. Several of these variations have been studied theoretically and will be mentioned later. Depending on the type of variation used, periodic unsteady-state processes may be broken down into three general categories: (a) pulsed operation, (b) chemical oscillators, and (c) controlled cycling. Only the latter mode of periodic operation will be considered in this work. For some classes of reactions, the operation of the reactor periodically can generate increases in the product yield of 5%-50% above the conventional steady-state values. Whether periodic operation can improve the product yield beyond the optimum steady-state depends strictly on the reaction system and the type of optimum involved (global or local). Several theoretical studies have been made which demonstrate the desirability of periodic reactor operation; however, no experimental work has been done in the area of competitive reaction systems to verify these results. It was the purpose of this work to perform experimental work to show that in some reaction systems improvements in product yields can be obtained by the periodic operation of the reactor and to investigate more fully the phenomena associated with periodic operation.

CHAPTER II

UNSTEADY-STATE PROCESSING

Unsteady-state operation is not novel to chemical and petrochemical processing. Many times plants operate close to steady-state but, in general, have variations in the systems which cause them to behave essentially in unsteady-state fashion. The question that arises then is whether this is favorable or detrimental to the process. Schrodt (56,57) maintains that significant benefits can be obtained by deliberately operating a system at unsteady-state conditions. He cites examples of the unsteady-state operation of distillation columns, extraction columns, packed bed absorbers, crystallizers, ion exchangers and chemical reactors, suggesting in each case that performance can be improved to some degree by unsteady-state operation. In addition, Horn (33) has investigated the performance of periodic countercurrent processes and shown that, theoretically, efficiency can be improved considerably over conventional steady-state. The optimal operation of a variable-volume stirred tank reactor was investigated by Lund and Seagrave (42) in a theoretical study and the results showed that the unsteady-state variation of the volume of the reactor could produce an increase in the yield of the desired product for some classes of reactions.

Pulsed Operation

Pulsed operation, as mentioned in the literature, generally refers to a periodic variation in one of the input variables to a reactor (flow rate, initial concentration, etc). Laurence and Vasudevan (38) and Ray (50) performed theoretical studies on the periodic operation of polymerization reactors. In both cases periodic operation was achieved by the sinusoidal variation of the monomer feed concentrations; neither study presented experimental results. Theoretical studies have also been made by Douglas and Rippin (23), Dorawala and Douglas (21), Renken (51), Ritter and Douglas (52), and Douglas (22) concerning the effect of a sinusoidal variation of feed concentration and the effect of the frequency of the variation on non-linear systems of reactions occurring in CSTR's. Again, in all cases, no experimental work was done to verify the theoretical results obtained from the analytical and numerical studies. Experimental work performed by Li (40) showed improvement in the extraction of benzoic acid from water into toluene in a perforated plate tower by pulsed operation (pulsed flow rate).

Chemical Oscillators

Chemical oscillators are reaction systems possessing inherent instabilities which cause natural oscillations in the system output while the input variables remain constant. In order for the system to exhibit this natural oscillation, the system parameters must fall within a specified range; that is, any given combination of parameters would not necessarily produce oscillation. Douglas and Rippin (23) have also studied chemical oscillators and the conditions necessary to cause

natural oscillations in non-linear systems. Experimental work in this area has been done by Baccaro, Gaitonde and Douglas (6), who designed a laboratory reactor to operate as a chemical oscillator for the hydrolysis of acetyl chloride. The object of the experimental work was to compare the actual oscillatory behavior with the behavior predicted by a mathematical model. Agreement was fairly good.

Controlled Cycling

Controlled cycling, which is also known as "bang-bang" or "on-off" operation is a type of periodic unsteady-state operation wherein the control variables of the system are deliberately varied with time in a square-wave or "bang-bang" manner. This type of operation can be applied to many different types of equipment in chemical unit operations.

Cannon (13,14) conceived the idea of controlled cycling about 1952. Later experimental work was performed by Gaska and Cannon (28) and McWhirter and Cannon (44). Their investigations into both sieve and screen plate columns and packed plate columns showed that controlled cyclic operation of separation columns could increase column throughput without sacrificing efficiency. Sommerfeld et al. (61) performed analog computer simulations of a controlled cycled distillation column. An improved separating ability of a column operated in this fashion was shown to be due to the effective plate efficiency being significantly greater than the point efficiency for any given plate. Chien et al. (16) and Robinson and Engel (54) simultaneously derived the analytical expressions describing the cyclic operation of a distillation column. Chien et al. (16) concluded that improvement in the

separating ability of a distillation column could be obtained by cyclic operation. Robinson and Engel (54) stated that controlled cycling at best should give separation comparable to that of a conventionally operated column with no liquid mixing on the trays. A subsequent experimental study performed by Schrodt et al. (58) separating an acetone-water mixture showed, however, that the primary advantage of cyclic operation was that two or more times the conventional column throughput could be obtained. May and Horn (46) have also studied the periodic operation of a distillation column but their primary concern was the stage efficiency and effect of mixing on periodic countercurrent processes.

Several studies on equipment other than distillation columns have also been made. Kowler and Kadlec (37) have shown experimentally that the optimal control of a periodic adsorber is "bang-bang" and that this mode of operation produces better separation than conventional steady-state operation. Bailey and Horn (8) have shown that cyclic operation of catalytic reaction systems improves catalyst selectivity and Bailey, Horn and Lin (9) have investigated the effects of heat and mass transfer resistance in the cyclic operation of a CSTR. Horn and Lin (32), Codell and Engel (17) and Matsubara et al. (45) have all investigated the periodic operation of CSTR's. The latter five studies, which entailed no experimental work, showed that for some classes of reactions, improved yield of a desired product could be obtained by the cyclic or periodic operation of the reactor.

Several experimental studies have been done recently in the area

of periodic operation. One of these included the operation and modelling of a periodic, countercurrent liquid-solid reactor by Dodds et al. (20) in which an ion exchange resin was transferred periodically from stage to stage of a Cloete-Streat stage-wise solid-liquid reactor counter-current to an aqueous sodium hydroxide stream. Results indicated that, for a certain range of operating conditions, unsteady-state operation (with periodic transfer of solid resin) was superior to continuous steady-state operation.

A second experimental study was performed by Ausikaitis and Engel (5). In this study, a CCTR (controlled cycled tank reactor) was investigated using the reaction between sodium thiosulfate and hydrogen peroxide. The purpose of the work was to investigate multiplicity of steady-states. Results indicated that this reactor (CCTR) could be operated stably in a region which would be unstable under normal steady-state operating conditions. This periodic operation of the CCTR also resisted efforts of transient upsets to cause the system to go unstable.

Optimization Theory

The optimal design of conventionally operated CSTR's has been treated by Aris (3,4) and Bellman (10) both of whom used dynamic programming as their optimization technique. Beveridge and Schechter (12) have compiled an excellent review of numerous optimization techniques which can be used to determine the optimal steady-state operating policy. One of the most powerful tools developed in recent years for the determination of optimal control policies is the Pontryagin Maximum Principle, which was published in English in 1962 from the original Russian

work of Pontryagin et al. (49). An excellent review of the Maximum Principle and some examples of its use are given by Rozonoer (55). Siebenthal and Aris (60) have applied the Maximum Principle to the control of CSTR's and Shatkhan (59) has applied it to the optimization of parallel chemical reactions. Bertucci and Lapidus (11) have attempted to simplify calculations by using a Modified Maximum Principle. This modification to the Maximum Principle, introduced by Chaprun (15) in 1967, removes the instability in the adjoint variable integration. Application of the Maximum Principle in most cases requires a knowledge of the calculus of variations. Gelfand and Fomin (29), Akhiezer (2) and Elsgolc (25) have all prepared texts on the calculus of variations.

Analoguous to the optimum (either global or local) which may exist in conventional steady-state operation, there may also exist an optimum periodic state. The determination of the optimal "bang-bang" control policy for linear and non-linear systems has been investigated by Edgar and Lapidus (24) in which the authors studied the minimum time control of a two-stage CSTR being operated periodically. Lin and Horn (32) investigated the optimization of a competitive second and first-order reaction system using the Pontryagin Maximum Principle, Bailey (7) studied optimal periodic processes in the limits of very fast and very slow cycling and Locatelli and Rinaldi (41) investigated optimal quasi-stationary periodic processes.

Experimental Reaction System

The reaction system chosen for this experimental work had to meet rigorous requirements regarding the ratio of activation energies,

overall rate of reaction, and stability. The reaction system which offered the most promise was the simultaneous alkaline hydrolysis of two carboxylic esters. A survey of the literature showed that the activation energies for most hydrolysis reactions occurring in pure water were not sufficiently far apart to give the desired increase in product yield by periodic operation. However, studies showed that the same reactions occurring in certain aqueous-organic solvent systems had significantly different activation energies. Therefore, the reaction system chosen was the simultaneous alkaline hydrolyses of methyl acetate and ethyl benzoate in a 70% aqueous-acetone medium (this will be defined more explicitly in Chapter VI). The alkaline hydrolysis of methyl acetate in various aqueous-organic solvents has been studied extensively by Davies and Evans (19), Gallagher et al. (27), Jones and Thomas (36) and Yager et al. (66). In addition, the alkaline hydrolysis of ethyl benzoate in aqueous-organic solvents has been studied by Evans et al. (26), Ingold and Nathan (34), Newling and Hinshelwood (47), Timm and Hinshelwood (62), Tommila (63), Tommila and Hinshelwood (64), and Tommila et al, (65). Reaction rate constants, activation energies, solvent effects and types of mechanisms have all been previously determined and the rate constants were verified experimentally in this work.

CHAPTER III

THE PONTRYAGIN MAXIMUM PRINCIPLE

In 1962 with the translation from Russian to English of the work of Pontryagin et al. (49), a powerful technique for the determination of optimal control policies was made available. This method, known as the Pontryagin Maximum Principle, is quite sophisticated and involves the usage of several theorems which will be merely stated here; no attempt to prove these theorems will be made, since the proofs are lengthy and have already been presented by Pontryagin and others (49). The Maximum Principle, as it applies to periodic chemical processes, however, will be described as thoroughly as possible.

All unsteady-state processes in the chemical industry can be described by a system of material and/or energy balances. These are often ordinary differential equations (linear or non-linear) which can be expressed in state variable form:

$$\frac{dx_i}{dt} = f_i(x_1,x_2,\ldots,x_n ; u_1,u_2,\ldots,u_r) \qquad i = 1,2,\ldots,n \qquad (3.1)$$

where $x_1,\ldots, x_n$ are the state variables (variables describing the state of the system, such as concentration, temperature, etc.) and $u_1,\ldots, u_r$ are the control variables of the system (variables which may be controlled, such as heat flux, flow rate, initial concentration of reactants, etc.). Since in periodic reactor operation, the be-

havior of the system (once pseudo-steady-state has been achieved) is identical from one period to the next, the time interval under consideration will be $0 \leq t \leq \tau$, where τ is the length of the period in dimensionless time units. In order that optimal control be achieved, the control variables will be allowed to be a function of time during the period, or

$$u_j = u_j(t), \qquad j = 1,2,\ldots, r \tag{3.2}$$

If the initial values of the state variables are known, a solution to Equations (3.1) can be uniquely determined.

The following consideration of the Pontryagin Maximum Principle is taken principally from the published work of L. S. Pontryagin et al. (49) in order that the approach to the solution of the problem be clear.

Consider the functional:

$$J = \int_0^{\tau} f_0(x_1,\ldots,x_n ; u_1,\ldots,u_r)dt \tag{3.3}$$

where $f_0(x_1,\ldots, x_n; u_1,\ldots, u_r)$ is a specified function. For any set of control policies U(t), specified over the interval $0 \leq t \leq \tau$, the value of J is uniquely determined. If there exist various sets of control functions, U(t), which transfer the controlled system from the initial state, X(0), to the final state, $X(\tau)$, then the object is to find that control set, U(t), which transfers the system from the initial

to final states and at the same time minimizes the value of the functional J.

It is now necessary to define a new state variable, x_0, which obeys the relation

$$\frac{dx_0}{dt} = f_0(x_1,\ldots,x_n ; u_1,\ldots,u_r) \tag{3.4}$$

in which f_0 is the same function which appeared in Equation (3.3). Integration of Equation (3.4) between t_0 and t yields x_0 in the following form:

$$x_0(t) = \int_{t_0}^{t} f_0(X(t^*) , U(t^*))dt^* \tag{3.5}$$

Setting $t_0 = 0$ and $t = \tau$ we obtain:

$$x_0(\tau) = \int_0^{\tau} f_0(X(t) , U(t))dt = J \tag{3.6}$$

In other words the optimal control policy is one which transfers the controlled system from the initial state to the final state in such a manner that the new state variable, x_0, is minimized.

In addition to the system of differential equations in the state and control variables, it is necessary to introduce a set of adjoint variables ($\psi_0,\psi_1,\ldots,\psi_n$) defined by

$$\frac{d\psi_i}{dt} = -\sum_{k=0}^{n} \frac{\partial f_k(X,U)}{\partial x_i} \psi_k \qquad i = 0,1,\ldots,n \qquad (3.7)$$

Equations (3.7) are a system of linear, homogeneous, differential equations, which for any given set of initial conditions, admits a unique solution, $\Psi = (\psi_0,\ldots, \psi_n)$. One additional quantity, known as the Hamiltonian of the system, is defined as:

$$\mathcal{H}(\Psi,X,U) = \sum_{k=0}^{n} \psi_k f_k(X,U) \qquad (3.8)$$

As a result of this definition, the original system of equations in the state variables and the system of equations in the adjoint variables can be rewritten as:

$$\frac{dx_i}{dt} = \frac{\partial \mathcal{H}}{\partial \psi_i} \qquad i = 0,1,\ldots,n \qquad (3.9)$$

$$\frac{d\psi_i}{dt} = -\frac{\partial \mathcal{H}}{\partial x_i} \qquad i = 0,1,\ldots,n \qquad (3.10)$$

The following definition is also necessary in order to develop the Maximum Principle:

$$\xi(\Psi,X) = \max \left|\mathcal{H}(\Psi,X,U)\right| \qquad (3.11)$$

That is, for fixed values of the elements of Ψ and X, ξ is the absolute value of the maximum of the Hamiltonian. The Pontryagin Maximum Prin-

ciple, then, which is a necessary but not sufficient condition for optimality, can be stated in the following theorem:

THEOREM 1. If $U(t)$, $0 \leq t \leq \tau$, is an admissible control vector such that the corresponding trajectory $X(t)$ begins at some point $X(0)$ at time $t = 0$ and passes through $X(\tau)$ at time $t = \tau$, then in order for the trajectory to be optimal, there must exist a non-zero, continuous vector function, $\Psi(t) = (\psi_0(t),\ldots, \psi_n(t))$, such that

I. for every t in the range $0 \leq t \leq \tau$ the Hamiltonian, $\mathcal{H}(\Psi,X,U)$, attains its maximum value at $U = U(t)$:

$$\mathcal{H}(\Psi,X,U) = \xi(\Psi,X) \tag{3.12}$$

II. at the final time, τ, the following equations must be satisfied:

$$\psi_0(\tau) \leq 0 \tag{3.13}$$

$$\xi(\Psi(\tau), X(\tau)) = 0 \tag{3.14}$$

In addition if $\Psi(t)$, $X(t)$ and $U(t)$ satisfy Equations (3.9) and (3.10), and condition I, then the functions $\Psi_0(t)$ and $\xi(\Psi(t), X(t))$ are constant. Therefore, Equations (3.13) and (3.14) are true for time $0 \leq t \leq \tau$.

CHAPTER IV

APPLICATION OF THE PONTRYAGIN MAXIMUM PRINCIPLE TO PARALLEL REACTIONS OCCURING IN A CSTR

The kinetics of parallel reactions occuring in a CSTR have been widely studied for conventional steady-state operation (39); however, studies of periodic reactor operation have been limited to theoretical analyses of systems of the type $2A \rightarrow B$, $A \rightarrow C$ or single reaction such as $2A \rightarrow B$. This is primarily due to the fact that some non-linearity in the system is thought to be necessary in order to obtain improvement via periodic operation. An experimental study of an oscillating reactor performed by Baccaro et al. (6) and theoretical studies of polymerization reactors performed by Laurence and Vasudevan (38) and Ray (50) all utilized a non-linearity in the reaction order, i.e. the reactions were at least second-order with respect to one of the reacting species. In these studies, the initial concentration of a reactant or chain initiator was varied sinusoidally in order to obtain periodic operation; however, no attempt to compare the results with conventional-steady-state operation was made.

A second non-linearity, which exists in all reaction systems, irrespective of their order, is the exponential temperature dependence of the reaction rate constant. Lin (32) has taken advantage of this non-linearity in a theoretical study to show that increases in product yield above the conventional-steady-state yield could be obtained by the periodic variation of the heat flux to or from the reactor. This

causes the temperature of the reactor to also vary periodically; and due to the exponential dependence of the rate constant on temperature, the non-linearity is utilized to its fullest advantage. Schrodt (56,57) explains the improved operation as the result of a driving force which changes with time, and whose time average value over one cycle is higher than the comparable steady-state driving force. It would appear, then, that in order to take advantage of the temperature non-linearity, it would not be necessary to have the non-linearity in the reaction order; and since reactions of the type $2A \rightarrow B$, $A \rightarrow C$ are not very common, consideration will be given primarily to reactions of the form $A+B \rightarrow C+D$, $A+E \rightarrow F+G$ which are first order with respect to each of the species reacting in both reactions (reactant A).

Parallel Reactions of the Form $2A \rightarrow B$, $A \rightarrow C$

It is difficult to think of a pair of reactions which is represented by this system of equations; however, it might conceivably describe a second order dimerization of some material accompanied by a pseudo-first-order hydrolysis or thermal decomposition.

Now consider the case of the two reactions shown below

$$2A \xrightarrow{k_1} B \tag{4.1}$$

$$A \xrightarrow{k_2} C \tag{4.2}$$

where reaction (4.1) is second-order and reaction (4.2) is first-order and the rate constants can be described by the Arrhenius relationship:

$$k_i = k_{i0} e^{-E_i/RT} \tag{4.3}$$

In this case it will be assumed that reaction (4.1) is desirable and reaction (4.2) is undesirable. Therefore, only the optimization of product B will be considered. If these reactions occur in a CSTR similar to the one shown in Figure 1, the dynamic material and energy balances for species A and B are given by Equations (4.4)-(4.6).

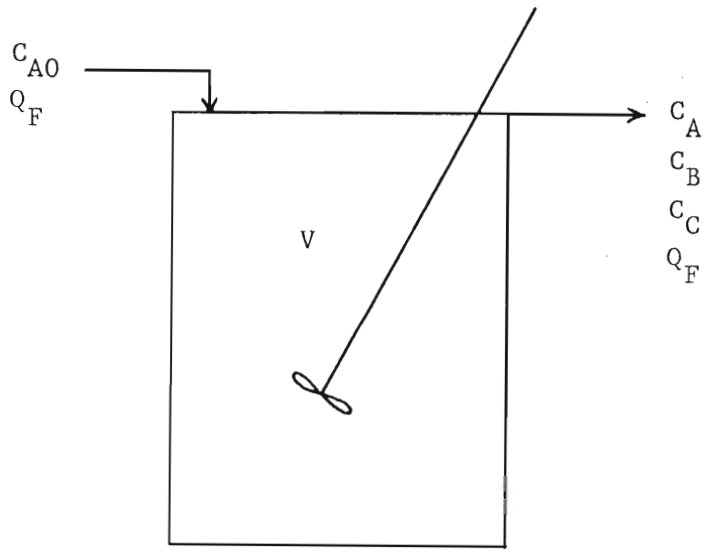

Figure 1. Diagram of a CSTR

$$\frac{dC_A}{dt'} = -k_{10}e^{-E_1/RT}C_A^2 - k_{20}e^{-E_2/RT}C_A + Q_F(C_{A0} - C_A)/V \qquad (4.4)$$

$$\frac{dC_B}{dt'} = k_{10}e^{-E_1/RT}C_A^2 - Q_F C_B/V \qquad (4.5)$$

$$\frac{dT}{dt'} = q/1000\rho_\ell C_p V + Q_F(T_0 - T)/V \qquad (4.6)$$

These equations can be simplified by the introduction of the following dimensionless quantities:

$$x_1 = C_A/C_{A0} \qquad (4.7)$$

$$x_2 = C_B/C_{A0} \qquad (4.8)$$

$$x_3 = RT/E_1 \qquad (4.9)$$

$$t = t'Q_F/V \qquad (4.10)$$

$$\rho = E_2/E_1 \qquad (4.11)$$

$$a_1 = Vk_{10}C_{A0}/Q_F \qquad (4.12)$$

$$a_2 = Vk_{20}/Q_F \qquad (4.13)$$

$$y = RT_0/E_1 + qR/1000\rho_\ell C_p E_1 Q_F \qquad (4.14)$$

where x_1, x_2 and x_3 are the state variables and y is the single control variable of the system. Substitution of these quantities into Equations

(4.4)-(4.6) yields Equations (4.15)-(4.17) which are in state variable form.

$$\frac{dx_1}{dt} = - a_1 x_1^2 e^{-1/x_3} - a_2 x_1 e^{-\rho/x_3} - x_1 + 1 = f_1 \qquad (4.15)$$

$$\frac{dx_2}{dt} = a_1 x_1^2 e^{-1/x_3} - x_2 = f_2 \qquad (4.16)$$

$$\frac{dx_3}{dt} = y - x_3 = f_3 \qquad (4.17)$$

Because of the definition of the constants a_1 and a_2 (as well as that of the dimensionless time t), the reactor volume, flow rate and initial concentration of reactant are constrained to remain constant. Therefore, the physical quantity which is being varied in order to change the value of the control variable (y) is the heat flux (q) to or from the reactor. The optimal control policy for this system can be found in several ways; the methods discussed in this work will consist of (1) the Pontryagin Maximum Principle and (2) a numerical solution.

Optimization by the Pontryagin Maximum Principle

As stated in Chapter III, in order to use the Pontryagin Maximum Principle, it is necessary to define a set of adjoint variables, $\psi(x,y,t)$. From the definitions of Chapter III, (Equation (3.7)), the adjoint variables are given by Equations (4.18)-(4.20).

$$\frac{d\psi_1}{dt} = \left\{2a_1x_1e^{-1/x_3} + a_2e^{-\rho/x_3} + 1\right\}\psi_1 + \left\{-2a_1x_1e^{-1/x_3}\right\}\psi_2 \qquad (4.18)$$

$$\frac{d\psi_2}{dt} = \psi_2 - 1 \qquad (4.19)$$

$$\frac{d\psi_3}{dt} = \left\{a_1x_1^2e^{-1/x_3} + a_2x_1\rho e^{-\rho/x_3}\right\}x_3^{-2}\psi_1 \qquad (4.20)$$

$$+ \left\{-a_1x_1^2e^{-1/x_3}\right\}x_3^{-2}\psi_2 + \psi_3$$

In conventional steady-state operation, the state and adjoint variables would approach some constant value and would then be time invariant. This is not true in periodic operation. The state and adjoint variables are a function of time and vary over the period (or cycle). It is therefore necessary to introduce the concept of time-averaged values into the discussion of this reaction system. The time-averaged value of a state variable will be denoted by a bar over the variable and is defined as:

$$\bar{x} = \frac{1}{\tau}\int_0^\tau x\,dt \qquad (4.21)$$

Since the control variable will also vary with time, a similar definition is made for it:

$$\bar{y} = \frac{1}{\tau}\int_0^\tau y\,dt \qquad (4.22)$$

In analogy with conventional-steady-state operation, it is the time-averaged values of the state variables which approach constant or pseudo-steady-state values as time progresses.

One last definition, then, is that of the objective function for this system. Letting species B (state variable x_2) be the desired product, then the objective function M is defined as:

$$M = \frac{1}{\tau} \int_0^{\tau} x_2 dt \tag{4.23}$$

This objective function corresponds to the objective function J in Chapter III except that it is now our desire to maximize M where J was minimized previously.

Prior to the solution of this system, the importance of a value for the constant ρ will be discussed. There are several constraints which must be met by equations (4.15)-(4.17) in conventional steady-state operation in order to assure an optimum steady-state. The first is:

$$\frac{dx_2}{dy} = 0 \tag{4.24}$$

and the second is

$$\sum_{i=1}^{3} \psi_i \frac{\partial^2 f_i}{\partial y^2} \leq 0 \tag{4.25}$$

Implicit differentiation of Equations (4.15)-(4.17) and re-arrangement yields the following equation for condition (4.24):

$$y_{opt} = \rho/\ell n[a_2(2\rho - 1)] \tag{4.26}$$

which restricts ρ to be greater than 0.5. In addition, Lin (32) has shown that condition (4.25) restricts ρ to be less than one in order for the stationary point to be a maximum. Reviewing the constraints we see that

$$0.5 < \rho < 1 \tag{4.27}$$

Therefore, for a value of ρ within these limits, there exists a stationary point for x_2 which is a maximum. It can also be shown, that for ρ within these limits, the value of the redundant state variable x_4 (C_C/C_{AO}) does not have a stationary point but increases monotonically with y.

Since Lin (32) has also shown that the optimal control policy was "bang-bang" operation (see Figure 2), this mode of variation of the control variable will be used throughout this thesis as the optimal control policy without further proof. As a check, the square wave variation was compared to triangular wave variation and found to be superior with respect to improvement of the desired product yield.

Prior to the use of the Maximum Principle, it is necessary to place some bounds on the control variable y. The lower bound will be fixed by the temperature of the incoming reactant stream (for heat flux into the reactor) or by the incoming temperature and the rate of cooling (for heat flux out of the reactor). Limitations on heat trans-

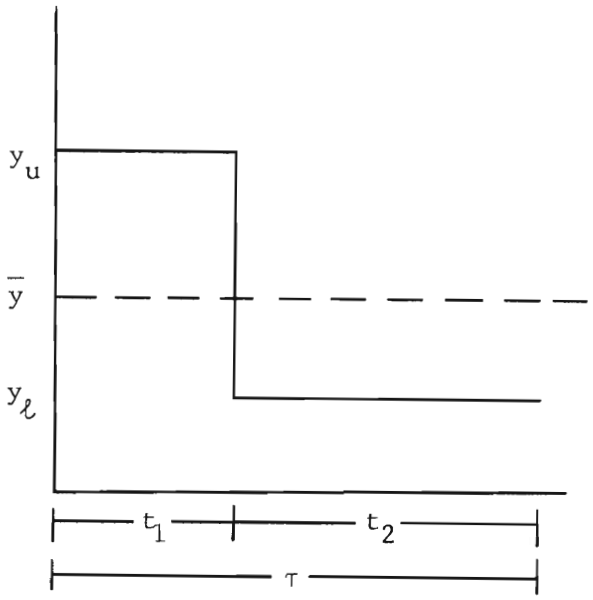

Figure 2. "Bang-Bang" Variation of Control Variable

fer rates, boiling points and other physical quantities will set a limit on the upper bound.

The optimal control policy can then be determined by integration of Equations (4.15)-(4.20) subject to the boundary conditions:

$$x_i(0) = x_i(\tau) \qquad i = 1,2,3 \tag{4.28}$$

$$\psi_i(0) = \psi_i(\tau) \qquad i = 1,2,3 \tag{4.29}$$

These boundary conditions apply specifically to periodic operation of a CSTR. The optimization procedure is carried out by guessing values for the state and adjoint variables and for t_1 and t_2 (see Figure 2). The system of Equations (4.15)-(4.20) is then integrated over one

period (or cycle). If boundary conditions (4.28)-(4.29) are obeyed, then the system is at its pseudo-steady-state condition for the control policy selected. If they are not obeyed, the initial values of the state and adjoint variables are then adjusted based on the difference between the initial and final values of both the state and adjoint variables during the first trial. The system of equations is integrated again using the new initial values and the process is repeated until the pseudo-steady-state is reached (boundary conditions (4.28) and (4.29) are met). Since the values of x_2 are now known as a function to time, it is possible to calculate the value of the objective function from Equation (4.23). In addition, since the values of t_1 and t_2 chosen were not necessarily the optimal values, Lin (32) showed that the value of the objective function could possibly be increased by selection of new values of t_1 and t_2 from Equations (4.30) and (4.31):

$$t_1^* = t_1 + \epsilon \frac{\partial M}{\partial t_1} \tag{4.30}$$

$$t_2^* = t_2 + \epsilon \frac{\partial M}{\partial t_2} \tag{4.31}$$

where

$$\frac{\partial M}{\partial t_1} = \frac{1}{\tau} \left\{ x_2 + \sum_{i=1}^{3} \psi_i f_i - M \right\}_{0 \le t \le t_1} \tag{4.32}$$

$$\frac{\partial M}{\partial t_2} = \frac{1}{\tau}\left\{x_2 + \sum_{i=1}^{3} \psi_i f_i - M\right\}_{t_1 \le t \le \tau} \qquad (4.33)$$

and ϵ is some small quantity. Using the new values of t_1 and t_2, a new pseudo-steady-state is obtained as previously described. This procedure is repeated until no further increase in M is achieved by varying t_1 and t_2. This is the optimum pseudo-steady-state. The final values of t_1 and t_2 along with the upper and lower bounds on the control variable fully describe the optimal control policy as determined by the Pontryagin Maximum Principle. By using this technique in a computer-aided study, Lin (32) suggested that increases in the yield of product B (state variable x_2) of the order of 5%-10% could be obtained (at the expense of product C) by periodic operation of this type; however, no experimental work was performed in support of these results.

Numerical Solution

The numerical integration technique used in finding the optimum pseudo-steady-state for this system of parallel reactions (Equations (4.1) and (4.2) is performed without the usage of the Pontryagin Maximum Principle and, as a result, is somewhat easier to use. The reason for its use will become apparent later.

In the conventional steady-state operation of this system of reactions in a CSTR, the value of the control variable y remains constant. Thus for each value of y there is a corresponding value of x_2. The continuous curve drawn through this locus of points (see bottom

curve of Figure 3) exhibits a maximum (for $0.5<\rho<1$) which is the optimum steady-state for conventional operation. No further increase in x_2 can be achieved by the simple variation of the parameter y to a new steady-state value. Periodic operation yields the family of curves above the steady-state curve. Since the control variable is constant at either the upper or lower bound during the entire period, Equation (4.22) then reduces to:

$$\bar{y} = (t_1 y_u + t_2 y_\ell)/\tau \tag{4.34}$$

where t_1 is the length of time (dimensionless) during which the control variable is at the upper limit and t_2 is the time during which it is at the lower limit. If we define $\phi = t_2/\tau$ (or the fraction of the period during which the control variable is at its lower limit), then fixing values of $\tau, \phi, \bar{y}$ and y_ℓ determines the value of y_u by Equation (4.35), which is obtained from Equation (4.34):

$$y_u = (\bar{y} - \phi\, y_\ell)/(1 - \phi) \tag{4.35}$$

The family of curves for periodic operation are a function then of ϕ at a given, constant value of y_ℓ. As can be seen from Figure 3, the value of $\bar{x}_2$ increase as ϕ increases for a given value of $\bar{y}$. The physical reason for this is that as ϕ becomes larger (and approaches 1.0), the upper limit, y_u, is getting very large in order to maintain a constant value of $\bar{y}$. Figure 4 (which is a plot of k_2 vs k_1 for a value of ρ less than one) will help elucidate the effect of an increase in y_u.

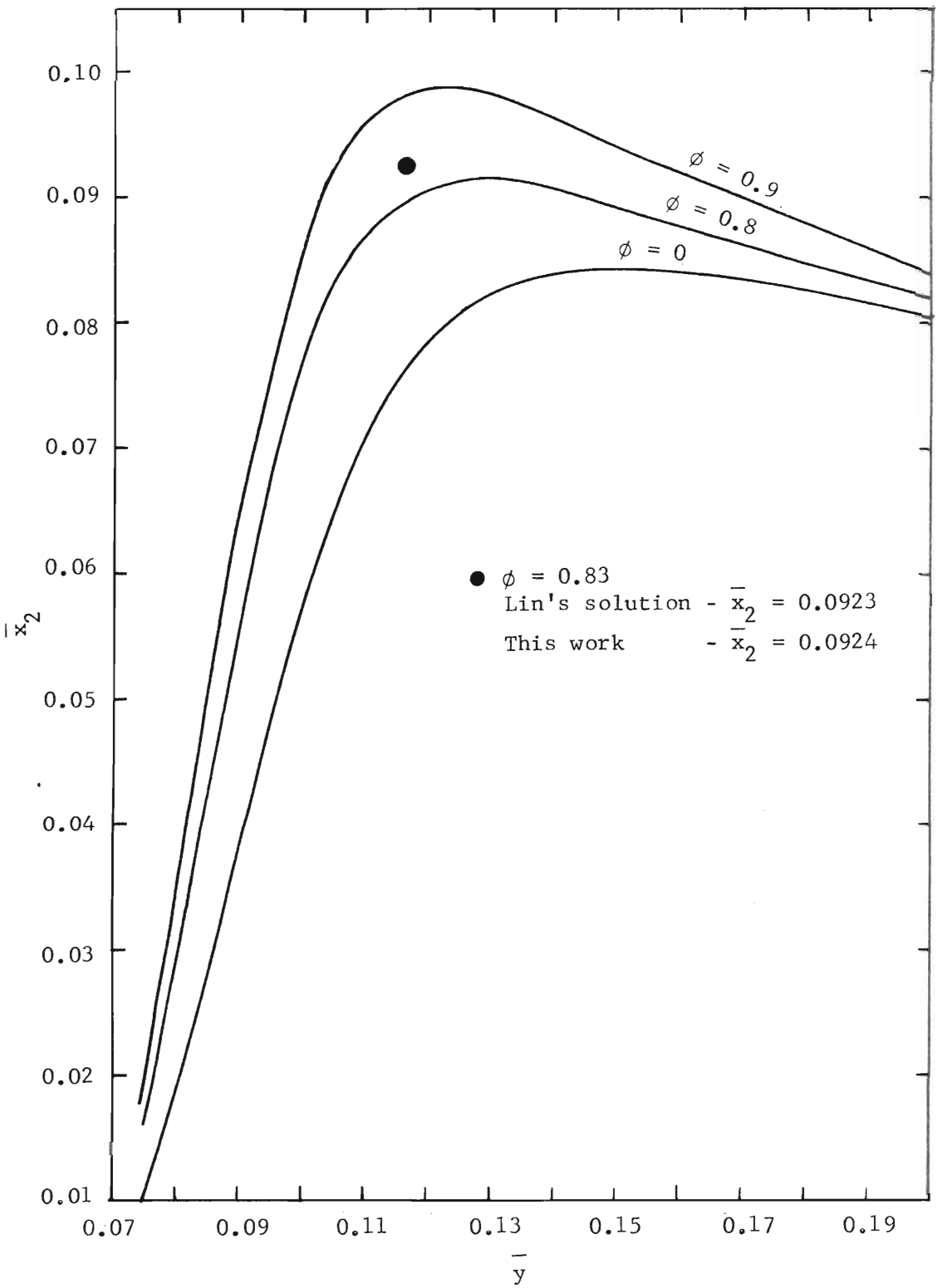

Figure 3. Dimensionless Concentration as a Function of the Time-Averaged Control Variable

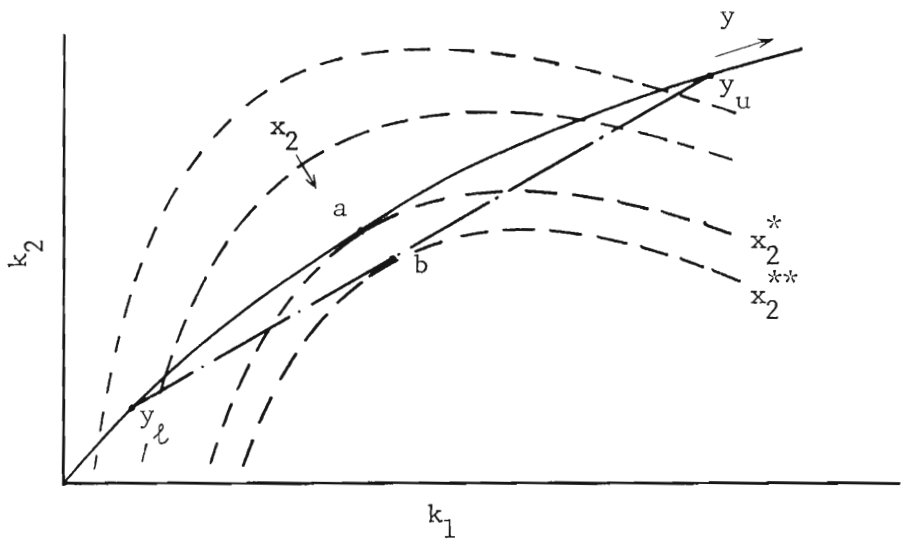

Figure 4. Plot of k_2 versus k_1 for $\rho<1$

The solid curved line is the locus of values of k_1 and k_2 as a function of temperature. The direction of increasing y is shown above the curve. The dotted curves are obtained by solving equations (4.15)-(4.17) for k_2 in terms of k_1 and x_2 and represent curves of constant x_2. The arrow indicates increasing values of x_2. The optimum conventional-steady-state is located at a value of x_2 whose dotted curve is tangent to the solid curve (point a) since only points on the solid curve are physically attainable. The very fast switching from a high value of the control variable (y_u) to a low value (y_ℓ) prevents the system from following its normal path down the solid curve and the dashed line joining points y_ℓ and y_u shows the pseudo-steady-state that results. As can be seen, the dotted line (x_2^{**}) which is tangent to the pseudo-steady-state line at point b represents a higher value of

x_2 than the optimum conventional-steady-state. Also the higher the value of y_u, the larger the value of x_2 attained.

In order to compare periodic operation with conventional-steady-state operation, one should make the comparison for the same value of $\bar{y}$. As can be seen from Figure 3, the optimum conventional-steady-state occurs at $\bar{y} = 0.149$ and $\bar{x}_2 = 0.0846$. The remaining curves represent periodic operation with a value of $y_\ell = 0.049$, and converge to the conventional-steady-state curve at this value of $\bar{y}$. This is reasonable, since a value of $\bar{y}$ below the lower limit has no physical meaning. As the lower limit is increased, the family of periodic curves is shifted to the right and always converges to the value of the lower limit on the conventional-steady-state curve. In comparison, periodic operation at a value of $\phi = 0.9$ and $\bar{y} = 0.149$ yields $\bar{x}_2 = 0.0940$ which represents a 11.1% increase in yield above the optimum conventional-steady-state value. It should be noted, however, that physical constraints on the upper limit of the control variable might preclude actual increases of this magnitude.

Since no experimental work has been done in this area, a chemical reaction system of the form $A + B \rightarrow C + D$, $A + E \rightarrow F + G$ was selected and operated periodically in order to compare actual pseudo-steady-state values with those predicted by the numerical solution. The equations for this system are slightly different and are given in the next section.

Parallel Reactions of the Form A+B → C+D, A+E → F+G

Since most of the theory discussed in the previous section also

applies to the system of reactions shown below, only the pertinent differences will be discussed.

The system examined in the present work is described by Equations (4.36) and (4.37):

$$A + B \xrightarrow{k_1} C + D \tag{4.36}$$

$$A + E \xrightarrow{k_2} F + G \tag{4.37}$$

Where reaction (4.36) is second-order overall and reaction (4.37) is configured to be pseudo-first-order with respect to A. The energy and material balances around a CSTR in which these reactions are occurring are given by Equations (4.38)-(4.40):

$$\frac{dC_A}{dt'} = - k_1 C_A C_B - k_2 C_A C_E + Q_F(C_{A0} - C_A)/V \tag{4.38}$$

$$\frac{dC_F}{dt'} = k_2 C_A C_E - Q_F C_F/V \tag{4.39}$$

$$\frac{dT}{dt'} = q/1000\rho_\ell C_p V + Q_F(T_0 - T)/V - \frac{U_0 A_0 (T - T_a)}{(1000) C_p \rho_\ell V} \tag{4.40}$$

Again, these equations can be simplified by the introduction of the following dimensionless state and control variables, and the stoichiometric relationships: $C_B = C_{B0} - C_C$ and $C_F = C_{A0} - C_A - C_C$:

$$x_1 = C_A/C_{A0} \tag{4.41}$$

$$x_3 = RT/E_1 \tag{4.42}$$

$$x_4 = C_F/C_{A0} \tag{4.43}$$

$$t = t'Q_F/V \tag{4.44}$$

$$\rho = E_2/E_1 \tag{4.45}$$

$$a_1 = Vk_{10}C_{A0}/Q_F \tag{4.46}$$

$$a_2 = Vk_{20}C_{A0}/Q_F \tag{4.47}$$

$$C_1 = U_0A_0/(1000C_p\rho_\ell Q_F) \tag{4.48}$$

$$C_2 = RT_a/E_1 \tag{4.49}$$

$$y = RT_0/E_1 + qR/1000\rho_\ell C_p E_1 Q_F \tag{4.50}$$

$$r_1 = C_{B0}/C_{A0} \tag{4.51}$$

$$r_2 = C_{E0}/C_{A0} \tag{4.52}$$

Rearrangement and substitution of these quantities into Equations (4.38)-(4.40) yields the system of equations in state-variable form as shown:

$$\frac{dx_1}{dt} = 1 - x_1 - a_1x_1(r_1 - 1 + x_1 + x_4)e^{-1/x_3} - a_2x_1(r_2 - x_4)e^{-\rho/x_3} \tag{4.53}$$

$$\frac{dx_2}{dt} = a_2 x_1 (r_2 - x_4) e^{-\rho/x_3} - x_4 \tag{4.54}$$

$$\frac{dx_3}{dt} = y - (1 + C_1)x_3 + C_1 C_2 \tag{4.55}$$

This system of equations can then be utilized to obtain optimum pseudo-steady-states by either (1) the Pontryagin Maximum Principle or (2) the numerical methods presented in the preceding section.

Optimization by the Pontryagin Maximum Principle

There is a unique difference between this system of reactions and the system presented previously. In the earlier system, it could be shown that the yield of the reaction which had the higher activation energy exhibited a maximum (or optimum value for the state variable x_2 when ρ was within the specified range). In addition, the yield of the reaction with the lower activation energy (the first-order reaction) increased monotonically with y. Analysis by construction of a figure similar to Figure 4 for product C in Equation (4.2) showed that its yield would only be decreased by periodic operation. It appeared then, that periodic switching of the heat flux to or from the reactor would aid the reaction with the highest activation energy. Implicit differentiation of Equations (4.53)-(4.55) resulted in the following conditions for $\frac{dx_2}{dy} = 0$:

$$y_{opt} = \rho / \ell n[a_2(\rho - 1)] \tag{4.56}$$

which differs from Equation (4.26) in that it contains the term ρ, and not 2ρ. This difference results from the fact that, although reaction (4.36) is second-order overall, it is only first-order with respect to the species reacting in both reactions (A). Equation (4.56) thus has meaning only for:

$$\rho > 1 \tag{4.57}$$

The system of reactions chosen for experimental work obeyed Equation (4.57), and therefore the state variable x_2 (C_C/C_{A0}) will have a maximum, and the state variable x_4 will increase monotonically with y. Intuition would still lead us to believe that it is x_4 (the product of the reaction with the higher activation energy) that could be improved by cycling; but in this case, the possibility of bettering the optimum steady-state, which would then be a local optimum rather than a global optimum, would be in doubt. Construction of a diagram similar to Figure 4 for this system of reactions ($\rho > 1$) yielded Figure 5. As can be seen from this figure, the system has no optimum (no dotted line tangent to the solid line), but periodic operation should result in higher yields of x_4 (at the expense of x_2).

Therefore, the Maximum Principle was applied to this system of reactions in an effort to optimize the value of x_4. Rather than determining the optimal values of t_1 and t_2, the Maximum Principle predicted the optimal control to be steady-state control at the upper limit. This occurred as a result of the absence of a global optimum

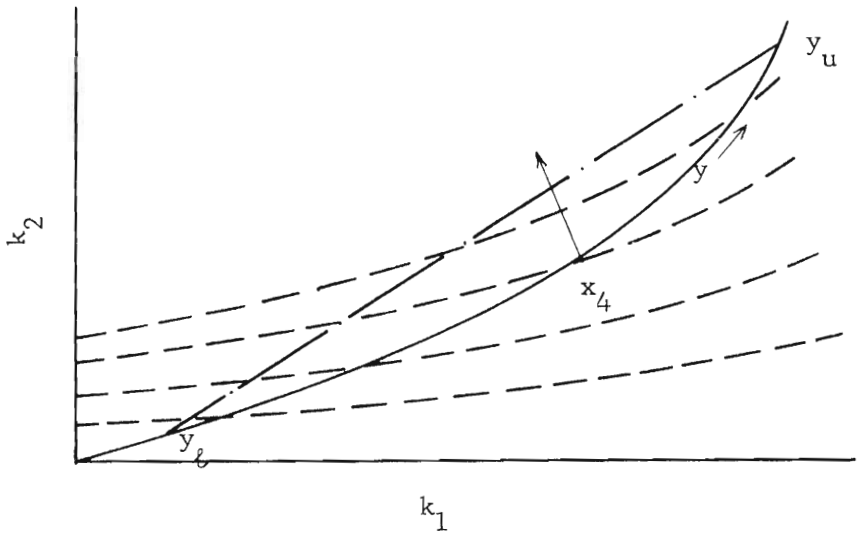

Figure 5. Plot of k_2 versus k_1 for $\rho>1$

between the two limits y_u and y_ℓ. Thus the procedure using the Maximum Principle was not effective in the absence of a global optimum; and consequently, the numerical technique previously described was used to predict the results of periodic operation.

Numerical Solution

Given a set of reactor conditions (flow rate, reactor volume, etc.), the conventional-steady-state value of x_4 as a function of the control variable y can be determined from Equations (4.53)-(4.55), using a multi-variable search technique such as Newton's Method (18) in three variables. The results are the locus of points forming the bottom curve of Figure 6 (ϕ=0). A plot like this could be constructed for every value of τ; however, for values of τ below approximately 1.0 (length of the cycle corresponds to the residence time), there is no practical difference in the curves for periodic operation. As before,

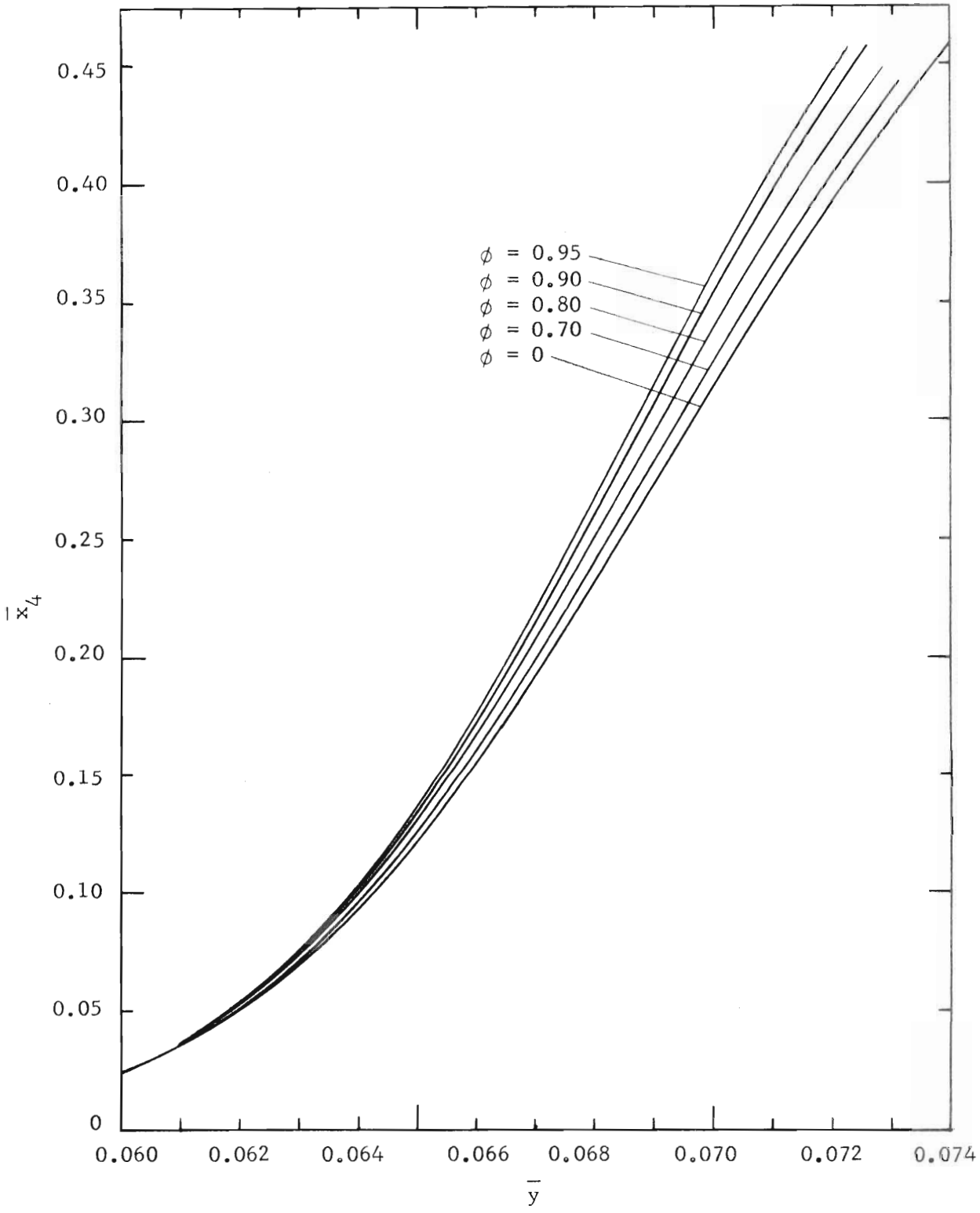

Figure 6. Effect of Periodic Variation of Heat Flux on $\bar{x}_4$

specification of y , $\bar{y}$, τ and ϕ allows construction of the family of curves above the conventional-steady-state curve. Clearly, there results improvement from periodic operation, and it is the purpose of this work to compare the predicted results of periodic reactor operation with experimental data obtained from the periodic operation of a laboratory reactor.

CHAPTER V

EXPERIMENTAL APPARATUS

In order to perform the experimental phase of this work, a continuous-flow, stirred tank reactor system was constructed. Particular effort was expended to keep the system as simple yet as flexible as possible, so that future work could be performed using the same equipment. A diagram of the reactor system is shown in Figure 7; Figures 8 and 9 give other views of the experimental reactor system. As can be seen from Figure 7, the reactants were gravity fed to constant-head flow controllers. These controllers were manual overflow devices which supplied stabilized flows of reactants to an assembly of rotameters. The rotameters were used to monitor the flows of reactants to the reactor through the primary cooling coils. The reactor itself was a simple CSTR with an electrical heating element, thermocouple and an electric stirrer driven by an explosion-proof motor. The reactions were quenched chemically with acid in a stirred-beaker sample collection system. The major components of the reactor system are described in more detail in the following sections.

Reactant Storage Tanks

The reactant storage tanks were three five-gallon polyethylene bottles. Each bottle was equipped with a spigot which was used as the main valve for controlling reactant flow from the storage vessels. The storage tanks containing the ester solutions were vented directly to

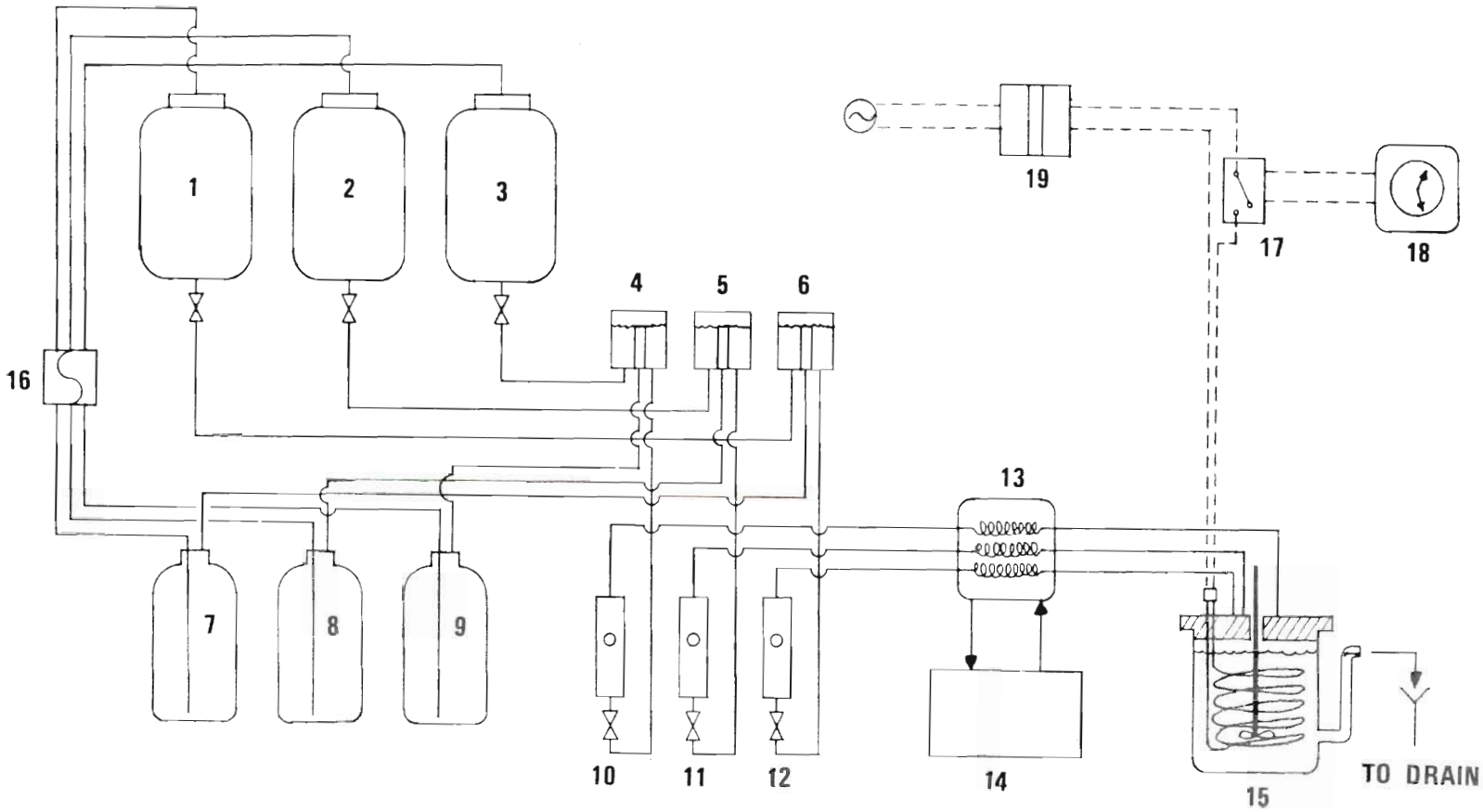

Figure 7. Flow Diagram of Experimental Reactor System

Table 1. Identification of Experimental Apparatus Components

Part No.	Description
1	methyl acetate storage tank
2	sodium hydroxide storage tank
3	ethyl benzoate storage tank
4-6	constant head flow controllers
7-9	reactant overflow tanks
10-12	reactant rotameters
13	reactant (primary) cooling coils
14	constant temperature bath
15	CSTR
16	flexible tubing pump
17	electrical relay
18	cycle timer
19	constant voltage transformer

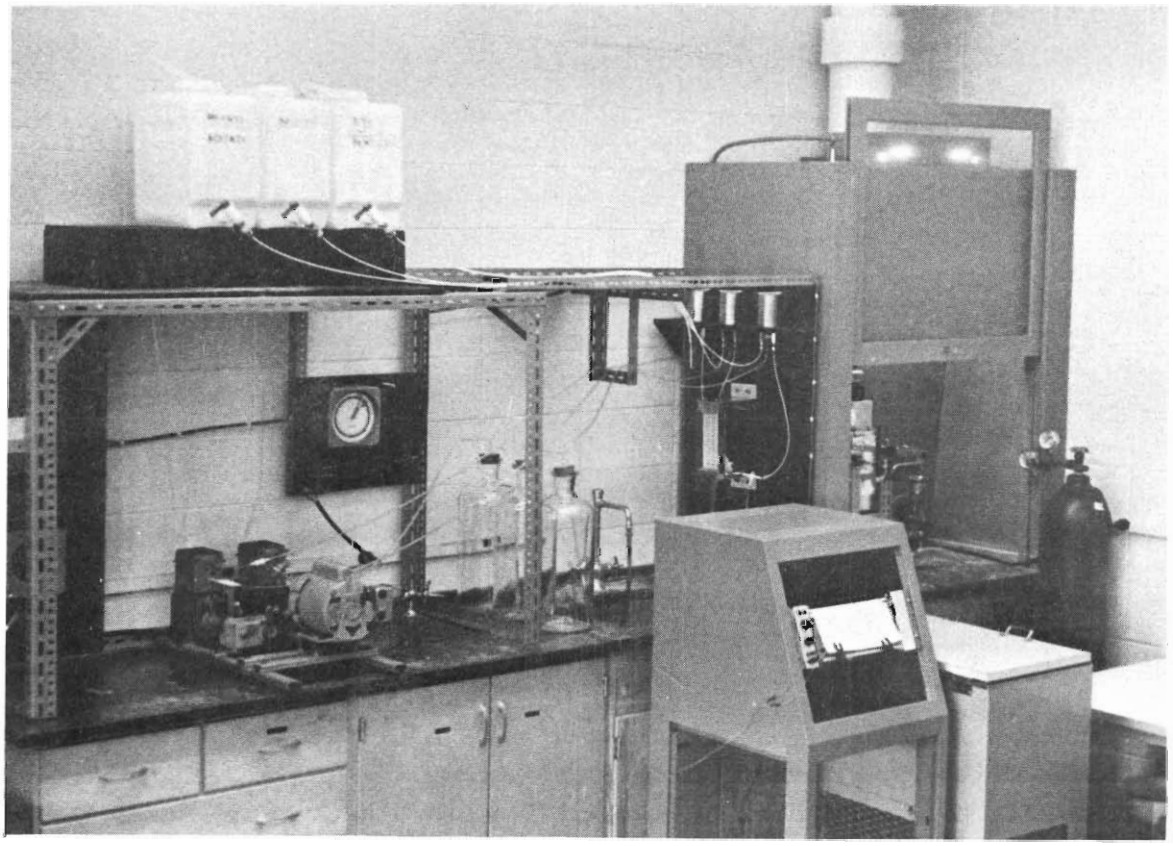

Figure 8. Overall View of the Experimental Reactor System

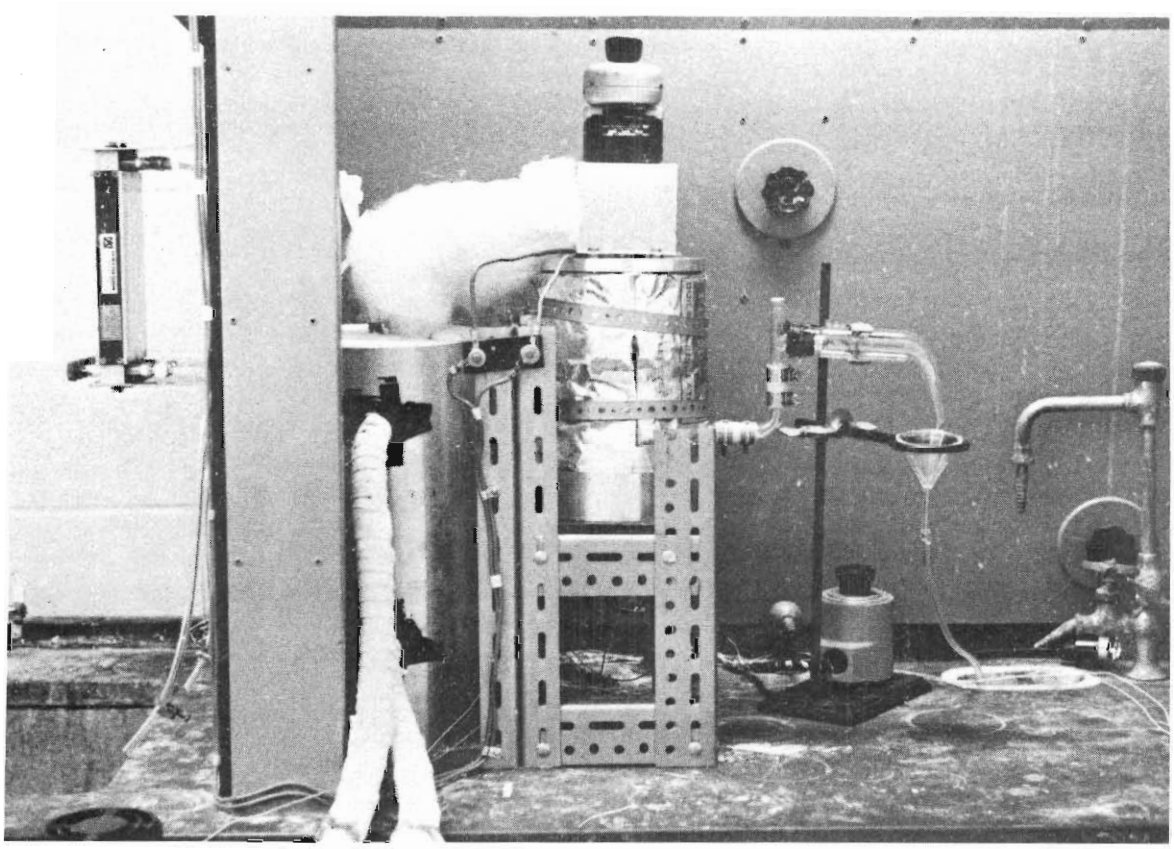

Figure 9. Photograph of Experimental CSTR and Reactant Cooling Unit

the atmosphere, and the tank containing the sodium hydroxide solution was vented through a tube containing "Ascarite" to prevent contamination by CO_2. The reactant storage tanks were located on a high platform, well above all other equipment, so that the reactant solutions could be gravity fed.

Constant Head Flow Controllers

The reactant storage tanks were connected to the constant-head flow controllers with 1/4" O.D. polyethylene tubing. The flow controllers (see Figure 10) used an overflow principle to supply reactant solution to the rotameters, thereby eliminating fluctuations in the flow rate of reactant to the CSTR, which would be caused by a changing liquid level in the reactant storage tanks.

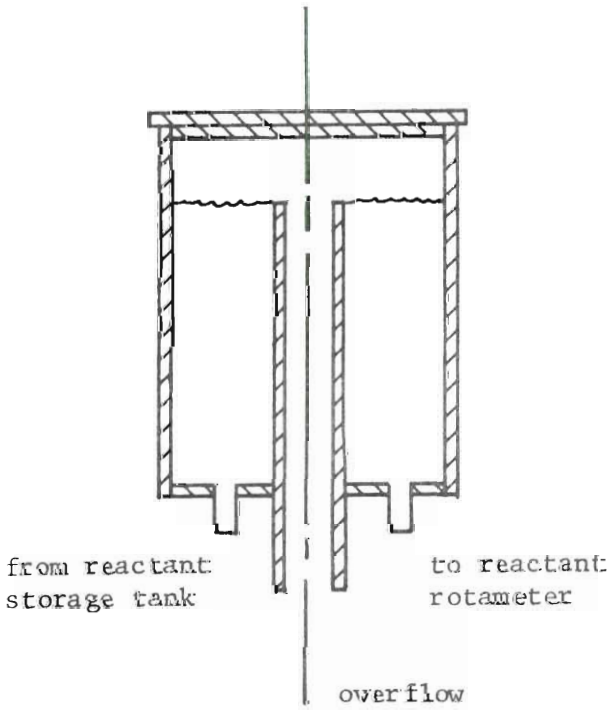

Figure 10. Constant Head Flow Controller

Overflow reactant solution from the center tube flowed by gravity to three 2.5-gallon glass receiving bottles. From there the solutions were returned to the reactant storage tanks by means of a Sigmotor flexible tubing pump driven by a General Electric 1/3 HP motor and equipped with a variable speed reducer.

Rotameters

The rotameters used to control reactant flow rate were mounted in a single unit (Matheson No. 642 PSV) and equipped with 150mm tubes (Matheson No. 603). Needle valves at the entrance to each tube allowed fine adjustments to be made in flow rate. A calibration curve for a 70% aqueous-acetone solution was constructed using an acetone-water mixture only and is presented in Appendix C. The solution used for calibration did not contain ester or sodium hydroxide; because the reactant solutions were relatively dilute, (e.g., <0.60 gmole/ℓ or 0.06 gmole/ℓ), it was assumed that the small amount of reactant present did not affect the flow characteristics. In addition, only one calibration curve was constructed, because the rotameter tubes as received from Matheson were assumed to be identical.

Reactant (Primary) Cooling Coils

Experimentally, the maximum allowable operating temperature of the reactor was the boiling point of the reactant solution, which is lower than that of pure water. To have restricted operation of the reactor from ambient temperature (~25^{o}C) to this upper bound would then have seriously reduced the measurable effects of periodic operation.

Since the series of simulated pseudo-steady-state curves emanated from a given lower limit, it was decided that the reactant streams should be cooled below ambient temperature. The degree of cooling determined the amount of measurable effect and, in order to better observe the effects of periodic reactor operation, the reactant streams were cooled to approximately -10°C. Each of the three reactant streams, after flowing through the rotameter tubes, passed through individual ten foot copper coils in the heat exchanger. A mixture of 50% ethylene glycol and 50% water was pumped through the shell side of the exchanger by a submersible pump located in a constant temperature bath (Model 66595, Precision Scientific Co.) which kept the coolant at -16°C. The holdup volume of the constant temperature bath was fifteen gallons compared to the 1.5 gallon holdup of the heat exchanger. The temperature of each of the reactant streams was monitored by a copper-constantan thermocouple in each of the exit lines of the exchanger. All lines and fittings between the heat exchanger and the reactor were made of polyethylene or nylon and surrounded by glass wool to minimize heat transfer between the lines and the surroundings.

Continuous Flow Stirred Tank Reactor

The CSTR was constructed from a cylindrical glass jar (Pyrex) approximately nine inches high and six inches in diameter. The jar, purchased from Will Scientific Company (Will Catalog, No. D-17156), was modified by adding a 5/8" thick-walled side arm near the bottom of the reactor to facilitate continuous operation. The various component parts of the reactor included: (1) a reactor cover with associated

fittings; (2) thermocouple; (3) heating element interfaced with a cycle timer and other necessary electrical equipment; (4) three blade impeller driven by an explosion proof electric motor; (5) overflow arm to maintain constant reaction volume. The reactor was wrapped with one inch fiberglass insulation to reduce heat loss. A photograph of the reactor is shown in Figure 11, and a more detailed description of the reactor components is given in the following sections.

Reactor Cover

The reactor cover was made of aluminum and was approximately 1 1/2 inches thick. It contained two holes for the electrical leads to the heating element, three holes drilled and tapped with 1/8-27 NPT threads to accommodate 400-1-2-316 Swagelok male connectors (for the incoming reactant lines), and one hole drilled and tapped with 1/8-27 NPT threads to accommodate a fitting (Omega Engineering Catalogue No. BRLK-316) used to fix the reactor thermocouple in place.

Thermocouple

During periodic operation, unlike conventional steady-state operation, the temperature of the reactor contents purposefully varies periodically as a function of time. In order to observe this temperature variation, a copper-constantan thermocouple (Omega Engineering) was installed in the reactor. Copper-constantan was chosen because of its good response in the temperature range of interest (-20^{0}C to 45^{0}C). The thermocouple wire was insulated with a Teflon coating and shielded with a two-hole ceramic insulator. The insulator was contained in a fine gauge stainless steel tube (3/16" O.D.) within the reactor. The thermocouple junction itself was left unshielded for faster response.

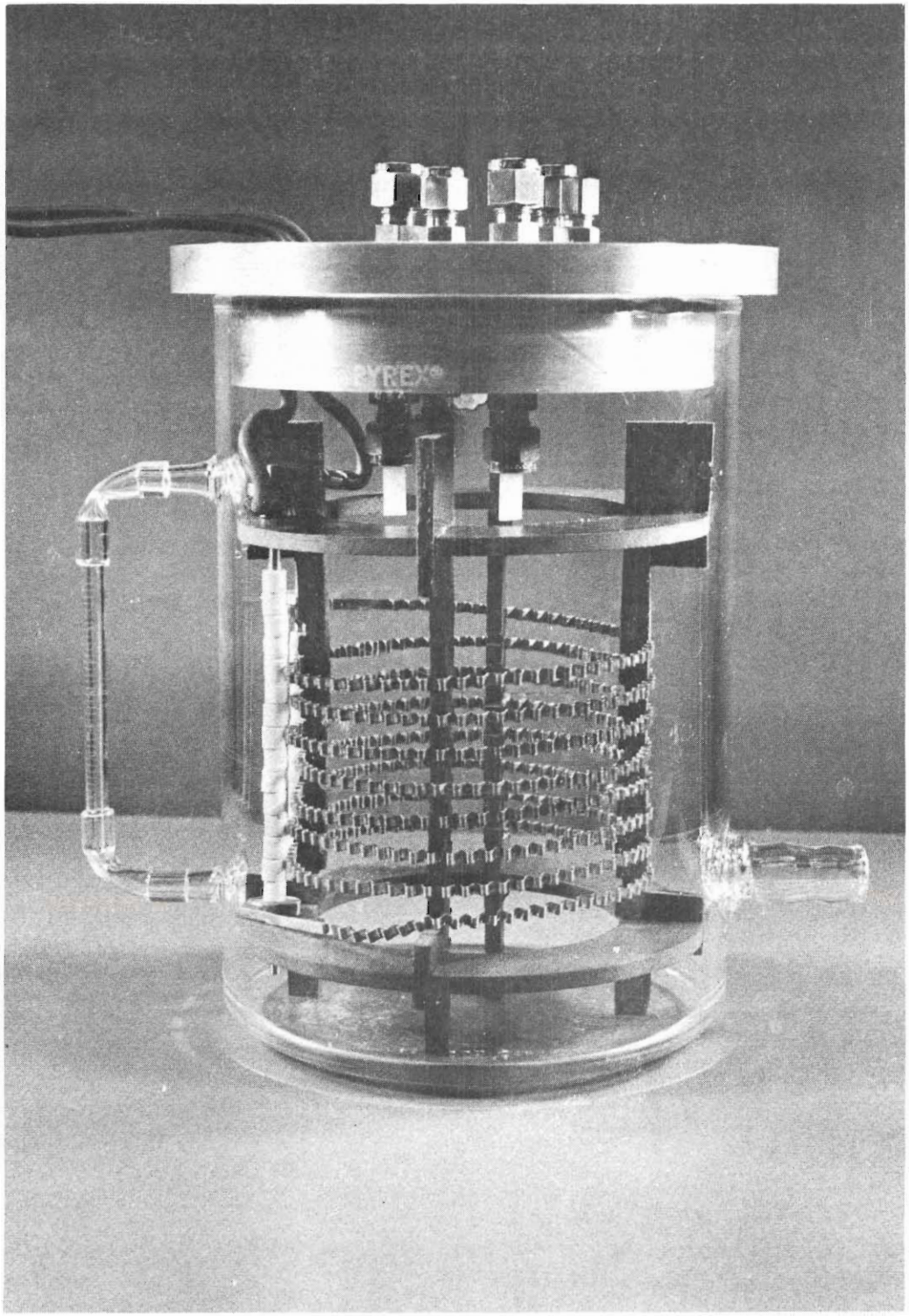

Figure 11. Photograph of Experimental CSTR

The stainless steel tube was mounted on the reactor cover (see Figure 11) as previously described and was capable of traversing the entire height of the reactor to detect the existence of any local temperature gradients. The copper and constantan leads from the thermocuple were connected to a terminal strip immersed in an ice-water bath. Copper leads then joined the terminal strip to a Honeywell Electronik 194 millivolt recorder which had an adjustable millivolt span and was calibrated with a potentiometer. The temperature of the reactor contents was then followed (to the nearest degree) as a function of time, and the attainment of thermal pseudo-steady-state was determined by the temperature profile; that is, when the temperature of the reactor contents was the same at the beginning and the end of a cycle (or period), thermal pseudo-steady-state was assumed to have been established.

Heating Element

Periodic reactor operation (or more specifically, periodic variation of the heat flux to the reactor) was achieved by placing a cyclically actuated heating element in the reactor. The heating element was made of Nichrome metal stripping which was corrugated in order to take up less space. The element was mounted on a non-conductor frame in helical fashion as shown in Figure 12. One eighth inch stainless steel rods were threaded and used as binding posts for the electrical connections. The support frame also served as a baffle system to promote mixing of the reactor contents. The electrical leads from the binding posts were of No. 10 copper wire and were connected to an electrical relay. The relay was activated and deactivated upon demand

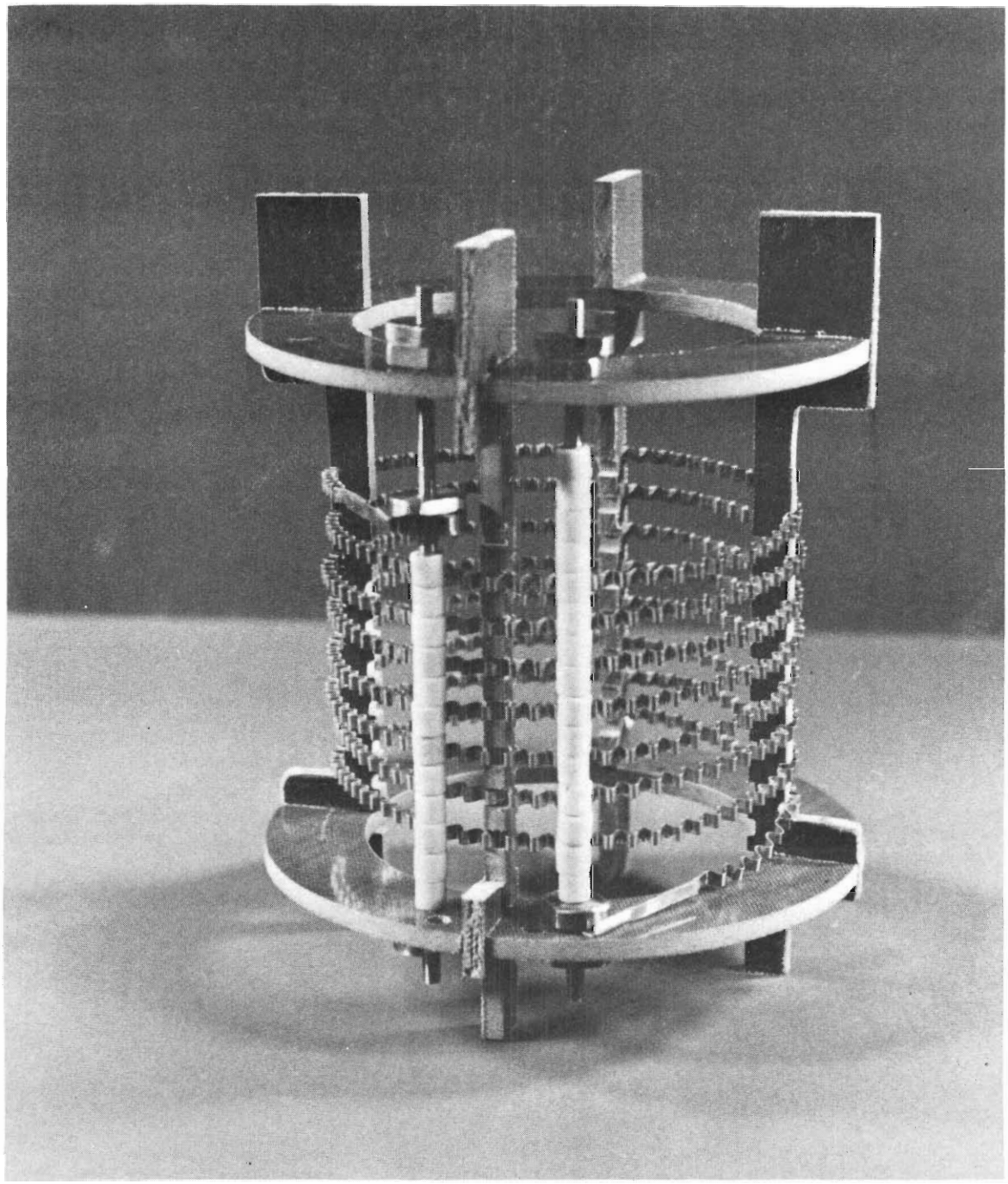

Figure 12. Experimental Heating Element

by an Eagle "Flexopulse" cycle timer(model HG94) which interrupted the flow of current to the heating element for a pre-selected period of time. The period of variation of the heat flux was determined prior to operation of the reactor system, and the amounts of "on time" and "off time" were manually set on the face of the timer. The on-off cycle was then repeated automatically by the timer for as long as desired without further adjustment.

Since the heat flux generated by the heating element was proportional to the power output, it was necessary to have a stable, adjustable power supply. The normal 110-volt power supply in the laboratory was subject to severe fluctuations which could cause errors in the experimental work. Thus, a constant-voltage transformer (2KVA, Sola No. 20-25-220) was installed to insure a constant voltage supply to the heating element. A variable transformer (Powerstat Type 126u) was placed between the constant voltage transformer and the relay so that the voltage could be adjusted to vary the power. Current to the heating element was monitored by a Triplett ammeter (0-30 amperes) and a GE precision ammeter (0-5 amperes). Voltage to the heating element was monitored with a GE precision voltmeter and a Honeywell digital voltmeter.

Electric Stirrer

The reactor contents were mixed with a stainless steel impeller with three blades. The impeller was driven by a variable speed, spark-proof, electric motor. Baffles in the reactor aided in complete mixing and prevented vorticity. A study (see Chapter VIII) was made to deter-

mine the mixing effectiveness of the impeller and the results were compared to an ideal mixing model. The mixing efficiency of the impeller was found to be excellent.

Overflow System

A simple overflow system was installed to maintain a constant volume of liquid in the reactor. The overflow arm (see Figure 9) was adjustable vertically so that the reactor volume could be changed if desired. A sightglass was installed and calibrated to indicate the reactor volume.

Sample System

The reactor effluent could either be diverted to waste containers or to a sample receiver. This latter vessel was a 2000-ml beaker supported on a magnetic stirrer and equipped with a Teflon coated stirring rod. Prior to reactor startup, the beaker, stirrer and a known volume of standard hydrochloric acid solution were weighed. After a sample was taken, the beaker and contents were again weighed. The difference between the initial and final weights was the weight of the sample. The sample, having been chemically quenched, was then allowed to attain room temperature and the volume of sample collected was calculated from the density at room temperature of the mixture (see Chapter VIII) and the sample weight.

Gas Chromatograph

After chemical quenching, the samples were partially analyzed using a Perkin-Elmer Model 810 Gas Chromatograph. The chromatograph contained two one-eighth inch OD, stainless steel columns each six feet

in length packed with Porapak Q. Nitrogen was used as the carrier gas and concentration was measured with a flame ionization detector. More details concerning the operation of the chromatograph are given in Chapter IX and Appendix E.

CHAPTER VI

DETERMINATION OF REACTION RATE CONSTANTS

As stated in previous chapters, the chemical system chosen for experimentation in this work was the simultaneous alkaline hydrolyses of methyl acetate and ethyl benzoate. These two reactions proceed as shown in Equations (6.1) and (6.2).

$$CH_3COOCH_3 + NaOH \xrightarrow{k_1} CH_3COONa + CH_3OH \qquad (6.1)$$

$$C_6H_5COOC_2H_5 + NaOH \xrightarrow{k_2} C_6H_5COONa + C_2H_5OH \qquad (6.2)$$

Both reactions (6.1) and (6.2) are second order overall. For both of these reactions, values for the second-order rate constants were found in the literature (36); but in order to use the numerical values found in the literature with confidence, it was necessary to verify their accuracy. Since one of the reactants (specifically, ethyl benzoate) is only slightly soluble in water, a solvent system composed of an aqueous-acetone solution was used. Further investigation showed that the rate of ester hydrolysis for these two esters varied as a function of the percentage of acetone in the solvent system. Data were available for the hydrolysis of both methyl acetate and ethyl benzoate in a 70% aqueous-acetone solution (which is defined throughout this work to mean 70 ml of acetone made up to 100 ml with distilled water) and it was decided that this composition would be acceptable for experimental

purposes. The detailed, step-by-step, experimental procedure used in determining the reaction rate constants is given in Appendix B, and the following is a summary of the techniques used and results obtained.

Alkaline Hydrolysis of Methyl Acetate

In an attempt to show the steric influence of the alkyl component in the alkaline hydrolysis of acetates and propionates, Jones and Thomas (36) investigated the alkaline hydrolysis of methyl acetate in a 70% aqueous-acetone solvent. It was found that the rate constant for the saponification obeyed the Arrhenius relationship

$$k = k_0 e^{-E/RT} \tag{6.3}$$

satisfactorily and the following constants were determined for methyl acetate: (1) $\log_{10} k_0(\ell/\text{gmole-sec.}) = 5.5$ and (2) $E = 8{,}800$ cal/gmole. The method used in determining these constants was that used by Davies and Evans (19) in a kinetic study of the acid and alkaline hydrolysis of several aliphatic esters and is described generally in the following section.

Rate Measurements

A 0.1N methyl acetate solution was prepared by weighing 0.01 moles of methyl acetate into a weighed, 100-ml volumetric flask. Care had to be observed (due to the volatile nature of the ester) to prevent evaporation during weighing. After the proper amount had been weighed into the flask, 70 ml of acetone and some distilled water were added and the mixture was allowed to sit at room temperature for approximately

one hour in order for the change in volume due to mixing to be complete. After an hour, the flask was filled to the mark with distilled water. The alkaline solution of the same concentration was prepared in a similar manner. The two flasks of ester and alkaline solutions were then placed in a constant temperature bath and allowed to come to the temperature of the bath. Changes in concentration were corrected for by noting the change in volume of the mixture due to temperature; however, since the change in volume due to the temperature change was almost the same for both solutions, their concentrations remained essentially equal. After thermal equilibrium was achieved, 25 ml of alkaline solution were transferred by volumetric pipet to a third volumetric flask (50-ml) also placed in the constant temperature bath. Similarly 25 ml of alkaline solution were transferred by means of a rapid delivery pipet and the stopwatch was started at one-half of the delivery of the sodium hydroxide solution. Samples were taken at various intervals and were pipetted into hydrochloric acid in order to quench the reaction. The time recorded for each sample was that time at which one-half of the sample had run into the quenching solution. The quenched solutions were then back titrated potentiometically with standard NaOH solution to their equivalence point in order to determine the concentration of acid present. The reactions occurring in these steps can be represented as follows:

a) hydrolysis reaction

$$RCOOR' + OH^- \rightarrow RCOO^- + R'OH \qquad (6.4)$$

b) quenching reactions

$$OH^- + H^+ \xrightarrow{\text{fast}} H_2O \qquad (6.5)$$

$$RCOO^- + H^+ \xrightarrow{\text{fast}} RCOOH \qquad (6.6)$$

Since the number of equivalents of hydrochloric acid used in the quenching solution was constrained to be stoichiometrically equal to the combined number of equivalents of sodium hydroxide and sodium acetate (i.e., equal to the original sodium hydroxide concentration times the number of milliliters of sample), then all of the HCl is used up in the quenching reactions and the back-titration yields the concentration of carboxylic acid (C_{CA}) formed in reaction (6.6), which is equal to the concentration of sodium acetate formed in reaction (6.4). Concentration versus time data were obtained this way; and since the reaction was second-order with the initial concentrations of reactants equal, Equation (6.7) was used to calculate the value of the rate constant for each sample. A tabulation of this data is found in Appendix A.

$$k = C_{CA}/[C^o_{NaOH}(C^o_{NaOH} - C_{CA})t] \qquad (6.7)$$

The arithmetic average of the rate constants for the samples was determined and this value was used as the value of the reaction rate constant at the given experimental temperature. The natural logarithms of the rate constants at various temperatures were plotted versus the reciprocal of the absolute temperature (see Figure 13). Data obtained in this

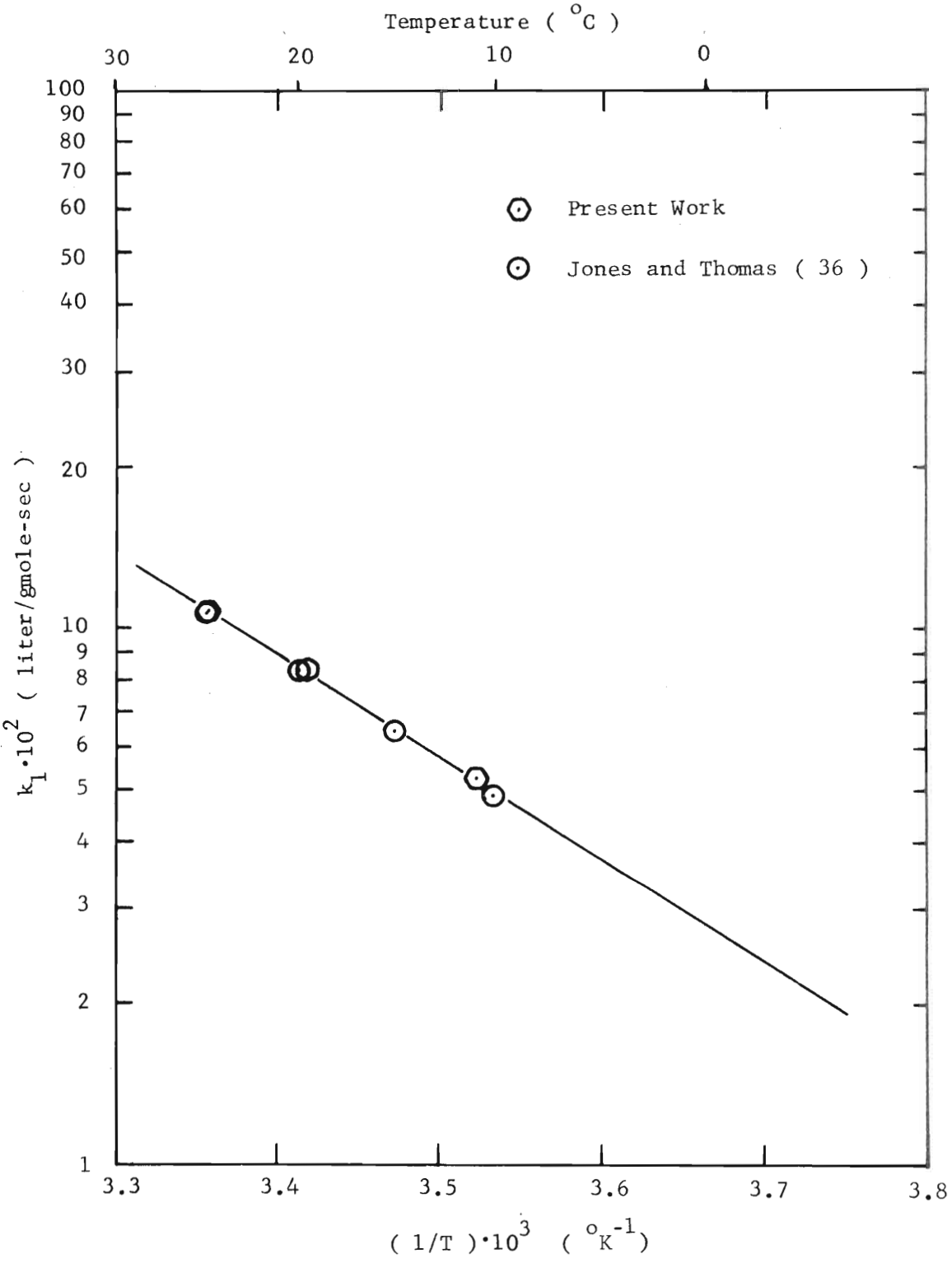

Figure 13. Reaction Rate Constant versus Reciprocal Temperature for the Alkaline Hydrolysis of Methyl Acetate

work as well as data obtained by Jones and Thomas (36) are shown and agreement is within experimental error (~2%). Both studies showed the activation energy for the saponification of methyl acetate in a 70% aqueous-acetone medium to be approximately 8,800 cal/gmole.

Alkaline Hydrolysis of Ethyl Benzoate

Tommila and co-workers (65) have performed investigations of the alkaline hydrolysis of ethyl benzoate in mixed solvent systems. Since ethyl benzoate is sparingly soluble in water, mixtures of acetone and water were investigated as solvents, and the effect of solvent composition on reaction velocities was studied. Among the compositions studied was the 70% aqueous-acetone mixture subsequently used in this work. Since ethyl benzoate is non-volatile, a slightly different experimental technique was used in this section, but results were in agreement with those given in the literature.

Rate Measurements

An alkaline solution (0.1N) was prepared by adding 70 ml of acetone to a 100-ml volumetric flask, followed by 10 ml of 1.0N NaOH and some water. This mixture was allowed to sit at room temperature for approximately one hour after which the flask was filled to the mark with distilled water. This flask was then placed in a constant-temperature bath and allowed to reach thermal equilibrium. At that time, approximately 0.01 mole (1.45ml) of ethyl benzoate was injected into the flask with a hypodermic syringe and the stopwatch was started. Weighing of the syringe before and after injection yielded the net weight of ethyl benzoate introduced into the reaction flask. A little

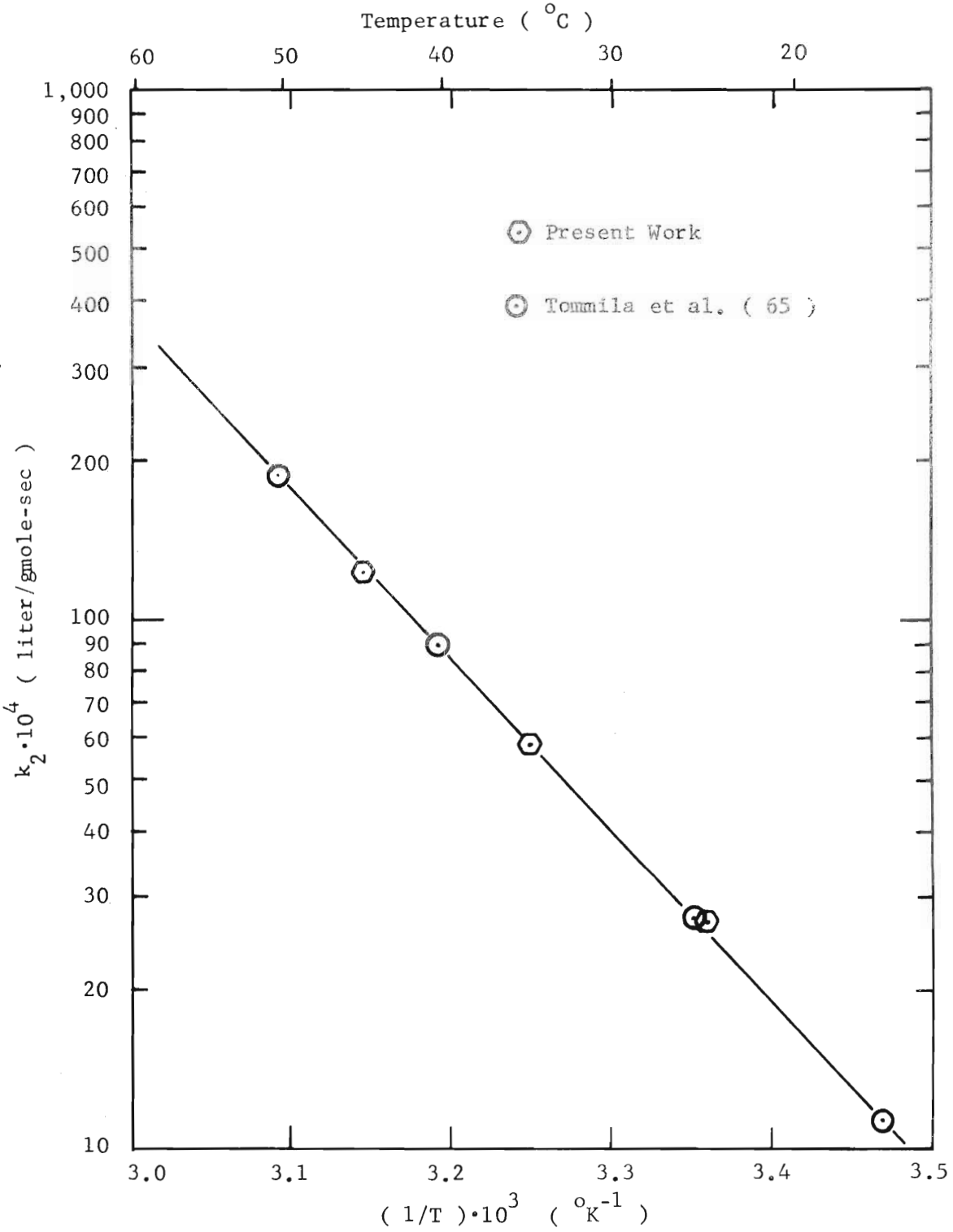

Figure 14. Reaction Rate Constant versus Reciprocal Temperature for the Alkaline Hydrolysis of Ethyl Benzoate

practice with this technique allowed injection of quantities extremely close to 0.01 mole. The initial concentrations again were corrected for change in volume due to the change in temperature from room temperature, although Tommila (65) states that the second-order reaction rate constant is essentially independent of the initial concentration of the reactants (indicating that the subject reaction is indeed second-order). Samples were taken at various times and the quenching technique previously described was used to determine the concentrations of products. Again, the arithmetic averages of the rate constants calculated for the samples by Equation (6.7) were used to represent the reaction rate constants at various temperatures. The experimental values from this work and that of Tommila are plotted in Figure 14. Again, as can be seen, agreement is within experimental error. The values of the activation energy and pre-exponential factor were (1) E = 14,500 cal/gmole and (2) $\log_{10} k_0(\ell/\text{gmole-sec.}) = 8.18$.

CHAPTER VII

COMPUTER SIMULATION OF PERIODIC OPERATION OF A CSTR

The objectives of this work were to demonstrate the phenomena associated with periodic reactor operation and to compare the experimental results obtained by operating the reaction system periodically with those predicted by a computer simulation of the reaction system. In general the computer simulation involves the mathematical construction of the governing differential equations for the system (mass and energy balances) and analytical or numerical integration thereof, subject to the constraints of the system (flow rates, volumes, densities, etc.). For very complex systems involving coupled non-linear differential equations, numerical integration is most often used.

The modeling of CSTR's is treated in most standard texts on reaction kinetics (3,39); however, there is no mention of periodic operation therein and very little said about unsteady-state operation in general. This chapter covers the mathematical modeling of periodic operation of the reaction system used in this work. The assumptions made concerning certain physical properties of the reaction mixture and the differential equations and boundary conditions (from Chapter IV) are given in the following sections. In addition, there is a brief discussion of the numerical techniques used.

Assumptions

In order to simplify the mathematical model as much as rationally possible, it was convenient to make the following assumptions concerning the reaction system:

1) The reactor contents were completely mixed (i.e., there were no thermal or concentration gradients in the reactor).

2) All electrical energy supplied to the heating element was dissipated to the liquid in the reactor.

3) The density and heat capacity of the liquid in the reactor remained essentially constant over the temperature range involved (i.e. an average value for the range was used).

4) The acid hydrolysis of the esters was neglected since these reactions are much slower than the alkaline hydrolysis (19) and the time required for analysis was small in comparison.

5) The thermal effects of both hydrolysis reactions were neglected since the concentrations of all reactants were very low.

6) The reaction rate constants obeyed the Arrhenius relationship over the temperature range of interest.

7) The reaction volume remained constant.

In order to verify the validity of some of these assumptions (1, 3, and 6), several auxiliary studies were made. Assumption (1) was tested by the injection of a dye into the reactor. The change in optical density of the effluent as a function of time was then measured using a Spectronic 20 spectrophotometer. This study will be described more fully in the next chapter. Assumption (3) was tested by measuring

the density of a 70% aqueous-acetone mixture as a function of temperature. The resulting curve is shown in Figure 15. While it was evident that the density of the mixture did vary with temperature, it was concluded that an average density for the operating temperature range would be satisfactory. Assumption (6) was verified by the study described in Chapter VI to determine reaction rate constants.

Mathematical Model

The material and energy balances comprising a mathematical model of the CSTR used in this work were given in Chapter IV. As stated in the previous chapter, the two reactions considered were the alkaline hydrolyses of methyl acetate and ethyl benzoate. These reactions were given by Equations (6.1) and (6.2):

$$CH_3COOCH_3 + NaOH \xrightarrow{k_1} CH_3COONa + CH_3OH \qquad (6.1)$$

$$C_6H_5COOC_2H_5 + NaOH \xrightarrow{k_2} C_6H_5COONa + C_2H_5OH \qquad (6.2)$$

and are represented by the following pair of equations:

$$A + B \xrightarrow{k_1} C + D \qquad (7.1)$$

$$A + E \xrightarrow{k_2} F + G \qquad (7.2)$$

where: A = sodium hydroxide

B = methyl acetate

C = sodium acetate

D = methanol

E = ethyl benzoate

F = sodium benzoate

G = ethanol

Derivations of the material balances for sodium hydroxide (A) and sodium benzoate (F) and an energy balance around the CSTR were given in Chapter IV by Equations (4.38) - (4.40). Invoking the assumptions described above, these equations were rewritten as Equations (4.53) - (4.55), which are in state variable form and are repeated below:

$$\frac{dx_1}{dt} = 1 - x_1 - a_1 x_1 (r_1 - 1 + x_1 + x_4) e^{-1/x_3} - a_2 x_1 (r_2 - x_4) e^{-\rho/x_3} \tag{4.53}$$

$$\frac{dx_2}{dt} = a_2 x_1 (r_2 - x_4) e^{-\rho/x_3} - x_4 \tag{4.54}$$

$$\frac{dx_3}{dt} = y - (1 + C_1) x_3 + C_1 C_2 \tag{4.55}$$

These three differential equations completely describe the behavior of the system. Other concentrations are obtained by simple stoichiometric relationships. Boundary conditions at the pseudo-steady-state for these differential equations were given by Equation (4.28).

$$x_i(0) = x_i(\tau) \qquad i = 1,3,4 \tag{4.28}$$

This merely states that the values of the state variables (or in reality the concentrations and temperature) must be the same at the end of the cycle (or period) as they were at the beginning. Since these values are not known initially, an iterative scheme was used to determine the boundary conditions. This scheme was as follows:

1) With a given switching policy, assume an initial value for each of the state variables.

2) Integrate over one cycle (τ) and examine the final values of the state variables ($x_i(\tau)$).

3) If Equation (7.3) is not satisfied, use Equation (7.4) to find the new initial values of the state variables.

$$\left| \frac{x_i(0) - x_i(\tau)}{x_1(0)} \right| \leq \epsilon_i \qquad i = 1,3,4 \tag{7.3}$$

$$x_i^*(0) = x_i(0) + [x_i(\tau) - x_i(0)]/2.0 \qquad i = 1,3,4 \tag{7.4}$$

In Equation (7.3) ϵ_i (e.g. 10^{-6}) is the convergence criterion which is some small specified quantity.

4) Repeat this procedure until the boundary conditions match within the specified accuracy. This method is similar to the bisection method used in determining roots of polynomial equations (18). It is simple and works well for small systems of equations, but is certainly not the only method available for determining the boundary conditions. For more complex systems, a method such as the matrix technique described by Lin (32) could be used. This method, which uses an iterative scheme

similar to Newton-Raphson interpolation, converges to the boundary conditions faster, but is somewhat bulky to use for small systems of equations; hence, the simpler method of Equation (7.4) was used. Once the boundary conditions are determined the behavior of the periodic system at the pseudo-steady-state (for the given switching policy) is completely specified.

Since Equations (4.53)-(4.55) are non-linear, fourth-order Runge-Kutta numerical integration of these equations was used. These operations were performed on a Univac 1108 digital computer and the program is given in Appendix D. With this background, the next section explains the use of the computer simulation to produce the theoretical curves with which the experimental data were compared.

Construction of Theoretical Curves

The family of curves shown in Figures 3 and 6 represent both conventional-steady-state operation ($\phi = 0$) and periodic operation ($0<\phi<1$). The numerical methods used in determining points on these curves are discussed in the following sections.

Conventional-Steady-State Curve

The points on the conventional-steady-state curve ($\phi = 0$) were determined by setting Equations (4.53)-(4.55) equal to zero. This resulted in three simultaneous, non-linear, algebraic equations in three unknowns (x_1, x_3, x_4) of the form given in Equations (7.5)-(7.7):

$$f = f(x_1, x_3, x_4) - b_1 = 0 \tag{7.5}$$

$$g = g(x_1, x_3, x_4) - b_2 = 0 \tag{7.6}$$

$$h = h(x_i, x_3, x_4) - b_3 = 0 \tag{7.7}$$

This system of equations was solved using Newton's method (18) in three variables. This technique utilizes the following algorithm to iterate on the variables:

$$x_1^{k+1} = x_1^{k} - \frac{\begin{bmatrix} b_1 & \frac{\partial f}{\partial x_3} & \frac{\partial f}{\partial x_4} \\ b_2 & \frac{\partial g}{\partial x_3} & \frac{\partial g}{\partial x_4} \\ b_3 & \frac{\partial h}{\partial x_3} & \frac{\partial h}{\partial x_4} \end{bmatrix}}{J(x_1, x_3, x_4)} \tag{7.8}$$

where:

$$J(x_1, x_3, x_4) = \begin{bmatrix} \frac{\partial f}{\partial x_1} & \frac{\partial f}{\partial x_3} & \frac{\partial f}{\partial x_4} \\ \frac{\partial g}{\partial x_1} & \frac{\partial g}{\partial x_3} & \frac{\partial g}{\partial x_4} \\ \frac{\partial h}{\partial x_1} & \frac{\partial h}{\partial x_3} & \frac{\partial h}{\partial x_4} \end{bmatrix} \tag{7.9}$$

and is the Jacobian of the system of equations. Equation (7.8) is written for the variable x_1; similar expressions were developed for x_3 and x_4. The iteration proceeded until the relative error between suc-

cessive values of x_1 for all state variables was less than 10^{-6}. For any value of y, then, a unique solution to Equations (4.53)-(4.55) could be found and the resulting values of x_4 plotted versus y to yield the conventional-steady-state curve. It is obvious that for conventional-steady-state operation, Equations (4.21) and (4.22) reduce to Equations (7.10) and (7.11);

$$\bar{x}_i = x_i \qquad i = 1, 3, 4 \tag{7.10}$$

$$\bar{y} = y \tag{7.11}$$

Pseudo-Steady-State Curves

The family of pseudo-steady-state curves ($0<\phi<1$) were constructed by the integration of Equations (4.53)-(4.55) over one cycle (period), using the iterative technique previously described, until the boundary conditions matched to within a relative error of less than 10^{-6}. The parameter ϕ was defined in Chapter IV as the fraction of the period during which the control variable is at its lower limit. As the value of ϕ increases toward an upper limit of one, the upper limit of the control variable (y_u) necessarily increases in order to maintain a constant value of $\bar{y}$. Obviously, a value of $\phi = 1.0$ implies that $y_u = \infty$; and in reality, approach to a value of ϕ close to 1.0 may be restricted by the upper limit of the control variable. After matching the boundary conditions, the time-averaged value of the state variable x_4 was obtained using Equation (4.21)

$$\bar{x}_4 = \frac{1}{\tau}\int_0^{\tau} x_4 dt \qquad (4.21)$$

The points thus obtained were plotted versus values of $\bar{y}$ to produce the family of pseudo-steady-state curves. Selection of the value of τ (the period) and the switching policy determined the value of $\bar{y}$ in all cases where the upper and lower bounds on the control variable y had been previously fixed.

CHAPTER VIII

PRELIMINARY EXPERIMENTAL STUDIES

Prior to making any experimental runs, three studies were undertaken in order to clear up questions which had arisen during the rate determination runs. The first concerned the change in volume which occurred during the mixing of acetone and water. The second concerned the variation of the density of a 70% aqueous-acetone solution with temperature and the third concerned the mixing efficiency of the three-blade impeller used for mixing the reactor contents.

Volume Change Determination

This study was easily accomplished by using only a 50-ml titrating burette and a 100-ml volumetric flask. First, 70.0 ml of acetone were pipetted into the volumetric flask. Then 30.0 ml of distilled water were added from the burette and the flask was stoppered, shaken and allowed to stand for one hour. At the end of one hour, the mixture level was observed to be below the mark on the flask. Consequently, excess water was added to bring the level in the flask up to the mark. Again the flask was stoppered, shaken and allowed to sit for an hour. This procedure was repeated several times until no further change in volume occurred. At that time, the total number of milliliters of distilled water added to the flask was read from the burette and found to be 34.0 ml. Therefore, in all subsequent preparations of reactant

solutions, 700 ml of acetone and 340 ml of distilled water plus reactant were mixed to form each liter of reactant solution. Thus the total of the water plus reactants was always equal to 340 ml per liter of reactant solution.

Density vs. Temperature Behavior

The objective of this study was to determine the effect of temperature on the density of a 70% aqueous-acetone solution. For this purpose, a 70% aqueous-acetone solution was prepared in a volumetric flask as indicated in the previous section. This flask was then thermostated in a constant temperature bath and the contents of the flask allowed to reach the bath temperature. At this time, the specific gravity of the solution was measured with a hydrometer. This procedure was repeated at different temperatures over the range anticipated in the subsequent experimental work. The results are shown in Table 2 and Figure 15.

As can be seen, the density over this range varies by only 5% and the subsequent usage of an average density would result in an error of only $\pm$ 2-3% well within the overall experimental error.

Mixing Efficiency Study

Although the heating element support frame in the reactor was also designed as a baffle system, the question of the effectiveness of mixing in the reactor naturally still arises. Accordingly, a preliminary experiment was performed in an effort to answer this question. The objective of this experiment was to compare the ideally predicted

Table 2. Density Versus Temperature for a 70% Aqueous-Acetone Solvent

Temperature (^{o}C)	Density (gm/ml)
-17.2	0.930
0.2	0.914
7.8	0.907
10.3	0.905
20.0	0.896
24.8	0.892
30.3	0.887
39.4	0.879

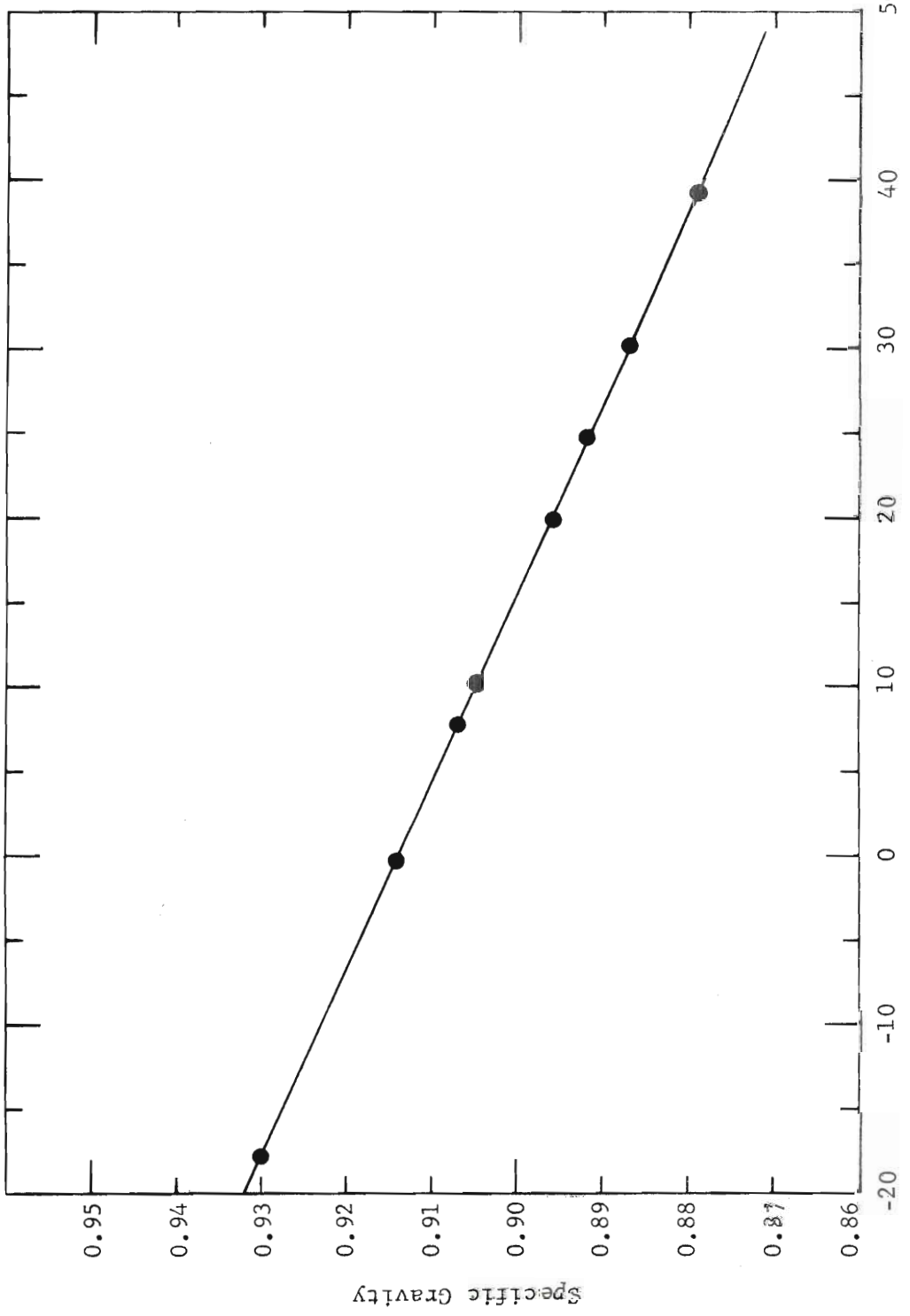

Figure 15. Specific Gravity as a Function of Temperature for a 70% Aqueous-Acetone Solvent System

behavior of the reactor vessel with its actual behavior; and if the two agreed within 5%, the reactor would be considered ideal.

A mathematical model of the reactor vessel was constructed assuming the volumetric flow rate (Q_F) and the reactor volume (V) were constant. At time t = 0, a concentrated solution of $KMnO_4$ was added instantaneously to the reactor. With the initial concentration of dye in the reactor equal to C_0, a material balance about the reactor for the dye can be described by Equation (8.1)

$$\frac{dC}{dt} = - (Q_F/V)C \tag{8.1}$$

Rearranging and integrating this equation from C_0 to C and from t = 0 to t = t, and defining $\alpha = Q_F/V$, Equation (8.1) becomes:

$$C = C_0 e^{-\alpha t} \tag{8.2}$$

This equation expresses the concentration as a function of time (with slug injection of material) for an ideally mixed reactor. Since concentration is not easily determined directly, the optical density (color intensity), was followed as a function of time. From the Beer-Lambert law

$$\text{Concentration} \propto \text{O.D.} \tag{8.3}$$

where O.D. is the optical density of the solution. Therefore, Equation

(8.2) can be rewritten as

$$O.D. = (O.D.)_0 e^{-\alpha t} \tag{8.4}$$

The optical density can then be plotted on semi-log paper versus time and if the result is a straight line with a slope of α, the reactor can be assumed to be ideally mixed. The experimental procedure involved establishing a constant flow of water through the reactor at approximately 100 ml/min (the flow used in the subsequent experimental runs). Once the flow rate was established and a constant volume of two liters was attained, the mixing impeller was started. Then 10 ml of concentrated $KMnO_4$ solution were injected into the reactor with a hypodermic syringe and a stopwatch was started. The optical dinsity of the effluent of the reactor was measured by taking ten-second samples and subjecting them to colorimetric analysis with a Bausch and Lomb Spectronic 20 spectrophotometer. The optical density was read directly from a logarithmic scale on the instrument and the results are given in Table 3. These data were plotted as previously described in semilogarithmic coordinates with the result shown in Figure 16. The slope of this line was calculated and found to be 0.05. The value of α determined from its definition is also 0.05. Since these numbers agreed extremely well, the reactor was considered ideally mixed and the ratio, V/Q_F, was taken as the mean residence time in the reactor computer simulations.

Table 3. Optical Density Versus Time Data For Mixing Efficiency Study

Sample No.	Time (min.)	Optical Density
1	1	0.360
2	3	0.328
3	5	0.297
4	7	0.270
5	9	0.244
6	11	0.217
7	15	0.177
8	20	0.137

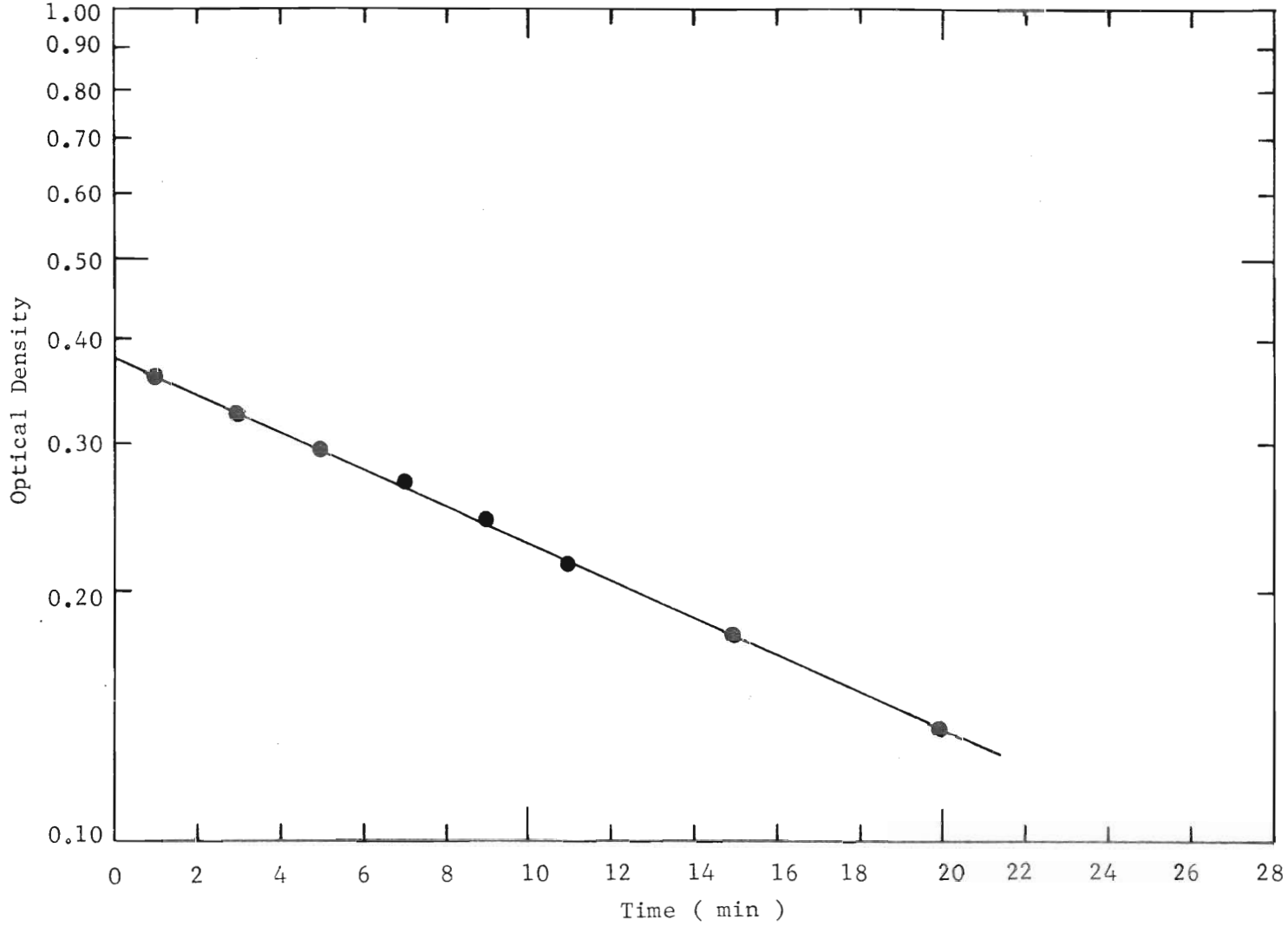

Figure 16. Optical Density as a Function of Time in the Determination of Reactor Mean Residence Time

CHAPTER IX

METHOD OF CHEMICAL ANALYSIS

Chemical analysis of the reaction products was the most difficult problem posed by this experimental system. The reactions involved were the alkaline hydrolyses of methyl acetate and ethyl benzoate, as shown in Equations (6.1) and (6.2):

$$CH_3COOCH_3 + NaOH \xrightarrow{k_1} CH_3COONa + CH_3OH \qquad (6.1)$$

$$C_6H_5COOC_2H_5 + NaOH \xrightarrow{k_2} C_6H_5COONa + C_2H_5OH \qquad (6.2)$$

These reactions occurred in a 70% aqueous-acetone solvent, which added two more species to the seven above. Reactor effluent samples were drained from the reactor into excess HCl, thereby converting the sodium acetate and sodium benzoate to acetic acid and benzoic acid, respectively; all excess sodium hydroxide was also neutralized. As a result, this left six species in the samples which could be analyzed for. One of these (ethyl benzoate) could be eliminated since it is in excess (its initial concentration is ten times that of the methyl acetate or sodium hydroxide); and its concentration changes very little during the reaction.

The first analytical method tried was gas chromatography using a Perkin-Elmer 820 gas chromatograph. This chromatograph was equipped

with a thermal conductivity cell detector; the concentrations used in this study however, were too small to be quantitatively measured and consequently this method of analysis was temporarily discarded.

The second analytical method tried involved the analysis of the methanol and ethanol products of the two reactions. Methanol was first oxidized to formaldehyde with $KMnO_4$. Then the formaldehyde was analyzed colorimetrically by reacting it with chromotropic acid (1,8 dihydroxynapthalene -3,6- disulfonic acid), which produces an intense purple color with as little as 20 μg/ml formaldehyde. Another part of the same sample was then analyzed for total alcohol by reacting the sample with a standard solution of $K_2Cr_2O_7$ in concentrated H_2SO_4. The excess $K_2Cr_2O_7$ was then determined colorimetrically by reaction with diphenyl carbazide, which produces a violet color with $K_2Cr_2O_7$. The amount of total alcohol present was calculated as the difference between the amount of $K_2Cr_2O_7$ remaining after the reaction with alcohol and the amount in an unreacted $K_2Cr_2O_7$ blank of identical size. The concentration of ethanol could then be determined by subtraction of the methanol concentration from the total alcohol concentration. This method proved excellent through the calibration stage (i.e., good calibration curves were obtained using standard solutions of methanol and ethanol). Upon implementing this method on actual reactor samples, however, impurities in the acetone (mostly methanol) rendered both tests unusable.

The third analytical method tried was ultraviolet spectroscopy. In the mixture of species to be analyzed, only two (ethyl benzoate and

benzoic acid) absorb appreciably in the UV region around 270 nm. A consideration here is that the ethyl benzoate interferes with the analysis of the benzoic acid, and consequently the two must be separated physically. Liquid-liquid extraction using carbon tetrachloride as the solvent was used to extract the unreacted ester, leaving the benzoic acid (which had been previously converted back to its sodium salt with sodium bicarbonate) in the aqueous phase. Tests performed with this method indicated that up to 50% of the benzoate ion was lost during the extraction and, consequently, this method was also discarded.

The analytical method finally decided upon for all of the analyses in this work consists of two stages: (1) titration for total carboxylic acid and (2) gas chromatographic analysis for ethanol.

Titrimetric Analysis

Of the five species which could be analyzed, two were carboxylic acids (acetic and benzoic). If the pKa values of two acids are at least 2 units apart, one titration would show two end points (one for each acid); and the complete analysis could then be done with a single titration. In reality, the pKa values for the subject acids are less than one unit apart (4.756 vs 4.213), and titration with a standard base solution shows only one break point for the total acid. As a result, this technique was used to determine total acetic plus benzoic acid in a sample.

One hundred milliliters of quenched sample were pipetted into a 300 ml beaker and a Teflon coated magnetic stirring bar was added. The beaker was placed on a magnetic stirrer, and the solution was ti-

trated potentiometrically with 0.100N NaOH using a Bechman pH meter with a combination glass-calomel electrode. Two end points were detected: (1) the excess HCl end point and (2) the carboxylic acid end point.

The initial concentrations of reactants were determined by sampling the reactant tanks during an experimental run. The samples of the two ester solutions were completely saponified with a known quantity of excess sodium hydroxide and the excess was back titrated to determine the ester concentration. The sodium hydroxide solution was titrated directly with standard HCl. Each of the reactant solutions were prepared at three times the desired reactor feed concentration so that when the three reactant streams were allowed to flow equally into the reactor, the initial concentrations would be correct.

Gas Chromatographic Analysis

The concentration of one additional species was needed in order to obtain a complete material balance. Ethanol seemed to be most promising in this regard. Also, since this was the species whose yield should be improved by periodic operation, it was felt that its concentration should be obtained directly and not by difference (as with the alcohol tests).

A Perkin-Elmer model 810 gas chromatograph with a flame ionization detector was made available for use; and it was then necessary to choose a column packing which would separate the ethanol from the other species. Several column packings were tried: (1) Chromasorb W with 10% silicone oil (DC-200), (2) Chromasorb W with a 10% Carbowax 20M and

(3) Porapak Q. The first of these packings is designed primarily for non-polar materials and performed poorly in separating the desired species. The second column packing is designed for polar materials. Due to its nature, however, the acetone solvent is eluted first, thus obscuring the ethanol peak. The third column packing is a porous polymer and requires no liquid phase coating. These features make it an excellent candidate when used with an ultra-sensitive flame ionization detector. In addition, this packing is recommended for polar compounds such as alcohols, esters, carboxylic acids, etc. Determination of the retention times for the two alcohols in this reaction system showed that the methanol and ethanol are eluted before the acetone solvent which is very desirable. This packing was thus selected for use in the gas chromatograph.

Two aluminum columns, each six feet long and one-eighth inch in outside diameter, were packed with 100-120 mesh Porapak Q and coiled into spirals. The optimum column operating conditions were determined by construction of a Van Deemter Plot (1,30,43) and are listed below in Table 4.

Reactor effluent samples quenched in acid were placed in a constant temperature bath at 25^{o}C and allowed to equilibrate before titration and gas chromatographic analysis. A five-microliter Hamilton syringe was then used to inject a known volume of quenched sample into the gas chromatograph. A typcial chromatogram is shown in Figure 17. The mass of ethanol in the sample was calculated by determining the area under the ethanol peak (by two different methods) and referring to

Table 4. Optimum Gas Chromatograph Operating Conditions

N_2 carrier gas flow rate	-	60 cc/min/column
H_2 flow rate	-	60 cc/min/column
Air flow rate	-	350 cc/min
Column temperature	-	145°C
Injector temperature	-	250°C
Attenuation	-	x50

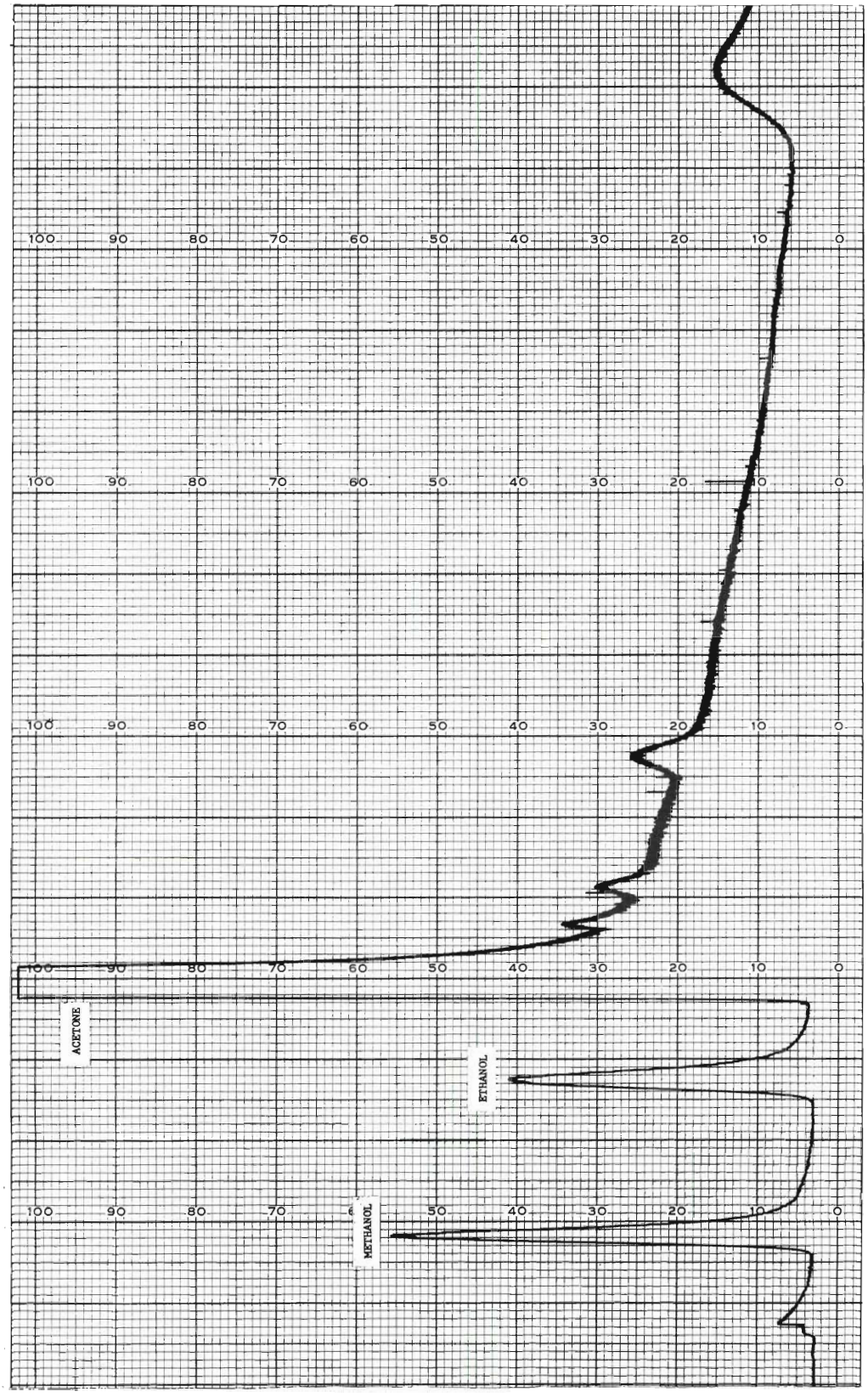

Figure 17. Typical Chromatogram from Chemical Analysis in This Work

a calibration curve constructed from standard ethanol solutions. Both a detailed description of the calibration procedure and the calibration curves are given in Appendix E.

The concentration of ethanol in the sample was determined as the ratio of its mass as determined above to the known volume injected. The concentration of methanol (or acetic acid) was then calculated by subtracting the ethanol concentration from the total acid concentration determined by titration. From these two concentrations and the initial concentration of reactants (as previously determined), a complete material balance could be obtained.

CHAPTER X

EXPERIMENTAL RESULTS AND DISCUSSION

The objective of this work was to obtain experimental data in an area where previously no data have been reported--periodic operation of a CSTR. As mentioned Chapter II, many theoretical studies have been made of CSTR's operated in periodic fashion; as a result, the mathematical model used in this work is of rather standard format. A few changes to the model, which will be mentioned later, were made in order to obtain a better fit of the experimental data with the model. It should be emphasized at this point, however, that the computer simulation of the reaction system was of secondary importance and, in some cases, was used only to show trends. Of primary importance was the gathering of experimental data on periodic reactor operation and the experimental verification of yield improvement through this mode of operation.

Selection of Reaction System

In order to obtain measurable increases in yield, it was necessary that the two reactions selected in the experimental work have activation energies whose ratio was greater than 1.5. In addition, the reactions had to proceed at a rate such that measurable amounts of products be formed over a reasonable period of time. Two different reaction systems were actually examined; one of them was discarded, how-

ever, due to analytical complications which could not be easily resolved.

The first reaction system examined was the simultaneous hydrolysis and aminolysis of benzoyl chloride. The hydrolysis reaction would be constrained to be pseudo-first-order by the presence of a large excess of water; the aminolysis reaction would be second-order (first-order with respect to each of the reacting species). These reactions appeared to be particularly promising because the ratio of their activation energies was 2.02. In addition reagent costs could be kept to a minimum by using reactant feed concentrations in the range of 0.01-0.001 gmole/liter. Numerous problems were encountered with this prospective system, however. Among these were: (1) the presence of a third coupling reaction when the original two reactions are carried out simultaneously in the same vessel, and (2) the inability to chemically quench the reactions during the sampling period. These problems rendered an experimental study almost impossible and, consequently, a second reaction system was chosen.

This second reaction system consisted of the simultaneous alkaline hydrolysis (saponification) of two carboxylic esters (methyl acetate and ethyl benzoate). It was found that: (1) these two reactions are not coupled, (2) reaction rate constants could be accurately determined by batch kinetic experiments and (3) chemical quenching of the reactions could be accomplished with any strong mineral acid, provided the acid is only slightly in excess and the samples are analyzed as quickly as possible. A search of the literature showed, however, that

these reactions occurring simultaneously in distilled water do not meet the requirement regarding the ratio of the activation energies. When these same reactions are carried out in various organic solvents, however, the activation energies are changed because of solvent interaction effects and the reactions become feasible for optimization by periodic operation (i.e., $E_2/E_1 > 1.5$). Among the feasible solvent systems are: (1) p-dioxane : water, (2) acetone : water, (3) tetrahydrofuran : water, (4) dimethyl sulfoxide : water, (5) methanol : water and (6) ethanol : water. The solvent system chosen for this work was acetone : water, with the primary consideration being cost. Since the quantity of acetone used during the experimental runs was large, the acetone (C P grade) was ordered in 55-gallon drums. This grade of acetone contains at least four impurities (as determined by gas chromatographic analysis), one of which is methanol. The presence of this methanol required modifications to the analytical procedure, which were discussed at length in Chapter IX, and will be returned to later in this chapter.

After the selection of the reaction and solvent system, a series of batch kinetic experiments was performed in order to verify the values of the reaction rate constants and activation energies reported in the literature. These experiments were described in Chapter VI and will not be discussed here at any length. It should be mentioned at this point, however, that the values of the activation energy and pre-exponential factor for the hydrolysis of ethyl benzoate were modified slightly in order to obtain a better fit between computer simulations and the experimental data. These kinetic parameters did agree within experimental

error with the values given in the literature, and were thus used as a starting point in the computer simulations.

Selection of Experimental Operating Conditions

After determination of the reaction rate constants, the experimental apparatus was assembled, and the preliminary mixing experiment was performed, as described in Chapter VIII. Next, the conditions at which the experimental runs should be made were determined. The residence time within the reactor was selected arbitrarily as twenty minutes. In this work the effect of periodic reactor operation was studied for only one cycle duration, which was chosen to be equal to the residence time (i.e., $\tau = 1$). This is not to say the $\tau = 1$ is necessarily the optimal cycle time. The purpose of this work, however, was not to determine the optimal operating policy, but to demonstrate experimentally yield improvements via periodic operation. Future work should include experiments conducted at other values of τ(0.1, 0.5, 1.5), and the results compared with those reported herein. Feed concentrations for methyl acetate, sodium hydroxide and ethyl benzoate of 0.001, 0.001 and 0.100 gmole/liter, respectively, were initially planned. The first two values proved to be too dilute for product determination by titration and, consequently, several different feed concentrations were tried. The final values used in all subsequent experimental runs were (1) 0.02 gmole/liter for the sodium hydroxide and methyl acetate and (2) 0.20 gmole/liter for the ethyl benzoate. Although an initial concentration of ethyl benzoate ten times that of the other reactants does not render its hydrolysis pseudo-first-order in the strictest sense,

this reaction does become competitive with the other hydrolysis reaction (which is the desired result).

Presentation of Experimental Results

The first periodic run was used to determine the number of cycles necessary for the reaction system to achieve pseudo-steady-state from a concentration standpoint. The system was started up and the thermal pseudo-steady-state, as determined from the reactor thermocouple output, was reached after four cycles. The first cycle after the thermal pseudo-steady-state was reached was denoted as cycle 1, and composite samples of the reactor product stream were taken over cycles 2, 4, 6, 8, and 10. The ethanol concentration in this stream was determined by gas chromatography as previously described and the results are shown in Figure 18. As can be seen from this figure, after two cycles this concentration has not quite reached the pseudo-steady-state (low by 7%). After four cycles the pseudo-steady-state concentration was found to level out at 0.159. It was decided from these results, that for all subsequent runs, composite samples taken over cycles 4 and 6 (after the attainment of the thermal pseudo-steady-state) would be representative samples. The remainder of the periodic runs and a conventional-steady-state run were made in order to gather data at five different values of ϕ (the fraction of the cycle during which the control variable is at its lower limit). The values of ϕ chosen were 0.95, 0.90, 0.80, 0.70 and 0.60. During these runs, careful measurements of both the voltage and current to the heating element were made in order to be able to calculate the power imput to the reactor. The temperature of the re-

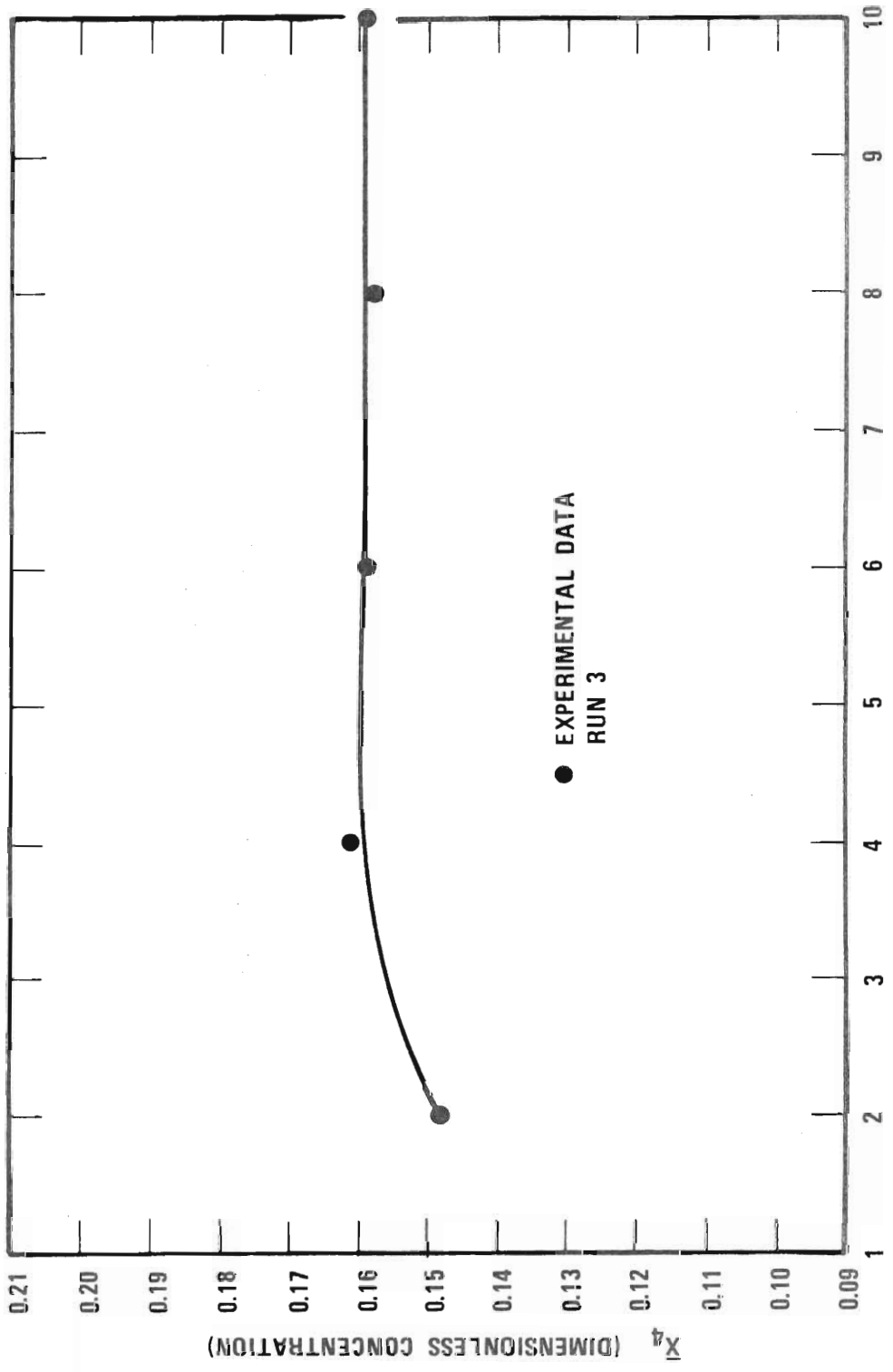

Figure 18. Experimental Determination of the Approach to Concentration Pseudo-Steady-State

actant solutions (T_0) was also monitored in order to use this value of T_0 in the computation of the control variable $\bar{y}$ at which the experimental values of $\bar{x}_4$ would be plotted.

Evaluation of Control Variable

The definition of y was given in Chapter IV:

$$y = RT_0/E_1 + qR/1000\rho_\ell C_p E_1 Q_F \qquad (4.50)$$

As can be seen from this definition, five different experimentally measured (T_0, q, Q_F) or inferred (ρ, C_p) quantities enter into this definition. The numerical value of the density for each run was determined from the density-temperature curve in Chapter VIII, using the experimentally determined average temperature of the cycle as the abscissa. The heat capacity of the reaction mass was computed from the heat capacities for pure acetone and pure water at the average temperature of the cycle, using a linear mixing rule based on mole fractions to obtain the heat capacity for the mixture. All of these inferred and measured values, including the values of $\bar{y}$ calculated from Equation (4.34), are given in Appendix F; the actual values of y_u and y_ℓ are also given there. The pseudo-steady-state concentration results for $\bar{x}_4$ were plotted versus the values of $\bar{y}$ as obtained above. Values of $\bar{x}_4$ from computer simulations (initially computed by assuming an adiabatic reactor and using the literature values of the activation energies) were also plotted on the same graph to compare the experimental and simulation results. The initial agreement was very poor. The curve for each value of ϕ seemed

to be offset horizontally from the model, and the slopes of these curves were slightly different from those suggested by the model. An explanation of the discrepancy between runs was sought and it was found that several factors were operative here.

The primary source of error was in the measurement of the reactant feed temperatures. It was found that, even though there were thermocouples in the inlet lines, sufficient heat was gained between the thermocouples and the reactor to change these temperatures (and hence the actual value of T_0). A change of only $1^{\circ}C$ distorts the value of $\bar{y}$ by the amount of .0003 unit. This was considered to be quite significant in view of the fact that, with the equipment used, it was impossible to hold the reactant feed temperatures within $\pm 3^{\circ}C$ from day to day.

A secondary source of error was in the measurement of the current to the heating element. While the voltage could be measured accurately enough (and remained very constant with the use of the constant voltage transformer), the current was found to vary over the cycle. This variation was primarily due to the change in the resistance of the heating element as it heated up. This behavior thus necessitated the use of an "average" value for the current; it is felt that this could be another source of error since the variation in current over the cycle was not always linear with time.

A third source of error resulted from the assumption that the heat capacity of the reaction mixture was the same as a 70% aqueous-acetone mixture. Since the ethyl benzoate concentration was 0.2 gmole/

liter (75 grams/liter), it was felt that this could possibly influence the heat capacity of the solution.

Finally, another source of error lay in the assumption that the reactor was adiabatic. The fact that this assumption was not valid became obvious when the steady-state experiment was performed with no heat flux from the heating element. During this run the first sample was taken when there was no heat flux to the reactor from the heating coil (if adiabatic, $T \approx T_0$). The steady-state temperature which resulted however, was five to ten degrees centigrade higher than it should have been if there were no heat losses to the surroundings from the reactant feed lines and reactor vessel. Accordingly, in an attempt to account for heat transfer to and from the reactor vessel, an extra term was added to the energy balance as shown in Chapter IV. The resulting dimensionless expression for the temperature in the reactor is repeated below:

$$\frac{dx_3}{dt} = y - (1 + C_1)x_3 + C_1C_2 \qquad (4.55)$$

During each of the experimental runs, the instantaneous temperature in the reactor vessel was monitored and recorded on a millivolt strip chart recorder (see Figure 19). In order to reduce the amount of error introduced into the value of $\bar{y}$ by the previously mentioned factors, it was decided that instead of calculating $\bar{y}$ from the power input and the other parameters in Equation (4.50), $\bar{y}$ would be determined from one experimental measurement (the instantaneous reactor temperature)

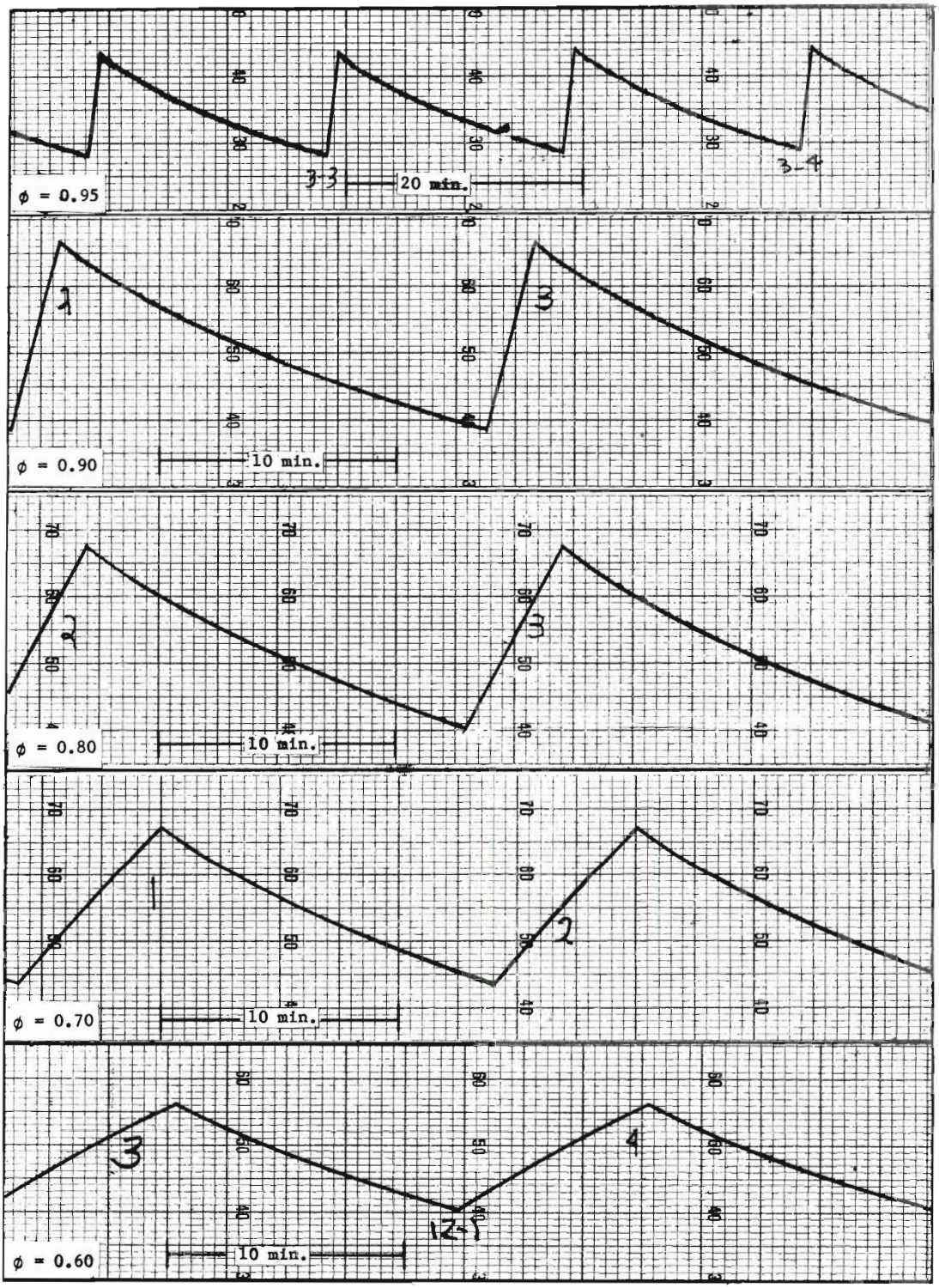

Figure 19. Experimental Temperature Profiles During Periodic Operation

Graphical integration of the reactor temperature profiles yielded numerical values of the average temperature ($\bar{x}_3$) for each sample taken. At steady-state Equation (4.55) becomes

$$y = (1 + C_1)x_3 - C_1C_2 \tag{10.1}$$

A similar procedure was employed in the case of pseudo-steady-state conditions. Equations (4.55) was integrated analytically and the time averaged value of state-variable x_3 was calculated. Since this derivation is rather lengthy, it is given in Appendix G and the results are shown:

$$\bar{y} = (1 + C_1)\bar{x}_3 - C_1C_2 \tag{10.2}$$

Since the value of $\bar{x}_3$ was graphically determined and the value of the constant C_2 was fixed by the ambient temperature, only the value of the constant C_1 was needed in order to plot $\bar{x}_4$ against $\bar{y}$.

In an effort to effect better agreement between the computer simulations and the experimental data, the pre-exponential factors, the activation energies and the constant C_1 were varied until a reasonable fit was obtained. The value of the activation energy for the hydrolysis of methyl acetate (E_1) was varied from 8,200 cal/gmole to 9,000 cal/gmole, while the value for the activation energy of the hydrolysis of ethyl benzoate (E_2) was varied from 13,000 cal/gmole to 14,750 cal/gmole. Pre-exponential factors were calculated for each activation

energy using the middle value of the experimental rate constant data from Chapter VI. No computer program was written to fit the simulation curves to the experimental data; however, approximately twenty-five different combinations of parameters were plotted before the best fit was obtained. It should be noted that since this was a semi-manual search, no attempt to obtain a best fit for $\bar{x}_2$ was made and, as a result, the fit of $\bar{x}_2$ data to the computer simulation would be expected to be poorer.

The results of this search indicated that varying E_1 did not have any significant effect on the simulation results, if the ratio E_2/E_1 were maintained constant. Therefore, rather than searching for E_1, the value of this parameter was retained as 8,800 cal/gmole (the literature value), and the parameters E_2 and C_1 were varied until a reasonable fit for $\bar{x}_4$ was obtained between the computed and experimental steady-state data. The final values used for these parameters are:

$$E_1 = 8{,}800 \text{ cal/gmole}$$

$$E_2 = 14{,}750 \text{ cal/gmole}$$

$$k_{10} = 1.8552 \times 10^{-7} \ell \text{/gmole-min}$$

$$k_{20} = 1.0283 \times 10^{10} \ell \text{/gmole-min}$$

$$C_1 = 0.037$$

$$C_2 = 0.0673$$

Comparison of Experimental and Simulation Results

The experimental data were then plotted, using Equation (10.2) to evaluate $\bar{y}$ from the measured values of $\bar{x}_3$, and the results for the five values of ϕ are shown in Figures 20 through 24. These results

have also been reduced to tabular form and are shown in Table 5. In calculating percent improvement, simulation results for conventional-steady-state were used as a basis.

As previously stated, the major emphasis in fitting the simulation curves to the experimental data was placed on fitting the values of $\bar{x}_4$. The experimental values of $\bar{x}_2$ (pseudo-steady-state yield of methanol) consequently, would not be expected to fit the model quite as well. An example of the fit of these data for $\bar{x}_2$ is shown in Figure 25 for a value of $\phi = 0.9$. As might be suspected, the fit is not as good; most of the experimental data, however, agree satisfactorily with the model. Two factors which might have contributed to the ragged nature of these titration data are: (1) variation in the sodium hydroxide titrant normality due to absorption of carbon dioxide and (2) poor endpoint behavior for the HCl, which thus introduces errors into the calculation of the total carboxylic acid present. In addition to these two factors, the precise position (on the pH scale) of the carboxylic acid endpoint would vary slightly as the amount of each acid in the mixture varied. While this last point may not be as significant as the other two, it could play a small part in the overall scatter of the titration data. Still another source of error might be that the value of $\bar{x}_2$ was obtained by subtracting the experimental values of $\bar{x}_4$ determined by chromatography from the total acid obtained by titration. Whenever a quantity is determined from the difference between two experimental measurements, the error in that quantity is naturally increased. While a good fit of all the experimental data with a model is certainly de-

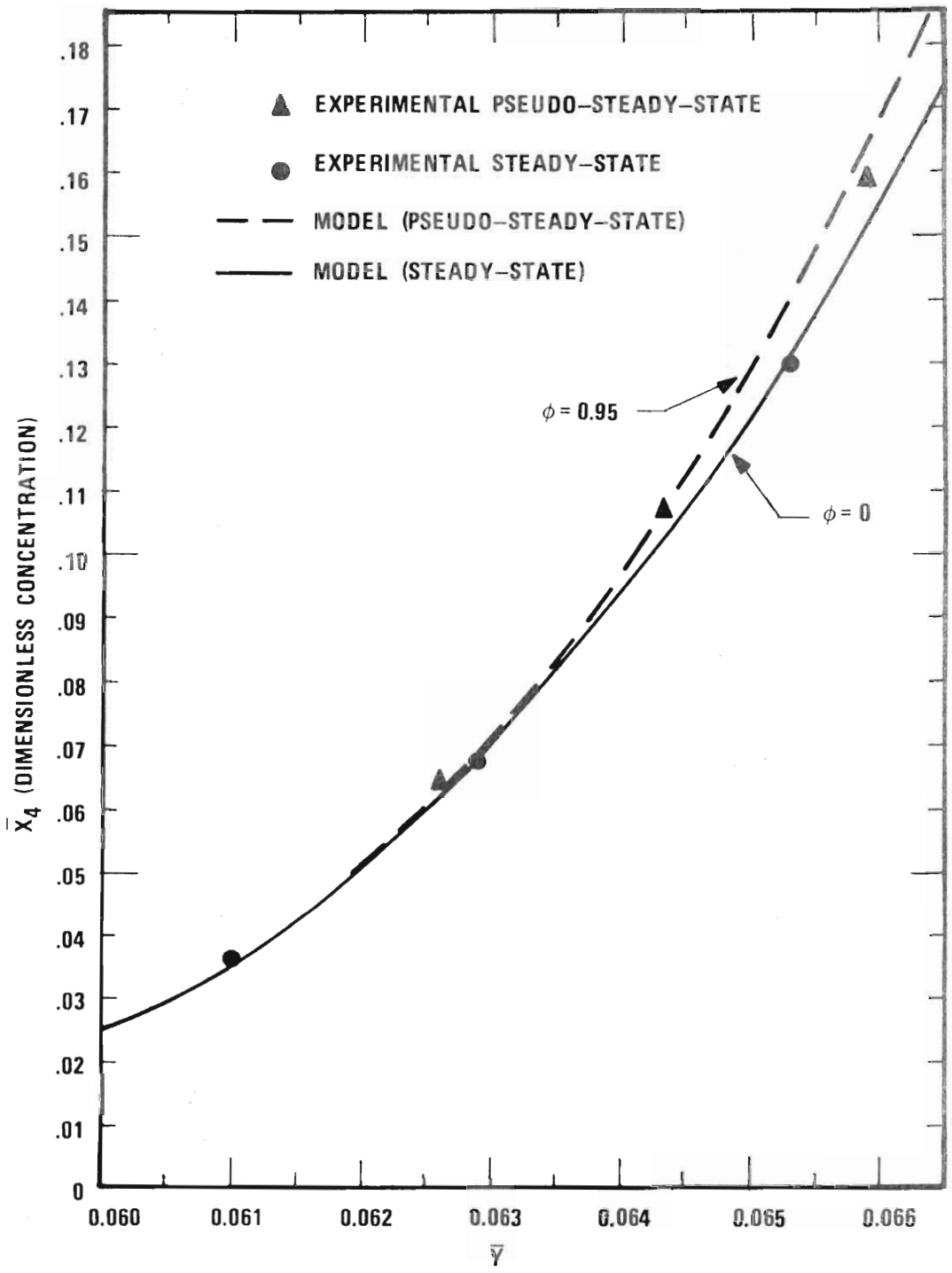

Figure 20. Dimensionless Concentration of Ethanol ($\bar{x}_4$) at ϕ = 0.95

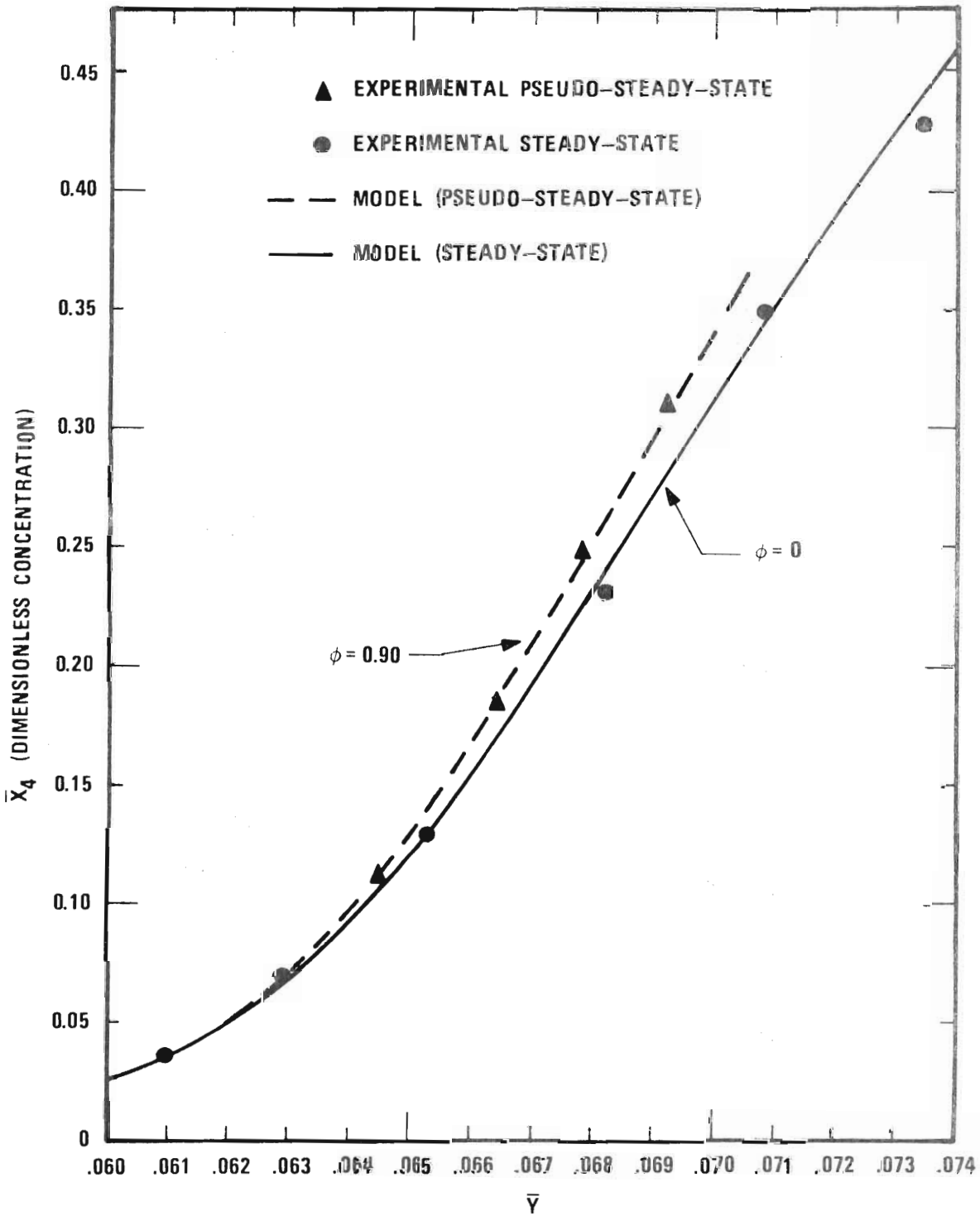

Figure 21. Dimensionless Concentration of Ethanol ($\bar{x}_4$) at ϕ = 0.90

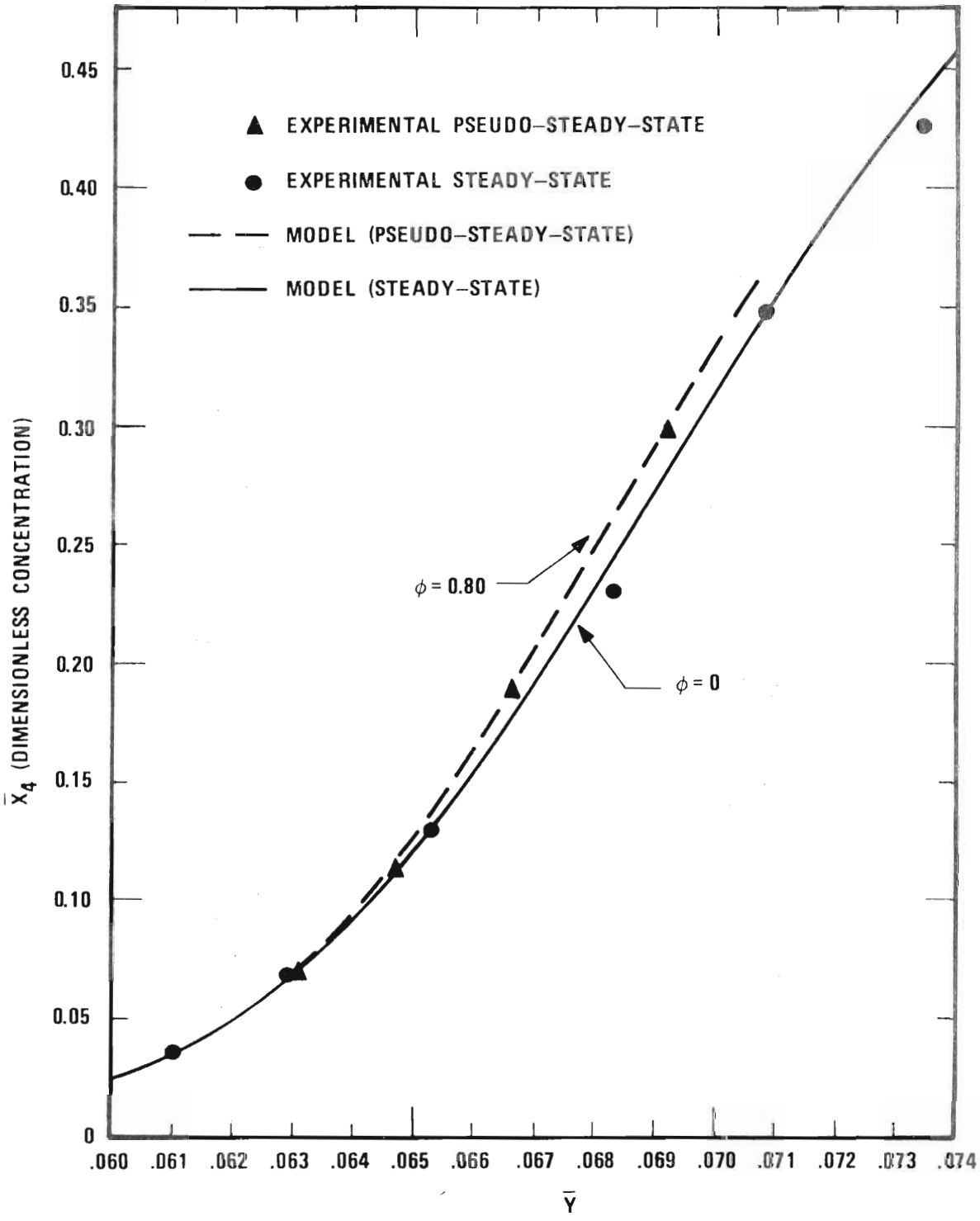

Figure 22. Dimensionless Concentration of Ethanol ($\bar{x}_4$) at ϕ = 0.80

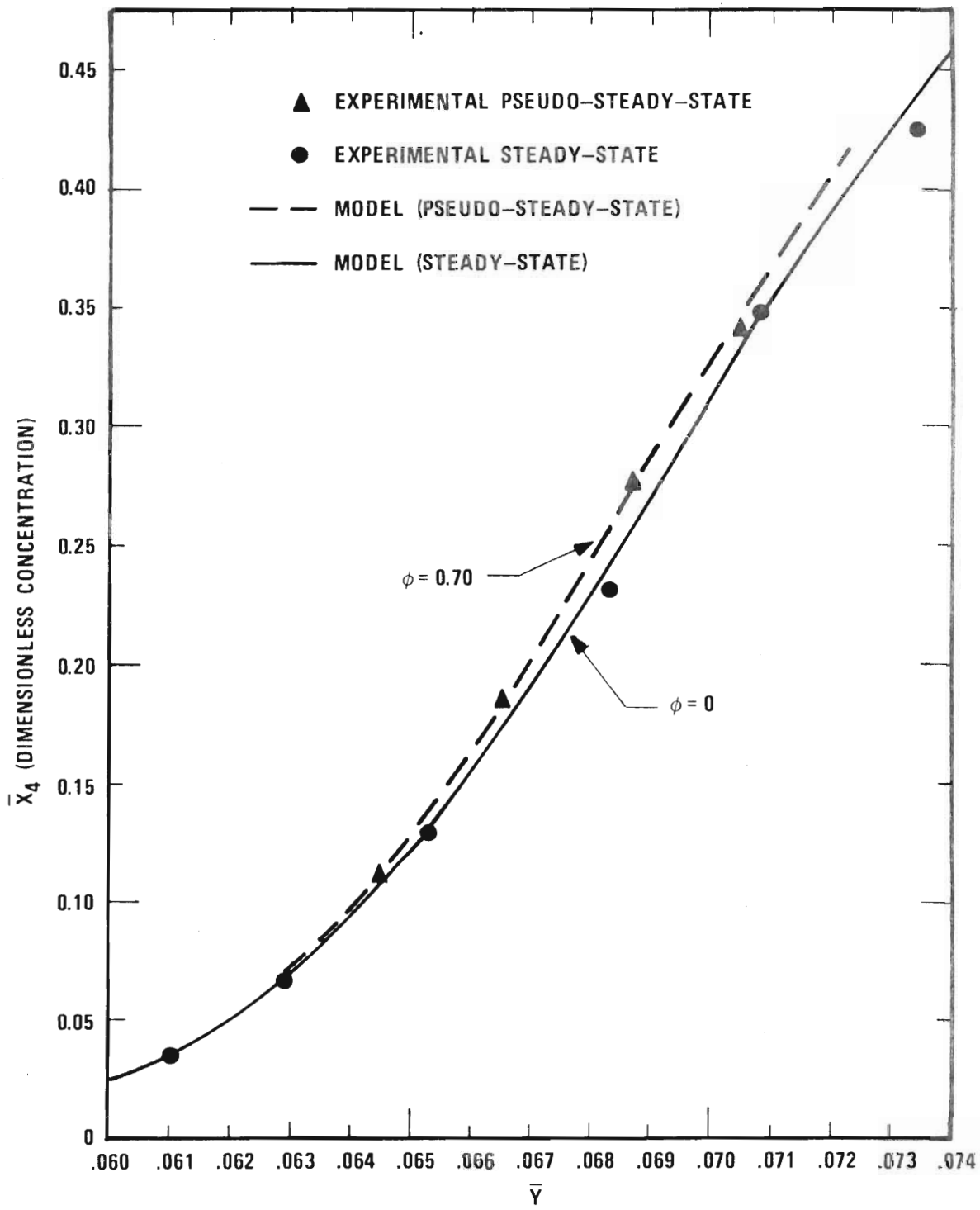

Figure 23. Dimensionless Concentration of Ethanol ($\bar{x}_4$) at ϕ = 0.70

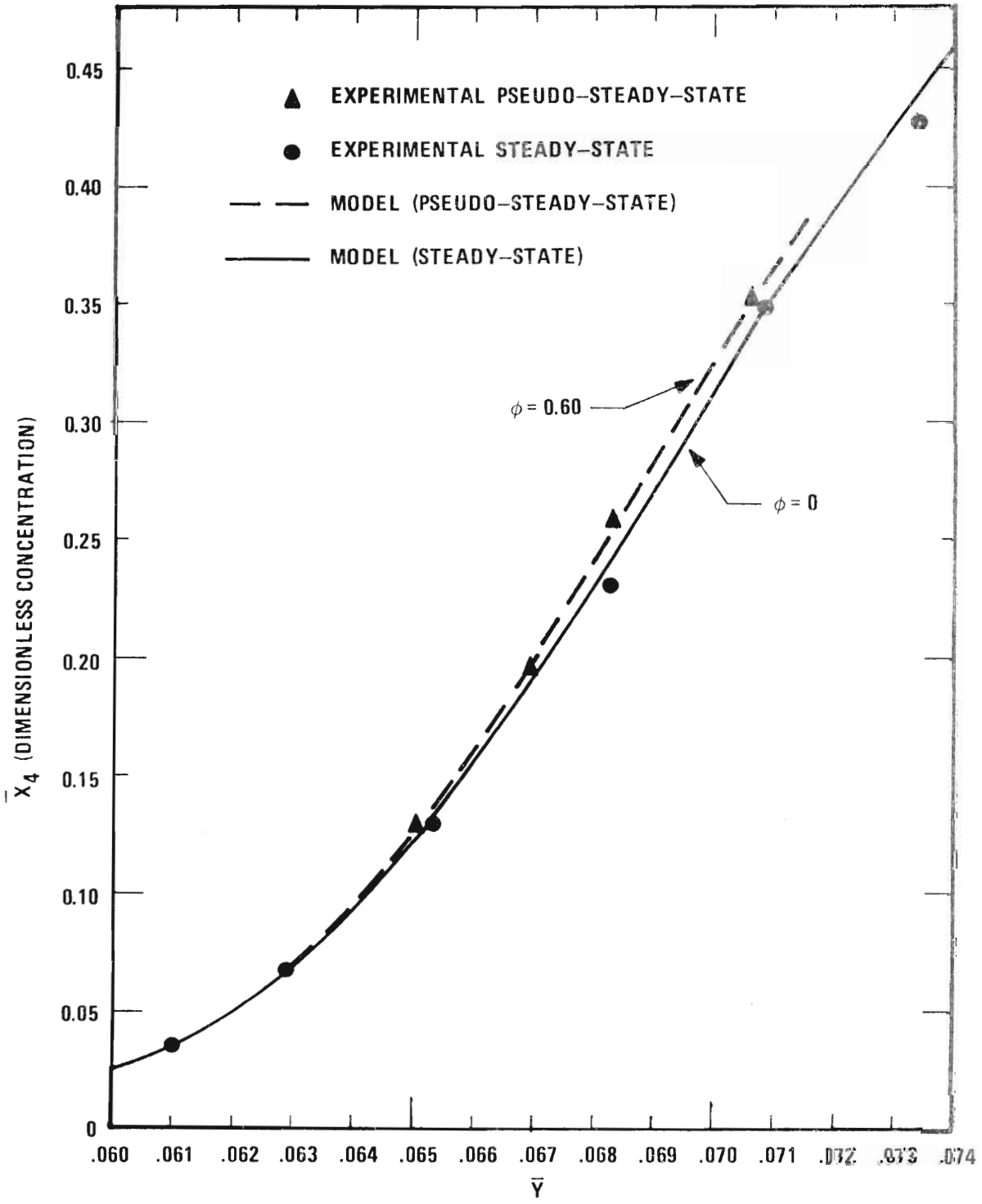

Figure 24. Dimensionless Concentration of Ethanol ($\bar{x}_4$) at ϕ = 0.60

Table 5. Percent Improvement in Yield of $\bar{x}_4$ over Steady-State Conditions

ϕ	$\bar{y}$	$\bar{x}_4$(exp.)	% Improvement in $\bar{x}_4$ Over Steady-State (experimental)	% Improvement in $\bar{x}_4$ Over Steady-State (calculated)
0.95	.0626	.064	4.6	1.3
	.0643	.107	5.9	4.6
	.0659	.159	4.6	8.1
0.90	.0645	.112	7.7	4.5
	.0664	.185	8.8	8.0
	.0678	.249	11.2	9.5
	.0692	.310	10.3	9.6
0.80	.0631	.071	- 0.7	1.5
	.0647	.113	0.3	3.8
	.0666	.190	7.4	6.4
	.0692	.298	5.9	7.2
0.70	.0645	.110	3.0	2.9
	.0665	.185	6.8	4.5
	.0687	.277	6.2	5.6
	.0705	.342	2.3	4.6

Table 5. Percent Improvement in Yield of $\bar{x}_4$ over Steady-State Conditions (Cont'd.)

ϕ	$\bar{y}$	$\bar{x}_4$(exp.)	% Improvement in $\bar{x}_4$ Over Steady-State (experimental)	% Improvement in $\bar{x}_4$ Over Steady-State (calculated)
0.60	.0651	.129	3.3	2.9
	.0669	.196	4.0	4.0
	.0683	.258	5.6	4.3
	.0706	.353	4.4	3.2

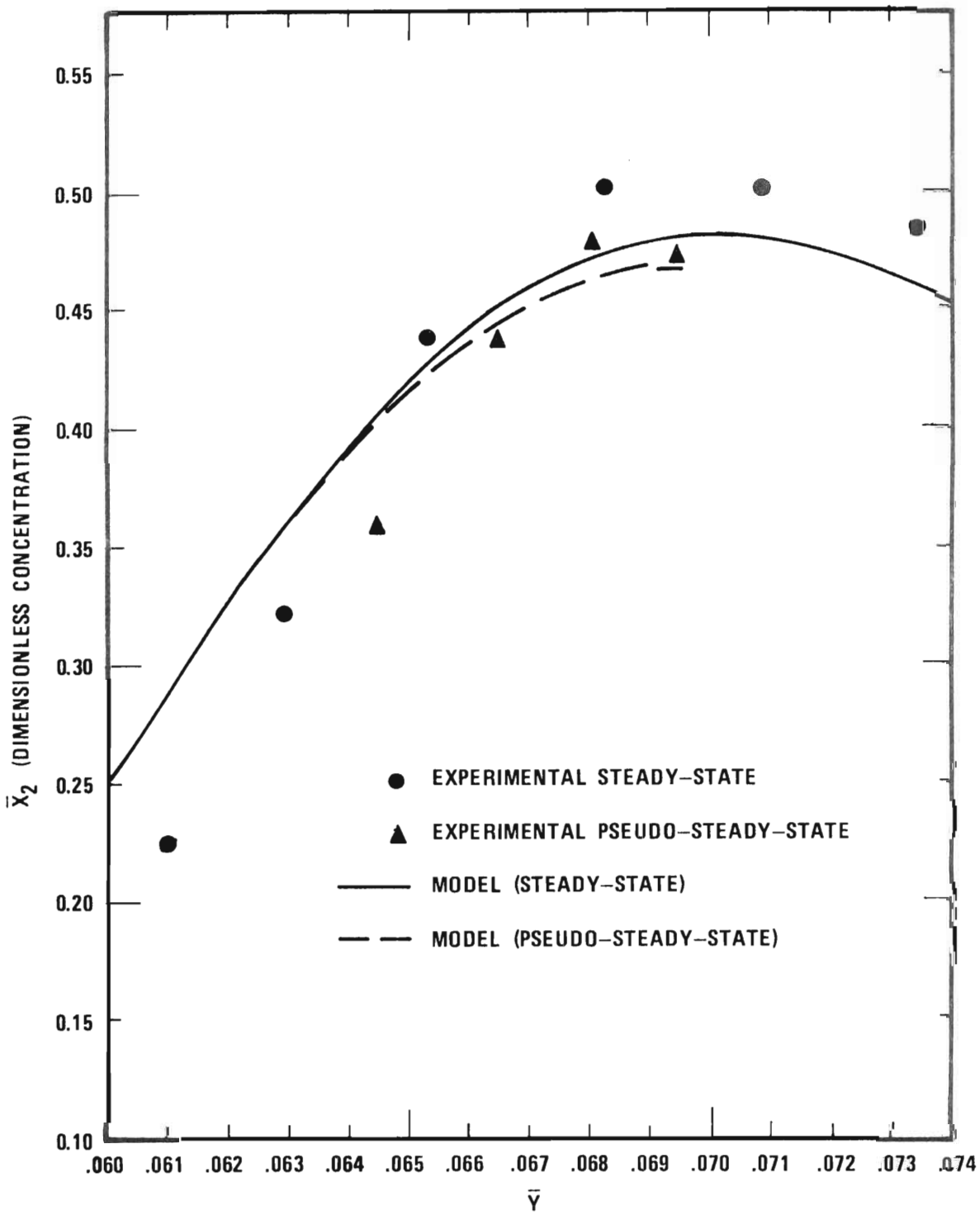

Figure 25. Dimensionless Concentration of Methanol ($\bar{x}_2$) at ϕ = 0.90

sirable, the primary purpose of this work remains the demonstration of the effects of periodic reactor operation.

Discussion of Results

The results obtained in this work are significant in that they demonstrate experimentally that the yield of certain reactions can indeed be improved by the periodic (or cyclic) operation of a CSTR. The mistake of making broad, sweeping assumptions regarding the applicability of this mode of operation to other reaction systems must not be made, however.

The reaction system used in this work was selected especially to demonstrate the effects of periodic operation of a CSTR. This basic goal was achieved as demonstrated in Table 5 and Figures 20-24. Yield increases in the ethanol of up to 11% were observed experimentally at the pseudo-steady-state. Since the overall experimental error is estimated to be less than 5%, it cannot be said that the increase in yield is due to experimental error. Increases in the ethanol yield were observed for almost all of the periodic experiments and were comparable to those predicted by computer simulation.

One question that inevitably arises regards the behavior of the yield of the other reaction product (methanol). The data presented in Figure 25 show that the time-averaged values of the concentration of the other product (methanol, which is equivalent to the sodium acetate concentration) is diminished by cycling (which is the expected result). The amount of decrease, however, is not necessarily equal to the amount of increase of the other species. Differences between the amount of

reactant remaining during periodic and conventional-steady-state-operation account for any discrepancies in the total conversion.

Another question which arises is the applicability of this mode of operation to reactions in the chemical process industry. Again, it should be stated that the parameters and reactions of this experimental system were selected especially for demonstration purposes. This option is obviously not generally available under commercial conditions. In this experimental system, the reactant solution was cooled to as low a temperature as possible in order to increase the measurable effects of cycling. A lower inlet reactant temperature results in a greater increase in the periodic yield, if all other conditions are kept constant, since the family of pseudo-steady-state curves originate from a point on the steady-state curve corresponding to the inlet reactant temperature. The cost of this amount of cooling would most probably more than offset any benefits obtained through cycling. The matter of heat transfer from the heating element is another factor to be considered. Under laboratory conditions an electrical strip heater is quite feasible and the heat transfer rate is quite good. In a larger system, the heating element would probably be a steam coil or jacket; and the heat flux between this element and the reaction mass would not be constant. This would cause the upper limit of the control variable (y_u) to be a variable (function of temperature) rather than a constant, and thus introduce new problems into the system.

In conclusion, it can be stated that the results of this work provide experimental proof that product yields in certain reaction sys-

tems, can be improved by the periodic (or cyclic) operation of a CSTR. Research should be continued in this area in an effort to extend the applicability of this mode of reactor operation to other, potentially practical systems.

CHAPTER XI

CONCLUSIONS AND RECOMMENDATIONS

Conclusions

From the experiments performed during the course of this investigation, the following conclusions result:

1. In certain competitive reaction systems, the yield of the product from the reaction with the higher activation energy can be increased (relative to its conventional steady-state value) by the periodic (or cyclic) variation of the heat flux to or from a CSTR.

2. For the same type of reaction systems, the yield of product from the reaction with the lower activation energy will be decreased as a result of cycling.

3. The family of pseudo-steady-state curves generated by periodic variation of a heat flux to the reactor emanate from the point on the steady-state curve corresponding to the reactant feed temperature.

4. The experimental results for this reaction system (the alkaline hydrolyses of methyl acetate and ethyl benzoate) show improvement in the yield of ethanol (a product of the reaction with the higher activation energy).

Recommendations

Many interesting problems arose during the performance of this experimental work. Some of them pertain to the reaction system and

equipment; others concern possible investigations which could be carried out to provide further data and operating experience in this field.

The following recommendations involve actual changes to the reactor configuration:

1. The constant-head feed controllers should be eliminated and replaced by three feed pumps or one flexible tubing pump which could more easily provide a constant feed to the reactor.

2. A drain line should be attached to the bottom edge of the reactor to drain its contents after each run.

3. The reactor insulation could be improved.

4. The reactant feed lines between the reactant cooler and the reactor should also have better insulation in order to reduce the amount of heat transfer from the surroundings.

5. Better instrumentation for the measurement of the reactant feed temperatures is needed.

6. A digital wattmeter with adjustable ranges should be installed to replace the voltmeter and ammeter used in this work.

7. An electronic or ball-and-disc integrator should be coupled with the gas chromatograph to facilitate any further chromatographic analysis.

8. Investigation of the effects of cycle time should be made using the same reaction system studied in this work.

The following recommendations pertain to future work in this general area of periodic reactor operation:

1. Since the solvent caused several analytical problems, a sys-

tem which could be run in only distilled water should be sought. The complete analysis could then be performed on a gas chromatograph (for all species).

2. The effect of periodic reactor operation on the yields of the products of consecutive reactions should be investigated. The alkaline hydrolysis of diethyladipate in distilled water would be an example of such a system.

3. Efforts should be directed toward the development of a general theory of periodic reactor operation to (1) enable better prediction of possible yield improvements (a priori) or (2) to possibly relate periodic reactor operation to conventional modes.

4. Other cyclic methods should be investigated. Some areas of interest might include (1) the cyclic variation of light energy to a photochemical reaction system, (2) the cyclic input of sonic energy to a reaction system or (3) the cyclic flucuation of flow rate to a CSTR.

5. Investigations into the applicability of periodic reactor operation to biochemical reaction systems where the reaction time is long could be of considerable interest. For these reactions, the "on" cycle could be scheduled to occur overnight or during periods of time when general power usage is not at a peak in order to reduce energy consumption during peak hours.

APPENDICES

APPENDIX A

REACTION RATE CONSTANT DATA

Table 6. Methyl Acetate Hydrolysis
Temperature = 10.8 ± 0.2 °C
Run Number R-8-a

Sample No.	Time(sec.)	C_{CA}(gmole/ℓ)	$k \cdot 10^2$(ℓ/gmole-sec)
1	131	0.0144	5.92*
2	308	0.0233	5.38
3	488	0.0292	5.42
4	669	0.0328	5.32
5	846	0.0355	5.35

Average = 5.37

* Discarded due to poor initial mixing

Table 7. Methyl Acetate Hydrolysis
Temperature = 19.6 ± 0.2 °C
Run Number R-9-a

Sample No.	Time(sec.)	C_{CA}(gmole/ℓ)	$k \cdot 10^2$(ℓ/gmole-sec)
1	136	0.0186	8.55
2	260	0.0266	8.56
3	368	--	--
4	609	0.0364	8.51
5	945	0.0404	8.53

Average = 8.54

Table 8. Methyl Acetate Hydrolysis
Temperature = 24.5 ± 0.2 °C
Run Number R-10-a

Sample No.	Time(sec.)	C_{CA}(gmole/ℓ)	$k \cdot 10^2$(ℓ/gmole-sec)
1	145	0.0216	10.3
2	203	0.0264	10.8
3	264	0.0298	10.9
4	317	0.0318	10.8
5	381	0.0340	10.9

Average = 10.7

Table 9. Ethyl Benzoate Hydrolysis
Temperature = 24.5 ± 0.2 °C
Run Number R-2-a

Sample No.	Time(sec.)	C_{CA}(gmole/ℓ)	$k \cdot 10^4$(ℓ/gmole-sec)
1	675	0.0162	28.6
2	1215	0.0244	26.6
3	1869	0.0334	26.8
4	2604	0.0412	26.9
5	3388	0.0464	25.6

Average = 26.9

Table 10. Ethyl Benzoate Hydrolysis
Temperature = 34.5 ± 0.2 °C
Run Number R-5-a

Sample No.	Time(sec.)	C_{CA}(gmole/ℓ)	$k \cdot 10^4$(ℓ/gmole-sec)
1	315	0.0166	63.2
2	907	0.0346	58.3
3	1510	0.0455	55.3
4	2141	0.0536	53.9
5	2889	0.0614	55.1

Average = 57.1

Table 11. Ethyl Benzoate Hydrolysis
Temperature = 44.5 ± 0.2 °C
Run Number R-6-a

Sample No.	Time(sec.)	C_{CA}(gmole/ℓ)	$k \cdot 10^4$(ℓ/gmole-sec)
1	133	0.0134	124
2	245	0.0220	123
3	364	0.0292	122
4	613	0.0401	118
5	910	0.0496	118

Average = 121

APPENDIX B

EXPERIMENTAL PROCEDURES

Reaction Rate Constant Determination

Methyl Acetate

1. Preparation of 0.1N Methyl Acetate Solution:
   a) Weigh a 100-ml volumetric flask.
   b) Into this flask weigh 0.7408 gm (0.01 mole) of methyl acetate.
   c) Measure 70 ml of acetone into a graduated cylinder and pour into the flask with the methyl acetate.
   d) Fill to the mark with distilled water and shake.
   e) Allow to sit at room temperature for one hour.
   f) Fill to the mark again with distilled water and place in a constant temperature bath.
2. Preparation of 0.1N Sodium Hydroxide Solution:
   a) Place 70 ml of acetone into a 100-ml volumetric flask.
   b) Pipet 10.0 ml of exactly 1.0N NaOH into this flask.
   c) Add distilled water to the mark and shake.
   d) Allow to sit at room temperature for one hour.
   e) Refill to the mark with distilled water.
   f) Place in a constant temperature bath.
3. Hydrochloric Acid Quenching Solution:
   a) Place 5 ml of 0.05N HCl into each of five 150-ml beakers.

b) Add 50 ml of distilled water to each beaker.

c) Add 5 drops of bromothymol blue indicator to each beaker.

4. Experimental Procedure:

a) Place a clean, 50-ml, glass-stoppered volumetric flask into a constant temperature bath.

b) Pipet 25 ml of 0.1N methyl acetate solution into the reaction flask (methyl acetate already at reaction temperature).

c) Pipet 25 ml of 0.1N NaOH solution into the reaction flask with a rapid delivery pipet.

d) Stopper immediately and shake vigorously for 5 seconds.

e) Begin stopwatch at delivery of one-half of the NaOH.

f) Take 5-ml samples at suitable intervals and pipet into the beakers containing the acid quenching solution.

g) Record the time of the sample as that time at which one-half of the 5-ml sample has been delivered to the quench solution.

h) Quench solution should remain yellow to yellow-green but not turn blue.

i) Back titrate with standard, carbonate-free 0.1N NaOH potentiometrically (typical titration curve is shown in Figure 26).

j) Calculate the number of milliequivalents of carboxylic acid present and from that calculate the concentration of sodium acetate.

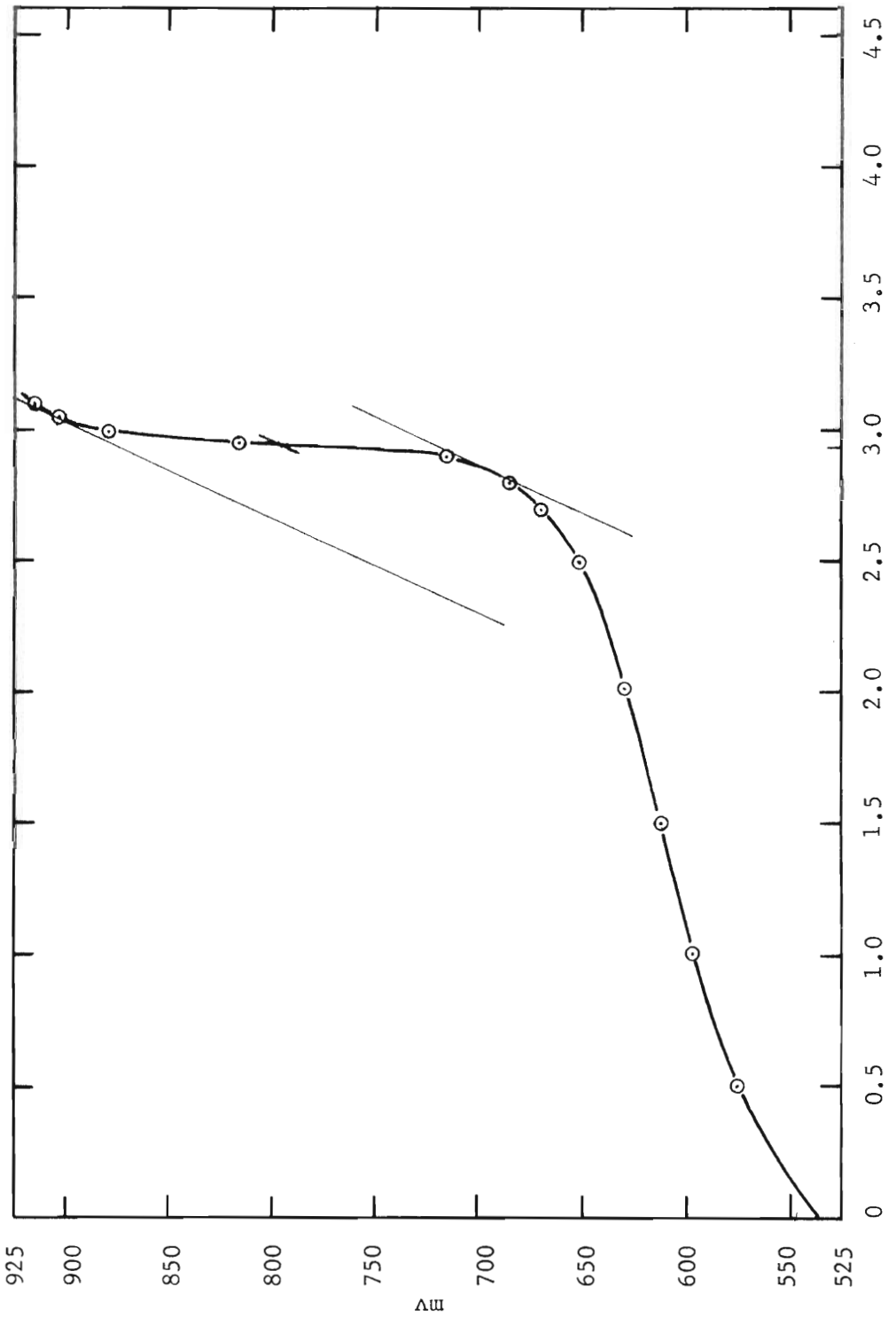

Figure 26. Titration Curve for the Titration of Acetic Acid or Benzoic Acid

Ethyl Benzoate

1. Preparation of 0.1N Ethyl Benzoate Solution:
    a) Using a 3-ml syringe, draw approximately 1.5 ml of ethyl benzoate into it.
    b) Weigh the syringe and ester.
    c) Inject the ester into a spare beaker and reweigh the syringe.
    d) Calculate the net weight of ester and convert to gmole.
    e) Practice this procedure until 0.01 gmole of ethyl benzoate can be weighed out.
2. Preparation of 0.1N Sodium Hydroxide Solution:
    a) Prepare same as in methyl acetate experiment.
    b) Place NaOH solution in a constant temperature bath.
3. Experimental Procedure:
    a) When the NaOH solution has come to the temperature of the bath, inject 0.01 gmole ethyl benzoate with a syringe into the flask containing the NaOH.
    b) Start the stopwatch at one-half of the delivery.
    c) Stopper and shake vigorously for 5 seconds.
    d) Take samples at suitable intervals.
    e) Place samples into the beakers containing quench solution as previously described.
    f) Analyze as previously described.

Experimental Run Procedure

Preparation of Reactant Solutions

1. Methyl Acetate (0.06N)
   a) Place 14,000 ml of acetone solvent into the 5-gallon reactant container.
   b) Add 6,705 ml of distilled water to the acetone and allow to sit overnight.
   c) Add 95 ml of methyl acetate (Fisher No. M-203) and agitate until thoroughly mixed.
2. Sodium Hydroxide (0.06N)
   a) Place 14,000 ml of acetone solvent into the 5-gallon reactant container.
   b) Add 6,680 ml distilled water and allow to sit overnight.
   c) Add 120 ml of 10.0 N NaOH (Fisher No. So-S-255) and agitate until throughly mixed.
3. Ethyl Benzoate (0.60N)
   a) Place 14,000 ml of acetone solvent into the 5-gallon reactant container.
   b) Add 5,080 ml of distilled water and allow to sit overnight.
   c) Add 1,720 ml of ethyl benzoate (Fisher No. 112) and agitate until mixed thoroughly.

Steady-State Run Procedure

1. Mix reactant solutions as indicated above.
2. Connect electrical jumper cable across cycle timer relay to give a steady current to the heating element.

3. Establish the flow of coolant through the reactant stream cooler to achieve coolant bath temperature of -16°C (+3°F).
4. Establish reactant stream flows at approximately 33 ml/min each. Allow the reactor to fill to half full before starting the mixing impeller.
5. Turn on constant voltage transformer.
6. Set millivolt recorder span to 5 mv and plug in leads from reactor thermocouple. Offset zero on scale so that full scale goes from -1.0 mv to 4.0 mv.
7. Turn on flexible tubing pump.
8. Establish a constant reactor temperature (as indicated by the reactor thermocouple output) and continue to run for four residence times at this temperature. This is to insure reaction steady-state as well as thermal steady-state conditions.
9. Withdraw a sample into the flask containing sufficient HCl to quench the reactions and remain in slight excess. Stir flask while sampling.
10. Change the Variac setting to increase the temperature in the reactor and repeat steps 8-9 until all samples at the various temperatures have been taken.

Pseudo-Steady-State Run Procedure

1. Mix reactant solutions as indicated above.
2. Turn on constant voltage transformer.
3. Establish the flow of coolant through the reactant stream cooler to achieve coolant bath temperature of -16°C (+3°F).

4. Adjust millivolt recorder as indicated in step 6 above.
5. Turn on flexible tubing pump.
6. Set cycle timer arms to the appropriate number of minutes "off" and "on".
7. Establish reactant stream flows at approximately 33 ml/min each. Allow the reactor to fill to half full before starting the mixing impeller.
8. Allow system 3-4 cycles to approach the thermal pseudo-steady-state and then wait for three more cycles. Take composite samples during cycles 4 and 6, mixing thoroughly while sampling. Again, an appropriate amount of HCl is present to quench the reactions during sampling and leave excess acid to be back-titrated.
9. Change the Variac setting to alter the power input (upper limit) to the reactor and repeat step 8.

APPENDIX C

ROTAMETER CALIBRATION CURVE

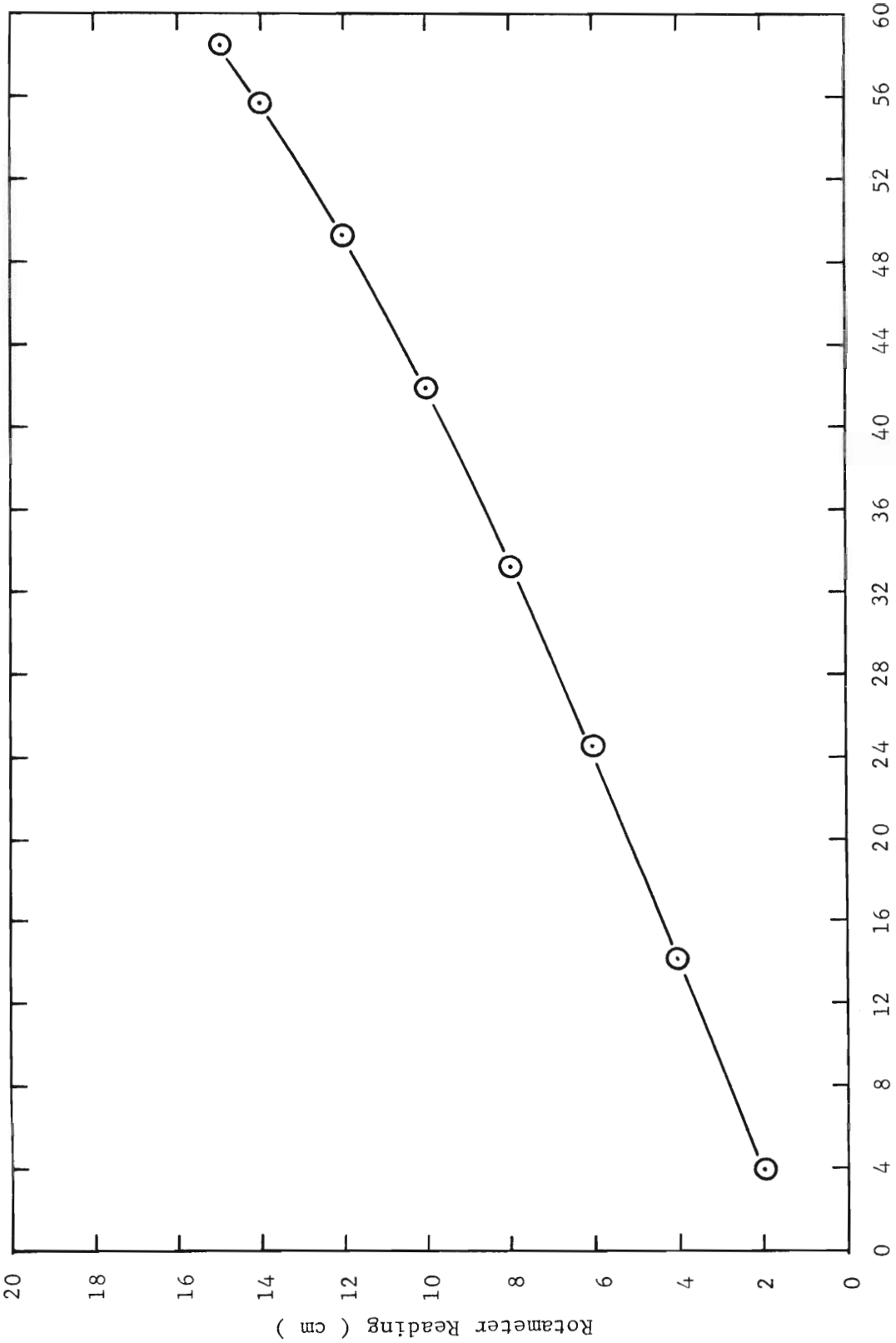

Figure 27. Rotameter Calibration Curve

APPENDIX D

PSEUDO-STEADY-STATE COMPUTER SIMULATION

```
      DIMENSION Y(20)
      EQUIVALENCE (X1,Y(1)),(X4,Y(2)),(X3,Y(3))
      COMMON/BLK1/A1,A2,RHO,R1,R2,T,TAU,EXP1,EXP2,CC,CD,CE,C1,C2
      READ 100, RHO,Q,V,CAO,AK10,AK20,R,E1,R1,R2
      READ 100,X10,X40,X30,C1,C2
      READ 100,DT,PDT
      READ 100,N,YL
      DO 223 I=1,N
      READ 100, YU,T1,T2,CP,DEN,SAMNO
  100 FORMAT(  )
      X1 = X10
      X4 = X40
      X3 = X30
      A1 = AK10*CAO*V/Q
      A2 = AK20*CAO*V/Q
  109 CONTINUE
      TAU = T1 + T2
      PRINT 555,SAMNO
  555 FORMAT(1H1,28X,14HSAMPLE NUMBER ,I3,/)
      PRINT 556
  556 FORMAT(14X,46HCH3COOCH3  +  NAOH  --K1--  CH3COONA  +  CH3OH  ,/,
     1  12X,51HC6H5COOC2H5  +  NAOH  --K2--  C6H5COONA  +  C2H5OH  ,///,
     2  21X,28HREACTOR OPERATING CONDITIONS,//,10X,4H****,
     3  47H**********************************************  ,//)
      PRINT 557,AK10,AK20,RHO,CAO,V,Q,DEN,CP,YU,YL,T1,
     1   T2,TAU,R1,R2
  557 0FORMAT(10X,24HK10 (LITERS/MOLE-MIN) = ,E15.8,/,
     1 10X,24HK20 (LITERS/MOLE-MIN) = ,E15.8 ,/,
     2 20X,14HRHO = E2/E1 = ,F10.5,/,
     3 14X,20HCAO (MOLES/LITER) = ,F10.3,/,
     4 8X,26HREACTOR VOLUME (LITERS) = ,F10.3,/,
     5 9X,25HFLOW RATE (LITERS/MIN) = ,F10.3,/,
     6 6X,28HSOLUTION DENSITY (GMS/CC) = ,F10.3,/,
     7 3X,31HHEAT CAPACITY (CAL/GM*DEG K) = ,F10.3,/,
     8 3X,31HCONTROL VARIABLE UPPER LIMIT = ,F10.6,/,
     1 3X,31HCONTROL VARIABLE LOWER LIMIT = ,F10.6,/,
     2 29X,5HT1 = ,F10.3,/,
     3 29X,5HT2 = ,F10.3,/,
     4 19X,15HPERIOD (TAU) = ,F10.3,/,
     5 24X,10HCBO/CAO = , F10.3,/,
     6 24X,10HCEO/CAO = , F10.3,/  )
      NP1 = IFIX(T1/DT + 0.1 )
      NP2 = IFIX(T2/DT + 0.1 )
      NPDT = IFIX( PDT + 0.1)
  110 CONTINUE
      SUM = 0.0
      TIME = 0.0
      T = YU
```

```
      X1IN = X1
      X2IN = 1.0 - X1 - X4
      X3IN = X3
      X4IN = X4
      NP3 = NP1 + NP2
      DO 10 N = 1,NP3
      IF(N.GT.NP1) T = YL
      CALL RKSUB(3,Y,TIME,DT)
      IF(X4.GT.1.0E2)  STOP
      X2 = 1.0 - X1 - X4
      SUM = SUM + X4*DT/TAU
10    CONTINUE
      ERR1 = ABS((X1IN - X1)/X1)
      ERR2 = ABS((X4IN - X4)/X4)
      ERR3 = ABS((X3IN - X3)/X3)
      ERRMAX = AMAX1(ERR1,ERR2,ERR3)
      ALIM = 1.0E-6
      IF(ERRMAX.LT.ALIM) GO TO 30
      X1 = X1IN + (X1 - X1IN)/2.0
      X3 = X3IN + (X3 - X3IN)/2.0
      X4 = X4IN + (X4 - X4IN)/2.0
      GO TO 110
30    CONTINUE
      KOUNT = 0
      TIME = 0.0
      T = YU
      PRINT 198
198   FORMAT(    2X,4HTIME,8X,2HX1,10X,2HX2,10X,2HX3,10X,2HX4,8X,1HY,/)
      PRINT 160,TIME,X1,X2,X3,X4,T
      DO 40 N = 1,NP3
      IF(N.GT.NP1) T = YL
      CALL RKSUB(3,Y,TIME,DT)
      X2 = 1.0 - X1 - X4
      TIME = DT*FLOAT(N)
      KOUNT = KOUNT + 1
      IF(KOUNT.LT.NPDT) GO TO 40
      PRINT 160,TIME,X1,X2,X3,X4,T
      KOUNT = 0
160   FORMAT(1X,F6.3,4(2X,F10.6),2X,F9.6 )
40    CONTINUE
      YBAR = (T1*YU + T2*YL)/TAU
      PHI = T2/TAU
      PRINT 177,SUM
      PRINT 178, YBAR,PHI
177   FORMAT(//,5X,'THE VALUE OF THE OBJECTIVE FUNCTION',
     1   ' M IS ',F9.5 ,//)
178   FORMAT(5X,7HYBAR = , F10.6,5X,6HPHI = ,F10.6 )
50    CONTINUE
223   CONTINUE
      STOP
      END
```

```
      SUBROUTINE DERIV(X,Y,DYDX)
      DIMENSION Y(20),DYDX(20)
      COMMON/BLK1/A1,A2,RHO,R1,R2,T,TAU,EXP1,EXP2,CC,CD,CE,C1,C2
      X1 = Y(1)
      X4 = Y(2)
      X3 = Y(3)
      EXP1 = EXP(-1.0/X3)
      EXP2 = EXP(-RHO/X3)
      DX1DT = 1.0 - X1 - A1*X1*(R1 - 1.0 + X1 + X4)*EXP1 - A2*X1*EXP2*
     1  (R2 - X4)
      DX2DT = - X4 + A2*X1*(R2 - X4)*EXP2
      DX3DT = -( 1.0 + C1 )*X3 + C1*C2 + T
      DYDX(1) = DX1DT
      DYDX(2) = DX2DT
      DYDX(3) = DX3DT
      RETURN
      END
```

```
      SUBROUTINE RKSUB(N,Y,X,DX)
      DIMENSION Y(20),DY1(20), DY2(20),DY3(20),DY4(20)
      DIMENSION U(20), DYDX(20)
      CALL DERIV(X,Y,DYDX)
      DO 20 I=1,N
      DY1(I) = DYDX(I)*DX
20    U(I) = Y(I) + DY1(I)/2.0
      Z = X + DX/2.0
      CALL DERIV(Z,U,DYDX)
      DO 40 I=1,N
      DY2(I) = DYDX(I)*DX
40    U(I) = Y(I) + DY2(I)/2.0
      CALL DERIV(Z,U,DYDX)
      DO 60 I=1,N
      DY3(I) = DYDX(I)*DX
60    U(I) = Y(I) + DY3(I)
      Z = X + DX
      CALL DERIV(Z,U,DYDX)
      DO 80 I=1,N
      DY4(I) = DYDX(I)*DX
80    Y(I) = Y(I) +(DY1(I) + 2.0*DY2(I) + 2.0*DY3(I)
     1      + DY4(I))/6.0
      RETURN
      END
```

SAMPLE NUMBER 124

$CH_3COOCH_3 + NAOH \xrightarrow{--K1--} CH_3COONA + CH_3OH$

$C_6H_5COOC_2H_5 + NAOH \xrightarrow{--K2--} C_6H_5COONA + C_2H_5OH$

REACTOR OPERATING CONDITIONS

****

K10 (LITERS/MOLE-MIN) =	.18552150+08
K20 (LITERS/MOLE-MIN) =	.10283100+11
RHO = E2/E1 =	1.67614
CAO (MOLES/LITER) =	.020
REACTOR VOLUME (LITERS) =	2.000
FLOW RATE (LITERS/MIN) =	.100
SOLUTION DENSITY (GMS/CC) =	.879
HEAT CAPACITY (CAL/GM*DEG K) =	.846
CONTROL VARIABLE UPPER LIMIT =	.085000
CONTROL VARIABLE LOWER LIMIT =	.061000
T1 =	.400
T2 =	.600
PERIOD (TAU) =	1.000
CB0/CA0 =	1.000
CE0/CA0 =	10.000

TIME	X1	X2	X3	X4	Y
.000	.225260	.450523	.067759	.324217	.085000
.100	.234511	.450192	.069395	.315297	.085000
.200	.214823	.463525	.070870	.321652	.085000
.300	.177234	.481722	.072200	.341044	.085000
.400	.135561	.496700	.073398	.367739	.085000
.500	.122364	.497483	.072199	.380154	.061000
.600	.133468	.489480	.071118	.377052	.061000
.700	.152716	.479657	.070144	.367628	.061000
.800	.175483	.469677	.069265	.354840	.061000
.900	.199969	.459943	.068473	.340088	.061000
1.000	.225260	.450523	.067759	.324217	.061000

THE VALUE OF THE OBJECTIVE FUNCTION M IS .34896

YBAR = .070600 PHI = .600000

STEADY-STATE COMPUTER SIMULATION

```
      READ 100,V,Q,AK10,AK20,CAO,RHO,R1,R2
      READ 100, X1,X4,X3,C1,C2
      READ 100,Y,DY,UPLIM
      PRINT 890
100   FORMAT(    )
890   FORMAT( 15X,'STEADY STATE COMPOSITIONS',//)
      PRINT 891
891   FORMAT(8X,'Y',8X,'X1',8X,'X2',8X,'X4',8X,'X3')
      A1 = AK10*CAO*V/Q
      A2 = AK20*CAO*V/Q
201   CONTINUE
200   CONTINUE
      IF(Y.GT.UPLIM) GO TO 501
      X3SQ = X3**2
      EXP1 = EXP(-1.0/X3)
      EXP2 = EXP(-RHO/X3)
      F = 1.0 - X1 - A1*(R1*X1 - X1 + X1**2 + X1*X4)*EXP1
     1   - A2*X1*(R2 - X4)*EXP2
      G = - X4 + A2*X1*(R2-X4)*EXP2
      H = Y - ( 1.0 + C1 )*X3 + C1*C2
      FX1 = -1.0 - A1*(R1 - 1.0 + 2.0*X1 + X4)*EXP1 - A2*(R2-X4)*EXP2
      FX4 = - A1*X1*EXP1 + A2*X1*EXP2
      FX3 = -A1*(R1*X1 - X1 + X1**2 + X1*X4)*EXP1/X3SQ
     1    - A2*X1*RHO*(R2-X4)*EXP2/X3SQ
      GX1 = A2*(R2-X4)*EXP2
      GX4 = -1.0 - A2*X1*EXP2
      GX3 = A2*X1*RHO*(R2-X4)*EXP2/X3SQ
      HX1 = 0.0
      HX4 = 0.0
      HX3 = - ( 1.0 + C1 )
      FF = F*(GX4*HX3 - HX4*GX3) - FX4*(G*HX3 - H*GX3)
     1     + FX3*(G*HX4 - H*GX4)
      GG = FX1*(G*HX3 - H*GX3) - F*(GX1*HX3 - HX1*GX3)
     1     + FX3*(GX1*H - HX1*G)
      HH = FX1*(GX4*H - HX4*G) - FX4*(GX1*H - HX1*G)
     1     + F*(GX1*HX4 - HX1*GX4)
      AJACOB = FX1*(GX4*HX3 - HX4*GX3) - FX4*(GX1*HX3 - HX1*GX3)
     1       + FX3*(GX1*HX4 - HX1*GX4)
      X1N = X1 - FF/AJACOB
      X4N = X4 - GG/AJACOB
      X3N = X3 - HH/AJACOB
      ERR1 = ABS((X1N - X1)/X1)
      ERR2 = ABS((X4N - X4)/X4)
      ERR3 = ABS((X3N - X3)/X3)
      ALIM = 1.0E-5
      ERRMAX = AMAX1(ERR1,ERR2,ERR3)
      IF(ERRMAX .LE.ALIM) GO TO 500
```

```
      X1 = X1N
      X4 = X4N
      X3 = X3N
      GO TO 200
  800 FORMAT(5X,F6.4,4F10.6)
  500 CONTINUE
      X2 = 1.0 - X1 - X4
      PRINT 800, Y,X1,X2,X4,X3
      Y = Y + DY
      GO TO 201
  501 CONTINUE
      STOP
      END
```

APPENDIX E

CALIBRATION OF GAS CHROMATOGRAPH

In order to determine the concentrations of the reaction products accurately, a Perkin Elmer Model 820 gas chromatograph was utilized. This model is equipped with a flame ionization detector which is capable of responding to virtually all organic compounds. Undetectable materials include water, carbon disulfide, hydrogen sulfide and most of the permanent gases. The lack of response to water makes this detector particularly suitable for analyzing aqueous systems. In addition, this detector is capable of measuring component mass flow rates as small as 10^{-12} grams/sec. This makes it extremely useful in the quantitative determination of very small concentrations of organic materials. The dynamic linear range of this detector is 10^{6}, making it possible to use a single calibration curve over six orders of magnitude of concentration.

The columns selected for use in this work were two one-eighth inch O.D. aluminum columns, each six feet long and packed with 100-120 mesh Porapak Q, which is "... a porous polymer composed of ethylvinylbenzene cross-linked with divinylbenzene to form a uniform structure of a distinct pore size."[1] Since there is no liquid phase, this packing is particularly suitable for use with a very sensitive flame ionization detector and results in a baseline which does not drift due to "bleeding"

---

[1] H. M. McNair and E. J. Bonelli, Basic Gas Chromatography, p. 59.

of any liquid phase. In addition, this packing does not deteriorate over a period of time when used at elevated temperatures (up to 250°C).

The primary advantage of Porapak Q, as applied to the reaction system studied in this research, was the fact that the two alcohols formed as reaction products were eluted before the acetone solvent, enabling precise analysis without solvent interference.

The gases used in the chromatographic analyses were all prepurified in order to insure minimum baseline interference. "Zero-gas" air (Matheson Gas Products) and prepurified hydrogen (Matheson Gas Products) were supplied for the flame, while prepurified nitrogen (Matheson Gas Products) was used as the carrier gas. Rotameters were installed in the nitrogen and air lines and were calibrated using a soap bubble meter. The optimum hydrogen flow rate was determined experimentally and then measured with a soap bubble meter; however, there was no rotameter in the hydrogen line.

In order to quantitatively analyze for the ethanol, it was necessary to construct a calibration curve. Accordingly, standard solutions of ethanol in water were prepared in concentrations of 66,132,330,660, 792, and 990 g/ml. The ethanol used for this calibration was 99.5% pure. Known quantities of these solutions were injected into the chromatograph using a Hamilton five-microliter syringe. The areas of the curves generated by these injections were measured by two different techniques for maximum precision. The first method was based on the assumption that the peaks were reasonably symmetric. The area was calculated by measuring the peak height and the width of the peak at one-

half of the peak height and then multiplying these two measurements. This area was plotted against mass injected and the results are shown in Figure 28. A least-squares fit of these data yielded Equation (E-1).

$$m = 0.0142 + 0.934953(a) \qquad \text{(E.1)}$$

where m = injected mass (nanograms)

a = peak area $(mm)^2$

The second method used to determine the areas was planimetry. Each of the curves previously analyzed by the first method was planed three times and the average area was plotted versus the mass injected. These results are given in Figure 29. A least-squares fit of these data yielded Equation (E-2).

$$m = 0.0382668 + 4540.5(a) \qquad \text{(E.2)}$$

where m = mass injected (nanograms)

a = planed area (planimeter units)

The difference between these two measurement techniques becomes more pronounced at higher concentrations. Increased tailing which occurs with injections of high concentrations causes area loss in the triangle method. This lost area in the peak "tail" can be accounted for by planimetry. At the lower concentrations, the planed area is in the neighborhood of .015 - .025 planimeter units. Obviously, an error of only .001 unit can mean an error of 4% -7% in the calculated concen-

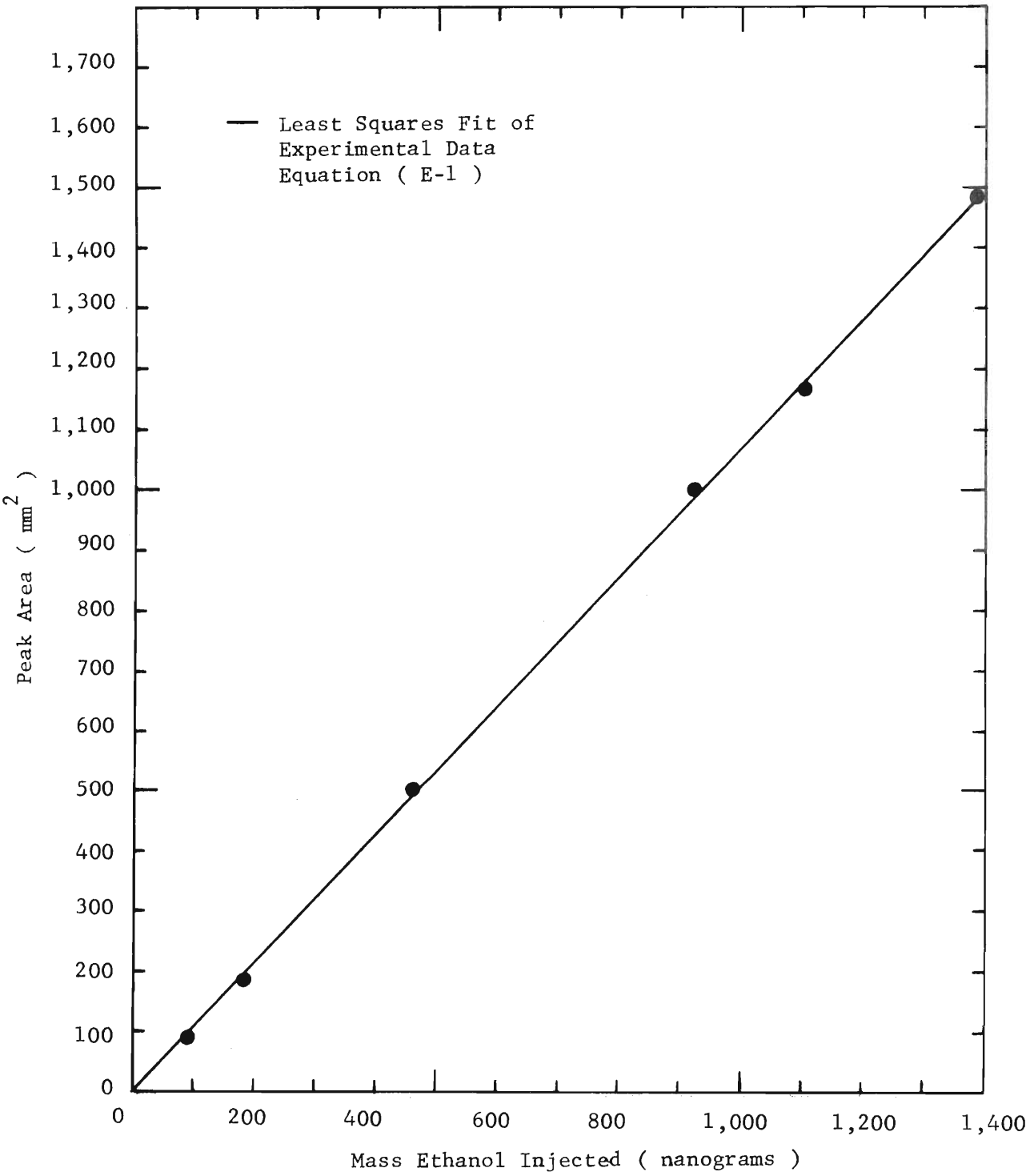

Figure 28. Gas Chromatograph Calibration Curve for Ethanol (Triangle Method)

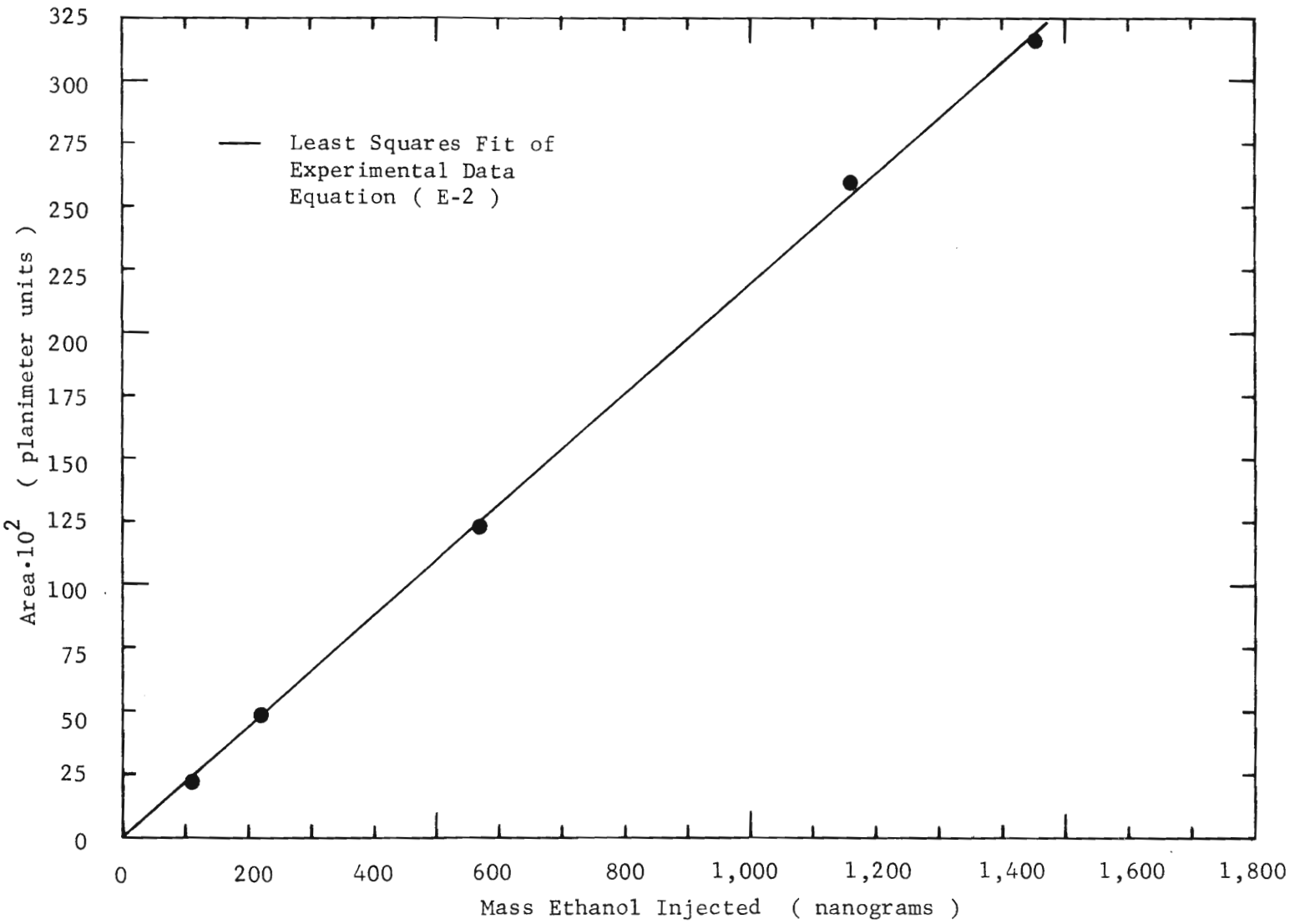

Figure 29. Gas Chromatograph Calibration Curve for Ethanol (Planimetry)

tration. At the higher concentrations, however, the normal area is .100 -.150 units and an error of .001 units would result in an error of less than 1% in the calculated concentration. Consequently, in all subsequent measurements, the planed area was used for larger, tailing peaks, while the triangle method was used for smaller, more symmetrical peaks. At the end of the experimental runs a third calibration curve was constructed. Again a least-squares fit through these data yielded Equation (E-3).

$$m = 0.03827 + 0.78251(a) \qquad \text{(E.3)}$$

where m = mass injected (nanograms)

a = peak area $(mm)^2$

The results are in satisfactory agreement with the previous calibration curves.

In order to compare the results for a given run, the chromatograms for Run 13 were analyzed using all three curves and the results are given in Table 12.

It is felt that the overall error in the chromatographic analysis was $\pm$ 3% using this combination of curves.

Table 12. Comparison of Area Measurements for Run 13

Sample No.	Eq. (E-1)	Eq. (E-3)	Eq. (E-2)
13-1	0.0366	0.0362	0.0381
13-2	0.0673	0.0674	0.0672
13-3	0.1341	0.1339	0.1299
13-4	0.2282	0.2282	0.2305
13-5	0.3183	0.3207	0.3484
13-6	0.3851	0.3880	0.4270

APPENDIX F

EXPERIMENTAL DATA

Table 13. Experimental Data from Run 3

Sample Number	3-1	3-2	3-3	3-4	3-5
$T_{avg.}$ (^{o}C)	19	19	19	19	19
$\rho_{avg.}$ (gm/ml)	0.899	0.899	0.899	0.899	0.899
E (volts)	118	118	118	118	118
I (amperes)	19.3	19.3	19.3	19.3	19.3
q (cal/min)	32,659	32,659	32,659	32,659	32,659
$C_{p,avg.}$ (cal/gm-^{o}K)	0.841	0.841	0.841	0.841	0.841
ϕ	0.95	0.95	0.95	0.95	0.95
y_{ℓ}	0.0610	0.0610	0.0610	0.0610	0.0610
y_u	0.1586	0.1586	0.1586	0.1586	0.1586
$\bar{y}$	0.0659	0.0659	0.0659	0.0659	0.0659
$\bar{x}_4$	0.148	0.161	0.159	0.158	0.159
$\bar{x}_4$ (avg.)	0.159	0.159	0.159	0.159	0.159
$\bar{x}_2$	0.437	0.423	0.425	0.437	0.439

Table 14. Experimental Data from Run 4

Sample Number	4-1	4-2	4-3	4-4
$T_{avg.}$ (^{o}C)	5	5	12	12
$\rho_{avg.}$ (gm/ml)	0.910	0.910	0.903	0.903
E (volts)	72	72	100	100
I (amperes)	11.1	11.1	15.8	15.8
q (cal/min)	11,461	11,461	22,658	22,658
$C_{p,avg.}$ (cal/gm-^{o}K)	0.836	0.836	0.838	0.838
ϕ	0.95	0.95	0.95	0.95
y_{ℓ}	0.0610	0.0610	0.0610	0.0610
y_u	0.0949	0.0949	0.1284	0.1284
$\bar{y}$	0.0627	0.0627	0.0644	0.0644
$\bar{x}_4$	0.0646	0.0642	0.107	0.107
$\bar{x}_4$ (avg.)	0.064	0.064	0.107	0.107
$\bar{x}_2$	0.358	--	0.438	--

Table 15. Experimental Data from Run 5

Sample Number	5-1	5-2	5-3	5-4
$T_{avg.}$ (^{o}C)	13	13	21	21
$\rho_{avg.}$ (gm/ml)	0.903	0.903	0.895	0.895
E (volts)	75	75	91.3	91.3
I (amperes)	11.7	11.7	14.8	14.8
q (cal/min)	12,590	12,590	19,377	19,377
$C_{p,avg.}$ (cal/gm-^{o}K)	0.839	0.839	0.843	0.843
ϕ	0.90	0.90	0.90	0.90
y_{ℓ}	0.0610	0.0610	0.0610	0.0610
y_u	0.0986	0.0986	0.1195	0.1195
$\bar{y}$	0.0648	0.0648	0.0669	0.0669
$\bar{x}_4$	0.107	0.112	0.186	0.184
$\bar{x}_4$ (avg.)	0.110	0.110	0.185	0.185
$\bar{x}_2$	0.478	--	0.472	--

Table 16. Experimental Data from Run 6

Sample Number	6-1	6-2	6-3	6-4
$T_{avg.}$ (^{o}C)	27	27	33	33
$\rho_{avg.}$ (gm/ml)	0.890	0.890	0.884	0.884
E (volts)	101.2	101.2	109.8	109.8
I (amperes)	17.0	17.0	18.7	18.7
q (cal/min)	24,671	24,671	29,444	29,444
$C_{p,avg.}$ (cal/gm-^{o}K)	0.843	0.843	0.845	0.845
ϕ	0.90	0.90	0.90	0.90
y_{ℓ}	0.0610	0.0610	0.0610	0.0610
y_u	0.1354	0.1354	0.1490	0.1490
$\bar{y}$	0.0684	0.0684	0.0698	0.0698
$\bar{x}_4$	0.249	0.238*	0.307	0.314
$\bar{x}_4$ (avg.)	0.249	0.249	0.310	0.310
$\bar{x}_2$	0.483	--	0.475	--

*Discarded

Table 17. Experimental Data from Run 7

Sample Number	7-1	7-2	7-3	7-4
$T_{avg.}$ (^{o}C)	7	7	14	14
$\rho_{avg.}$ (gm/ml)	0.908	0.908	0.902	0.902
E (volts)	53.9	53.9	64.2	64.2
I (amperes)	8.2	8.2	10.1	10.1
q (cal/min)	6,338	6,338	9,299	9,299
$C_{p,avg.}$ (cal/gm-^{o}K)	0.839	0.839	0.842	0.842
ϕ	0.80	0.80	0.80	0.80
y_{ℓ}	0.0610	0.0610	0.0610	0.0610
y_u	0.0798	0.0798	0.0889	0.0889
$\bar{y}$	0.0648	0.0648	0.0666	0.0666
$\bar{x}_4$	0.0684	0.0732	0.115	0.115
$\bar{x}_4$ (avg.)	0.071	0.071	0.115	0.115
$\bar{x}_2$	--	--	--	--

Table 18. Experimental Data from Run 8

Sample Number	8-1	8-2	8-3	8-4
$T_{avg.}$ (^{o}C)	22	22	33	33
$\rho_{avg.}$ (gm/ml)	0.894	0.894	0.884	0.884
E (volts)	73.3	73.3	82.1	82.1
I (amperes)	11.9	11.9	13.9	13.9
q (cal/min)	12,509	12,509	16,365	16,365
$C_{p,avg.}$ (cal/gm-^{o}K)	0.844	0.844	0.846	0.846
ϕ	0.80	0.80	0.80	0.80
y_{ℓ}	0.0610	0.0610	0.0610	0.0610
y_u	0.0986	0.0986	0.1105	0.1105
$\bar{y}$	0.0685	0.0685	0.0709	0.0709
$\bar{x}_4$	0.191	0.190	0.303	0.294
$\bar{x}_4$ (avg.)	0.190	0.190	0.299	0.299
$\bar{x}_2$	--	0.429	--	0.553

Table 19. Experimental Data from Run 9

Sample Number	9-1	9-2	9-3	9-4
$T_{avg.}$ (^{o}C)	13	13	21.5	21.5
$\rho_{avg.}$ (gm/ml)	0.903	0.903	0.895	0.895
E (volts)	43.8	43.8	53.0	53.0
I (amperes)	6.8	6.8	8.5	8.5
q (cal/min)	4,271	4,271	6,422	6,422
$C_{p,avg.}$ (cal/gm-^{o}K)	0.839	0.839	0.841	0.841
ϕ	0.70	0.70	0.70	0.70
y_{ℓ}	0.0610	0.0610	0.0610	0.0610
y_u	0.0738	0.0738	0.0803	0.0803
$\bar{y}$	0.0648	0.0648	0.0668	0.0668
$\bar{x}_4$	0.107	0.113	0.185	0.185
$\bar{x}_4$ (avg.)	0.110	0.110	0.185	0.185
$\bar{x}_2$	--	0.386	--	0.490

Table 20. Experimental Data from Run 10

Sample Number	10-1	10-2	10-3	10-4
$T_{avg.}$ (^{o}C)	31	31	38.5	38.5
$\rho_{avg.}$ (gm/ml)	0.886	0.886	0.880	0.880
E (volts)	61.2	61.2	66.7	66.7
I (amperes)	10.1	10.1	11.3	11.3
q (cal/min)	8,864	8,864	10,808	10,808
$C_{p,avg.}$ (cal/gm-^{o}K)	0.845	0.845	0.846	0.846
ϕ	0.70	0.70	0.70	0.70
y_{ℓ}	0.0610	0.0610	0.0610	0.0610
y_u	0.0877	0.0877	0.0938	0.0938
$\bar{y}$	0.0690	0.0690	0.0708	0.0708
$\bar{x}_4$	0.268	0.285	0.341	0.342
$\bar{x}_4$ (avg.)	0.277	0.277	0.342	0.342
$\bar{x}_2$	--	0.505	--	0.507

Table 21. Experimental Data from Run 11

Sample Number	11-1	11-2	11-3	11-4
$T_{avg.}$ (^{o}C)	15.5	15.5	23	23
$\rho_{avg.}$ (gm/ml)	0.900	0.900	0.893	0.893
E (volts)	39	39	47	47
I (amperes)	6.1	6.1	7.2	7.2
q (cal/min)	3,412	3,412	4,853	4,853
$C_{p,avg.}$ (cal/gm-^{o}K)	0.841	0.841	0.842	0.842
ϕ	0.60	0.60	0.60	0.60
y_{ℓ}	0.0610	0.0610	0.0610	0.0610
y_{u}	0.0712	0.0712	0.0756	0.0756
$\bar{y}$	0.0651	0.0651	0.0668	0.0668
$\bar{x}_4$	0.127	0.132	0.195	0.197
$\bar{x}_4$ (avg.)	0.129	0.129	0.196	0.196
$\bar{x}_2$	--	0.410	--	0.471

Table 22. Experimental Data from Run 12

Sample Number	12-1	12-2	12-3	12-4
$T_{avg.}$ (^{o}C)	29	29	39	39
$\rho_{avg.}$ (gm/ml)	0.888	0.888	0.879	0.879
E (volts)	51	51	57.5	57.5
I (amperes)	8.4	8.4	9.5	9.5
q (cal/min)	6,143	6,143	7,833	7,833
$C_{p,avg.}$ (cal/gm-^{o}K)	0.845	0.845	0.846	0.846
ϕ	0.60	0.60	0.60	0.60
y_{ℓ}	0.0610	0.0610	0.0610	0.0610
y_u	0.0795	0.0795	0.0848	0.0848
$\bar{y}$	0.0684	0.0684	0.0705	0.0705
$\bar{x}_4$	0.258	0.258	0.361	0.344
$\bar{x}_4$ (avg.)	0.258	0.258	0.353	0.353
$\bar{x}_2$	--	0.516	--	0.492

Table 23. Experimental Data from Run 13

Sample Number	13-1	13-2	13-3	13-4	13-5	13-6
$T_{avg.}$ (^{o}C)	-2	6	16.5	29	40	51
$\rho_{avg.}$ (gm/ml)	0.916	0.909	0.899	0.888	0.878	0.870
E (volts)	0	15.8	23.7	32	36	40.5
I (amperes)	0	2.58	3.97	5.1	6.0	7.0
q (cal/min)	0	585	1,349	2,340	3,098	4,065
$C_{p,avg.}$ (cal/gm-^{o}K)	0.836	0.838	0.841	0.845	0.848	0.850
ϕ	0	0	0	0	0	0
y_{ℓ}	0.0610	0.0610	0.0610	0.0610	0.0610	0.0610
y_u	--	--	--	--	--	--
$\bar{y}$	0.0610	0.0628	0.0653	0.0682	0.0706	0.0733
$\bar{x}_4$	0.0366	0.0672	0.130	0.230	0.348	0.427
$\bar{x}_4$ (avg.)	--	--	--	--	--	--
$\bar{x}_2$	0.226	0.322	0.437	0.502	0.502	0.485

APPENDIX G

DERIVATION OF EQUATION FOR CONTROL VARIABLE

Equation (4.55) must be separated into two differential equations as shown below:

$$\frac{dx_3^I}{dt} = y_u - (1 + C_1)x_3 + C_1C_2 \qquad 0 \le t \le t_1 \qquad (G.1)$$

$$\frac{dx_3^{II}}{dt} = y_\ell - (1 + C_1)x_3 + C_1C_2 \qquad t_1 \le t \le \tau \qquad (G.2)$$

Defining the following constants

$$a_1 = y_u + C_1C_2 \qquad (G.3)$$

$$a_2 = (1 + C_1) \qquad (G.4)$$

$$a_3 = y_\ell + C_1C_2 \qquad (G.5)$$

the solutions to Equations (G.1) and (G.2) are

$$x_3^I = \frac{a_1 - C_3' e^{-a_2 t}}{a_2} \qquad (G.6)$$

$$x_3^{II} = \frac{a_3 - C_4' e^{-a_2 t}}{a_2} \qquad (G.7)$$

where C_3' and C_4' are constants resulting from integration and rearrangement.

The boundary conditions for Equations (G.1) and (G.2) (assuming pseudo-steady-state) are :

$$x_3^I(t_1) = x_3^{II}(t_1) \tag{G.8}$$

$$x_3^I(0) = x_3^{II}(\tau) \tag{G.9}$$

Using these boundary conditions to solve for C_3' and C_4' , the final solutions for x_3 are :

$$x_3^I = \frac{a_1 - (a_1 - a_3) \dfrac{(1 - e^{-a_2(\tau - t_1)})}{(1 - e^{-a_2\tau})} e^{-a_2 t}}{a_2} \tag{G.10}$$

$$x_3^{II} = \frac{a_3 - (a_1 - a_3) \dfrac{(1 - e^{a_2 t_1})}{(1 - e^{-a_2\tau})} e^{-a_2 t}}{a_2} \tag{G.11}$$

The time-averaged value of x_3 was obtained from Equations (G.10) and (G.11) as shown below :

$$\bar{x}_3 = \frac{1}{\tau} \int_0^{\tau} x_3 dt \tag{G.12}$$

$$\bar{x}_3 = \frac{1}{\tau} \left\{ \int_0^{t_1} x_3^I dt + \int_{t_1}^{\tau} x_3^{II} dt \right\} \tag{G.13}$$

Inserting Equations (G.10) and (G.11) into Equation (G.13) and performing the necessary integration, Equation (G.13) becomes :

$$\bar{x}_3 = \frac{1}{\tau}\left\{ \frac{a_1}{a_2} t_1 + \frac{a_3}{a_2} (\tau - t_1) \right\} \qquad (G.14)$$

Inserting the definitions of constants a_1, a_2 and a_3 into Equation (G.14) we obtain:

$$\bar{x}_3 = \frac{1}{\tau}\left\{ \frac{y_u + C_1 C_2}{1 + C_1} t_1 + \frac{y_\ell + C_1 C_2}{1 + C_1} (\tau - t_1)\right\} \qquad (G.15)$$

Rearranging and recalling that $t_2 = \tau - t_1$ we obtain :

$$(1 + C_1)\bar{x}_3 = \frac{1}{\tau}\left\{ y_u t_1 + y_\ell t_2 \right\} + \frac{1}{\tau}\left\{ C_1 C_2 t_1 + C_1 C_2 t_2 \right\} \qquad (G.16)$$

By Equation (4.34) the first term on the right-hand side of this equation is defined to be $\bar{y}$. Therefore :

$$\bar{y} = (1 + C_1)\bar{x}_3 - C_1 C_2 \qquad (G.17)$$

which is given in Chapter X as Equation (10.2).

BIBLIOGRAPHY

1. Ambrose, D., Gas Chromatography, Page Brothers, Ltd., London, England (1971).

2. Akhiezer, N. I., The Calculus of Variations, Blaisdell Pub. Co., New York, New York (1963).

3. Aris, R., The Optimal Design of Chemical Reactors, A Study in Dynamic Programming, New York, Academic Press, 1961.

4. Aris, R. and N. R. Amundson, "An Analysis of Chemical Reactor Stability and Control," Chem. Eng. Sci., 7, No. 3, 121-147 (1958).

5. Ausikaitis, J. and A. J. Engel, "Adiabatic Operation of a Cycled Stirred Tank Reactor," Paper presented to the Seventy-fourth National Meeting of AIChE, March 1973.

6. Baccaro, G. P., N. Y. Gaitonde and J. M. Douglas, "An Experimental Study of Oscillating Reactors," AIChE J., 16 (2), 249 (1970).

7. Bailey, J. E., "Optimal Periodic Processes in the Limits of Very Fast and Very Slow Cycling," Automatica, 8, 451-454 (1972).

8. Bailey, J. E. and F. J. M. Horn, "Cyclic Operation of Reaction Systems: The Influence of Diffusion on Catalyst Selectivity," Chem. Eng. Sci., 27, 109 (1972).

9. Bailey, J. E., F. J. M. Horn and R. C. Lin, "Cyclic Operation of Reaction Systems: Effects of Heat and Mass Transfer Resistance," AIChE J., 17 (4), 818 (1971).

10. Bellman, R. E., Dynamic Programming, Princeton University Press, 1957.

11. Bertucci, J. A. and L. Lapidus, "A Modified Maximum Principle," AIChE J., 19 (3), 664-665 (1973).

12. Beveridge, G. S. G. and R. S. Schechter, Optimization: Theory and Practice, McGraw-Hill Book Co., New York, New York, 1970.

13. Cannon, M. R., "Here's a New Liquid Extractor Which Depends on Pulse Flow for Operation," Oil Gas J., 54, 68 (1956).

14. Cannon, M. R., "Here's a New Distillation, Absorption and Extraction Column," Oil Gas J., 51, 268 (1952).

15. Chaprun, B. E., "Solution of Optimization Problems by the Maximum Principle," Auto. Remote Control, 11, 126 (1967).

16. Chien, H. H., J. T. Sommerfeld, V. N. Schrodt, P. E. Parisot, Studies of Controlled Cyclic Distillation," Separation Science, 1 (3), 2 (1966).

17. Codell, R. B. and A. J. Engel, "A Theoretical Study of a Controlled Cycle Stirred Reactor," AIChE J., 17 (1), 220-225 (1971).

18. Conte, S. D. and Carl de Boor, Elementary Numerical Analysis, 2e, McGraw-Hill Book Co., New York, New York (1972).

19. Davies, Gwyn and David P. Evans, " The Influence of Alkyl Groups Upon Reaction Velocities in Solution. Part IV. The Alkaline and Acid Hydrolyses of the Ethyl Esters of the Lower Saturated Aliphatic Acids in Aqueous Acetone," Journal of the Chemical Society of London, 1940, 339 (1940).

20. Dodds, R.; P. I. Hudson; 1. Kershenbaum and M. Streat, "The Operation and Modelling of a Periodic Countercurrent Solid-Liquid Reactor," Chem. Eng. Sci., 28, 1233-1248 (1973).

21. Dorawala, T. G. and J. M. Douglas, "Complex Reactions in Oscillating Reactors," AIChE J., 17 (4), 974 (1971).

22. Douglas, J. M., "Periodic Reactor Operation," I&EC Process Design and Development, 6, No. 1, 43 (1967).

23. Douglas, J. M. and D. W. T. Rippin, "Unsteady State Process Operation," Chem. Eng. Sci., 21, 305 (1966).

24. Edgar, T. F. and L. Lapidus, "The Computation of Optimal Singular Bang-Bang Control," AIChE J., 18 (4), 774 (1972).

25. Elsgolc, L., Calculus of Variations, Pergamon Press, Reading, Mass. (1961).

26. Evans, D. P.; J. J. Gordon and H. B. Watson, "Studies of the ortho-Effect. Part III. Alkaline Hydrolysis of Benzoic Esters," J. Chem. Soc., 1937, 1430-1432 (1937).

27. Gallagher, G. A.; J. G. Miller and A. R. Day, "Solvent Effects and Ester Interchange in Basic Hydrolysis of Esters," J. Amer. Chem. Soc., 79, 4324-4327 (1957).

28. Gaska, R. A. and M. R. Cannon, "Controlled Cycling Distillation," I&EC, 53, 8, 630 (1961).

29. Gelfand, I. M. and S. V. Fomin, Calculus of Variations, Prentice-Hall Pub. Co., Engelwood Cliffs, N. J. (1963).

30. Grant, D. W., Gas-Liquid Chromatography, Van Nostrand Reinhold Company, London, England (1971).

31. Horn, F. J. M., "Periodic Countercurrent Processes," I&EC Process Design and Development, 6, No. 1, 30 (1967).

32. Horn, F. J. M. and R. C. Lin, "Periodic Processes: A Variational Approach," I&EC Process Design and Development, 6, (1), 21 (1967).

33. Horn, F. J. M. and R. A. May, "Effect of Mixing on Periodic Countercurrent Process," I&EC Fundamentals, 7, No. 3, 349 (1968).

34. Ingold, Christopher K. and Wilfred S. Nathan, "Mechanism of, and Constitutional Factors Controlling, the Hydrolysis of Carboxylic Esters. Part VIII. Energies Associated with Induced Polar Effects in the Hydrolysis of Substituted Benzoic Esters," J. Chem. Soc., 1936, 222-225 (1936).

35. Javinsky, M. A. and R. H. Kadlec, "Optimal Control of a Continuous Flow Stirred Tank Chemical Reactor," AIChE J., 16 (6), 916 (1970).

36. Jones, R. W. A. and J. D. R. Thomas, "Steric Influence of the Alkyl Component in the Alkaline Hydrolysis of Acetates and Propionates," J. Chem. Soc., 1966, 661 (1966).

37. Kowler, D. E., The Optimal Control of a Periodic Adsorber, PhD Thesis, Univ. of Michigan, 1969.

38. Laurence, R. L. and G. Vasudevan, "Performance of a Polymerization Reactor in Periodic Operation," I&EC Process Design and Development, 7, No. 3, 427 (1968).

39. Levenspiel, O., Chemical Reaction Engineering, John Wiley & Sons, N. Y., 1965.

40. Li, W. H., "Liquid-Liquid Extraction in a Pulsed Perforated-Plate Column," PhD Thesis, Georgia Institute of Technology, 1952.

41. Locatelli, A. and S. Rinaldi, "Optimal Quasi-Stationary Periodic Processes," Automatica, 6, 779-785 (1970).

42. Lund, M. M. and R. C. Seagrave, "Optimal Operation of a Variable Volume Stirred Tank Reactor," AIChE J., 17 (1), 31 (1971).

43. McNair, H. M. and E. J. Bonelli, Basic Gas Chromatography, Varian Aerograph, Consolidated Printers, Berkeley, California (1968).

44. McWhirter, J. R. and M. R. Cannon, "Controlled Cycling Distillation ... in a Packed Plate Column," I&EC, 53 (8), 632-4 (1961).

45. Matsubara, M.; Y. Nishimura and N. Takahashi, "Periodic Operation of a CSTR," Chem. Eng. Sci., 28, 1369-1385 (1973).

46. May, R. A. and F. J. M. Horn, "Stage Efficiency of a Periodically Operated Distillation Column," I&EC Process Design and Development, 7, No. 1, 61 (1968).

47. Newling, W. B. S., and C. N. Hinshelwood, "The Kinetics of the Acid and the Alkaline Hydrolysis of Esters," J. Chem. Soc., 1936, 1357-1361 (1936).

48. Patai, Saul, The Chemistry of Carboxylic Acids and Esters, Interscience Publishers, New York, New York (1969).

49. Pontryagin, L. S.; V. G. Boltyanskii; R. V. Gamkrelidze and E. F. Mishchenko, The Mathematical Theory of Optimal Processes, John Wiley and Sons, Inc., New York, New York (1962).

50. Ray, W. H., "Periodic Operation of Polymerization Reactors," I&EC Process Design and Development, 7, No. 3, 422 (1968).

51. Renken, A., "The Use of Periodic Operation to Improve the Performance of Continuous Stirred Tank Reactors," Chem. Eng. Sci., 27 (11), 1925 (1972).

52. Ritter, A. B. and J. M. Douglas, "Frequency Response of Nonlinear Systems," I&EC Fundamentals, 9, No. 1, 21 (1970).

53. Robinson, R. G., PhD Dissertation, Pennsylvania State University, University Park, Pa., 1964.

54. Robinson, R. G. and A. J. Engel, "An Analysis of Controlled Cycling Mass Transfer Operations," I&EC, 59 (3), 22-9 (1967).

55. Rozonoer, L. T., "L. S. Pontryagin Maximum Principle in the Theory of Optimum Systems," Auto. and Remote Control, 20 (10,11,12), 1288-1302, 1405-1421, 1517-1532 (1959).

56. Schrodt, V. N., "On-Off Operations," International Science and Technology, No. 61, 62-70 (1967).

57. Schrodt, V. N., "Unsteady-State Processing," I&EC, 59, No. 6, 58 (1967).

58. Schrodt, V. N., J. T. Sommerfeld, O. R. Martin, P. E. Parisot and H. H. Chien, "Plant-Scale Study of Controlled Cyclic Distillation," Chem. Eng. Sci., 22, 759-67 (1967).

59. Shatkhan, F. A., "Application of the Maximum Principle to the Optimization of Parallel Chemical Reactions," Auto. and Remote Control, 25, No. 3, 344-348 (1964).

60. Siebenthal, C. D. and R. Aris, "The Application of the Pontryagin Maximum Principle to the Control of a Stirred Reactor," Chem. Eng. Sci., 19, 729-746 (1964).

61. Sommerfeld, J. T., V. N. Schrodt, P. E. Parisot and H. H. Chien, "Studies of Controlled Cyclic Distillation," Separation Science, 1 (2), 245 (1966).

62. Timm, E. W. and C. N. Hinshelwood, "The Activation Energy of Organic Reactions. Part III. The Kinetics of Acid Hydrolysis of Esters," J. Chem. Soc., 1938, 862-869 (1938).

63. Tommila, Eero, "The Influence of the Solvent on Reaction Velocity. Part II. Alkaline Hydrolysis of Ethyl Benzoate and Benzyl Acetate in Mixed Solvents," Suomen Kemistilehti, B25, 37 (1952).

64. Tommila, E. and C. N. Hinshelwood, "The Activation Energy of Organic Reactions. Part IV. Transmission of Substituent Influences in Ester Hydrolysis," J. Chem. Soc., 1938, 1801-1810 (1938).

65. Tommila, Eero; Anja Nurro; Raija Muren; Sinikka Merenheimo and Eila Vuorinen, "The Influence of the Solvent on Reaction Velocity. XVIII. The Dependence of the Substituent Effect on the Solvent in the Alkaline Hydrolysis of Benzoic Esters," Suomen Kemistilehti, B32, 115 (1959).

66. Yager, B. J.; C. B. Kay; J. D. Mastrovich and L. E. Whittington, "The Variation of Saponification Rate Constants of Three Aliphatic Esters in Several Aqueous-Organic Solvent Systems," Texas Journal of Science, 21 (1), 3-11 (1969).

VITA

Robert Charles Schucker was born on January 10, 1945 in Altoona, Pennsylvania. Shortly thereafter his family moved to Columbia, South Carolina where he attended grammar and high schools. He was graduated from University High School in 1963 and attended the University of South Carolina from which he received a Bachelor of Science in Chemical Engineering in 1968. He continued at the University of South Carolina and received a Master of Engineering in Chemical Engineering in 1970. During the last six months of his graduate work at U.S.C. and until June 1971 , he worked for Carolina Eastman Company in Columbia, South Carolina as an engineer in Process Improvement and Development. In 1971 he attended Georgia Institute of Technology where he was employed as a Graduate Teaching Assistant during 1971-72 in the School of Chemical Engineering. He is a member of the American Institute of Chemical Engineers, Tau Beta Pi and Omicron Delta Kappa.

Mr. Schucker is married to the former Rebecca Lynn Crawford of Amelia Island, Florida and they have one daughter, Laura Leigh.